

**A Study of the Third Dimension
in the Thunder Bay Silver Veins:
Fluid Inclusion and Stable
Isotope Results.**

by

Ross Lawrence Sherlock



Submitted in partial fulfillment
for the degree of

Master of Science

Faculty of Arts and Science
Lakehead University
Thunder Bay, Ontario
Canada

May, 1989

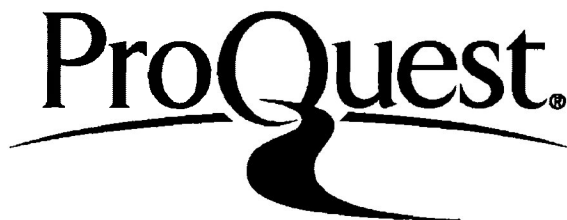
ProQuest Number: 10611796

All rights reserved

INFORMATION TO ALL USERS

The quality of this reproduction is dependent upon the quality of the copy submitted.

In the unlikely event that the author did not send a complete manuscript and there are missing pages, these will be noted. Also, if material had to be removed, a note will indicate the deletion.



ProQuest 10611796

Published by ProQuest LLC (2017). Copyright of the Dissertation is held by the Author.

All rights reserved.

This work is protected against unauthorized copying under Title 17, United States Code
Microform Edition © ProQuest LLC.

ProQuest LLC.
789 East Eisenhower Parkway
P.O. Box 1346
Ann Arbor, MI 48106 - 1346

Master of Science (1989) Lakehead University (Geology)

Title: A Study of the Third Dimension in the Thunder Bay
Silver Veins: Fluid Inclusion and Stable Isotope
Results.

Author: Ross Lawrence Sherlock

Supervisor: Dr. S.A. Kissin

Number of Pages: ix, 180

Abstract

Historic drill core from the Shuniah Mine and more recent drill core from the Keystone and Porcupine Mines have provided the basis for a study of these past silver-producing veins as a function of depth. Precipitation was initiated from a boiling fluid at temperatures in excess of 370°C. Cooling of the fluid and precipitation of calcite and sulfides followed generally at 100°C. Several episodes of deposition separated by fracturing events are evidenced. From fluid boiling temperatures the depth of emplacement for the veins is 1 km with the pressure regime alternating between hydrostatic and lithostatic. The ore-depositing solutions appear, therefore, to have arisen from depth and deposited their ores in proximity to diabase sills, which cap the various vein systems, in response to hydrologic factors.

Stable isotope studies reveal that carbon in vein calcite was possibly derived from oxidation of amorphous carbon in the Gunflint and Rove Formations ($\delta^{13}\text{C} = -33$ per mil), which host the silver lodes. Calcite as well, does not occur at great depth in the vein systems. $\delta^{18}\text{O}$ in calcite increases with depth, from calculated negative to positive values, suggesting that the ore-depositing fluid was a basinal-type brine that became increasingly mixed with meteoric water towards the surface. Fluid salinities are low to moderate, but invariably undersaturated, also supporting mixing. The dominant salts are NaCl, MgCl_2 and to a lesser extent CaCl_2 .

Acknowledgements

This project was supported by the Ontario Geoscience Research Fund, Grant 300 to Dr. S.A. Kissin. I would like to thank Dr. Kissin for his guidance and friendship over the course of this study. Anne Hammond and Reino Viitala provided assistance in sample preparation. Sam Spivak drafted some of the better looking figures. I would like to thank Dr. Cummings and Dr. Franklin of the Geological Survey of Canada for providing the Shuniah and Creswell drill core samples. John Scott of the Ontario Ministry of Northern Development and Mines provided samples from Silver Islet.

I wish to thank the faculty and my fellow students for their input and thought provoking discussions on various aspects of this project. Finally I thank Elizabeth, without her nothing would be possible.

Table of Contents

Abstract	1
Acknowledgments	ii
Table of Contents	iii
List of Figures	vi
List of Tables	ix
List of Photographs	ix

Chapter one

Introduction	1- 1
Previous Work	1- 1
Regional Geology	1- 2
Thunder Bay Silver District	1-10
Port Coldwell veins	1-10
Island Group	1-12
Mainland Group	1-13
Proposal	1-15

Chapter two

Methodology	
Fluid Inclusion Study	2- 1
Stable Isotopes	2- 6
X-Ray Diffraction Techniques	2- 8

Chapter three

Port Arthur Group Introduction	
Shuniah Mine	
History	3- 1
Geology	3- 5
Thunder Bay Mine	
History	3- 9
Geology	3-10
Joint Set Study	3-11
Fluid Inclusion Study	
Shuniah Mine	
Eutectic Temperatures	3-15
Salinity	3-17
Paragenesis	3-19
Homogenization Temperatures	3-23
Thunder Bay Mine	
Fluid Inclusion Study	3-31

Stable Isotope Data	
Shuniah Mine	3-37
Thunder Bay Mine	3-41
Silver Islet Grab Samples	3-42

Chapter four

Creswel Group	
Porcupine Mine History	4- 1
Keystone Mine History	4- 3
Creswel Mines Limited	4- 3
Geology of the Creswel Property	4- 5
Fluid Inclusion Study	
Porcupine Mine	
Eutectic Temperatures	4-15
Salinity	4-17
Homogenization Temperatures	4-19
Paragenesis	4-21
Keystone Mine	
Eutectic Temperatures	4-24
Salinity	4-26
Homogenization Temperature	4-26
Paragenesis	4-29
Stable Isotope Data	4-32
Comparison of Porcupine and Keystone Mines	4-36

Chapter five

Implications of the Fluid Inclusion Study	
Homogenization Temperature	5- 1
Freezing Data	5- 5
Implications of the Mineralogy	
Paragenesis	5- 8
Controls on Mineral Deposition	5-10
Mineralogy	5-13
Implications of Stable Isotope Data	
Oxygen Isotope Data	5-15
Carbon Isotope Data	5-20
Elemental Carbon Isotope Data	5-22

Chapter six

Summary	6- 1
Conditions of the ore-forming systems	6- 4
Model for the Formation of the Thunder Bay	6-10
Silver Veins.	
Recommendations for Future Research	6-13

References	Reference 1 to 8
Appendix one	Appendix 1-1 to 1-15
Appendix two	Appendix 2-1
Appendix three	Appendix 3-1 to 3-3
Appendix four	Appendix 4-1 to 4-5
Appendix five	Appendix 5-1 to 5-2

List of Figures

	Page
Figure 1-1	Geology of the Lake Superior Syncline..... 1- 9
Figure 1-2	Two belts of silver veins with vein..... 1-11 locations.
Figure 1-3	Study area showing the mines examined..... 1-16
Figure 2-1	Fluid Inclusion Thermocouple 2- 3 Calibration, January 1988.
Figure 2-3	Fluid Inclusion Thermocouple 2- 4 Calibration, September 1988.
Map 3-1	Geology and location map for the Port 3- 0 Arthur Group.
Figure 3-1	Vertical projection of the Shuniah Mine... 3- 3
Figure 3-2	Horizontal projection of the Shuniah Mine. 3- 4
Figure 3-3	Generalized cross section of the upper.... 3- 6 portions of the Shuniah Mine.
Figure 3-4	Cross section of the Shuniah Mine at..... 3- 8 shaft number three.
Figure 3-5	Area over which the joint set study was .. 3-12 undertaken, shows the division of the area into tectonic blocks based on the study.
Figure 3-6	Compilation of the joint set data..... 3-13
Figure 3-7	Histogram of eutectic temperatures 3-16 from the Shuniah Mine.
Figure 3-8	Histogram of salinity determinations 3-18 for the Shuniah Mine.
Figure 3-9	Paragenetic diagram for the Shuniah Mine... 3-20
Figure 3-10	Homogenization temperatures of fluid 3-25 inclusions hosted in calcite I as a function of depth.
Figure 3-11	Homogenization temperatures of fluid 3-26 inclusions hosted in calcite II as a function of depth.

Figure 3-12	Boiling curve for fluid inclusions 3-28 hosted in quartz I as a function of depth.
Figure 3-13	Boiling curve for fluid inclusions 3-29 hosted in quartz II as a function of depth.
Figure 3-14	Histogram of eutectic temperatures 3-33 from the Thunder Bay Mine.
Figure 3-15	Histogram of salinity determinations 3-34 for the Thunder Bay Mine.
Figure 3-16	Paragenetic diagram for the Thunder 3-35 Bay Mine.
Figure 3-17	Histogram of homogenization temperatures .. 3-36 for the Thunder Bay Mine.
Figure 3-18	Oxygen isotope variations as a function ... 3-40 depth, data is for the Port Arthur Group.
Map 4-1	Geology and location map for the Creswel .. 4- 0 Group.
Figure 4- 1	Porcupine Mine cross section showing the .. 4- 7 mine workings.
Figure 4- 2	Porcupine Mine cross section showing the .. 4- 9 orientation of D.D.H. 68-3.
Figure 4- 3	Porcupine Mine cross section showing the .. 4-10 orientation of D.D.H. 68-13 & 68-12.
Figure 4- 4	Detailed map of Keystone number six vein... 4-12
Figure 4- 5	Cross section of the workings at the 4-13 Keystone number six vein.
Figure 4- 6	Cross section of the Keystone Mine showing.. 4-14 the vertical projection of D.D.H. 68-4, 68-5, 68-6.
Figure 4- 7	Histogram of eutectic temperatures for ... 4-16 the Porcupine Mine.
Figure 4- 8	Histogram of salinity determinations 4-18 for the Porcupine Mine.
Figure 4- 9	Histogram of homogenization temperatures ... 4-20 for fluid inclusions hosted in quartz for the Porcupine Mine.

Figure 4-10	Graph of the homogenization temperatures ... 4-22 of fluid inclusions hosted in calcite as a function of depth for the Porcupine Mine.
Figure 4-11	Paragenetic diagram for the Porcupine Mine.. 4-23
Figure 4-12	Histogram of eutectic temperatures for 4-25 the Keystone Mine.
Figure 4-13	Histogram of salinity determinations 4-27 for the Keystone Mine.
Figure 4-14	Histogram of homogenization temperatures ... 4-28 for fluid inclusions hosted in quartz for the Keystone Mine.
Figure 4-15	Graph of the homogenization temperatures . . 4-30 of fluid inclusions hosted in calcite as a function of depth for the Keystone Mine.
Figure 4-16	Paragenetic diagram for the Keystone Mine .. 4-31
Figure 4-17	Variations in the Creswel Group oxygen 4-34 isotope variations as a function of depth.
Figure 5- 1	Variations in oxygen isotope data as a 5-16 function of depth. Data is combined from the Port Arthur and Creswel Groups.
Figure 5- 2	Graph of deuterium vs oxygen isotopic 5-17 ratios showing reference waters and the limits of this studies oxygen data.
Figure 5- 3	Graph demonstrating the variation in 5-21 carbon isotope ratios for the different wall-rock lithologies.
Figure 6- 1	Model for the Formation of the Thunder Bay . 6-11 Silver Veins.

List of Tables

	Page
Table 1-1 Proterozoic Stratigraphy and Radiometric ... Age Determinations for the Thunder Bay District.	1- 4
Table 3-1 Port Arthur Group Stable Isotope Data	3-38 3-39
Table 4-1 Creswel Group Stable Isotope Data	4-33

List of Photographs

Photograph 3-1 Fluid inclusion precipitated from a .. non-boiling fluid.	3-21
Photograph 3-2 Fluid inclusions precipitated from a .. boiling fluid.	3-21
Photograph 3-3 Hydrothermal quartz grains showing zoning due to pulses of boiling fluid.	3-22
Photograph 3-4 Large primary fluid inclusion hosted .. in calcite	3-24

Introduction

The Thunder Bay silver camp was most active between 1863 to 1911, with a total production of 4,701,000 ounces of silver (Franklin et al., 1986). Although this activity has been overshadowed by the production of five hundred million ounces of silver at Cobalt, Ontario, the Thunder Bay mining boom played a very important role in the development of northwestern Ontario. The most notable mine of the Thunder Bay silver camp, historically and geologically, is the Silver Islet Mine. However, Ingall (1888) described seventy-one veins from the Thunder Bay silver district that had some form of development work. Since the close of mining in 1911, there have been sporadic attempts to reopen old mines, but no new developments have occurred.

Previous Work

Comprehensive descriptive accounts of the vein systems have been published by Curtis (1887) and Ingall (1888). These geologists were able to visit the mines before the workings were filled in. This allowed them to describe and sample the properties in a detail that is not possible with today's exposure. Their work, and that of others, was summarized in a comprehensive report by Tanton (1931). Much

of today's understanding of the detailed geology is based on the work of these authors.

Franklin (1970) completed the first recent work on the area. Franklin et al. (1986) published Pb isotope data along with a comprehensive summary of the area. A number of studies have been completed at Lakehead University; the veins studied are Rabbit Mountain (Mosley, 1977); Beaver Junior (Cole, 1978); West Beaver (Maunula, 1979); Island Belt (Smyk, 1984); Creswel Group (Chambers, 1986) and a survey of the Mainland and Island Belts (Jennings, 1987).

Regional Geology

The Proterozoic rocks of northwestern Ontario unconformably overlie the older Archean rocks of the Superior Structural Province. As summarized by McGlynn (1970), the Archean terrane consists of two northeast-trending metamorphic belts, termed the Wawa-Shebandowan and the Quetico Subprovinces. The Wawa-Shebandowan Subprovince is composed of mafic and felsic volcanics, and sedimentary strata, with numerous intrusions. The belt has been intensely deformed and grades from greenschist in the west to amphibolite metamorphic grade in the east. The Quetico Subprovince is composed of greywacke, migmatitic gneiss and felsic intrusions. The Quetico belt

grades from greenschist at its margins to sillimanite facies at its center.

The Proterozoic strata consists of Aphebian, Paleohelikian, and Neohelikian terranes. The Aphebian terrane is composed of the Animikie Group, which is formed by the Gunflint and Rove Formations. The Paleohelikian terrane is composed of the Sibley Group, which is formed by the Pass Lake, Rossport and Kama Hill Formations. The Neohelikian terrane is composed of the Osler Group and various contemporaneous intrusions. The intrusive rocks include the Logan sills, Pine River-Mount Mollie gabbro, and the Pigeon River dikes (Table 1-1).

The earliest group, of Aphebian age, is the Animikie Group. This Group includes the Gunflint Formation, which is conformably overlain by the Rove Formation. The Gunflint Formation represents deposition in a stable shelf environment (Shegelski, 1982). The Gunflint Formation averages 145 m in thickness and has a lateral range of 177 km (Goodwin, 1956), which extends from Gunflint Lake east of Thunder Bay to the Slate Islands near Schreiber (Kustra et al., 1977). The Gunflint is considered an iron formation, since its lithologies are dominated by iron rich chemical sediments with minor tuffaceous components (Franklin et al., 1986). There exists a complete spectrum between chert and carbonate facies in the iron formation. It is thought that

Table 1-1

Proterozoic Stratigraphy and Radiometric Age Determinations for the Thunder Bay District

Osler Group	Tholeiitic basalt minor rhyolite and sedimentary strata.			
Contemporaneous mafic intrusives	Pine River-Mount Mollie Gabbro			
	Pigeon River Dikes	0.9-1.1 Ga	K-Ar	Hanson & Malhotra (1971)
	Logan Sills	1.3 Ga	K-Ar	Hanson & Malhotra (1971)
		0.99-1.1 Ga	paleomag	Robertson & Fahrig (1971)
		0.73-1.06 Ga	K-Ar	Robertson & Fahrig (1971)
		1.109 ± 0.2 Ga	U-Pb	Davls & Sutcliffe (1984)
----- <u>Intrusive Contact</u> -----				
Sibley Group	Kama Hill Formation			
	Rossport Formation	1.345 ± 0.033 Ga	Rb-Sr	Franklin (1970) recalculated
	Pass Lake Formation			with $\lambda = 1.42 \times 10^{-11}$
----- Unnamed period of mild deformation and metamorphism -----				
		1.6-1.7 Ga		Sims & Morey (1972)
----- Penokean Orogeny -----				
		1.85 Ga		Sims & Morey (1972)
----- <u>Unconformity</u> -----				
Animikie Group	Rove Formation	1.57 Ga	Rb-Sr	Peterman (1966)
		1.556 ± 0.064 Ga	Rb-Sr	Franklin (1978)
	Gunflint Formation	1.6 ± 0.5 Ga	K-Ar	Hurley <u>et al.</u> (1962)
		1.63 ± 0.024 Ga	Rb-Sr	Kovach & Faure (1969)
		2.08 ± 0.25 Ga	Sm-Nd	Stille & Claire (1986)
----- <u>Unconformity</u> -----				
Archean Terrane				

the carbonate is primary and the siliceous component is due to diagenetic processes (Shegelski, 1982).

Goodwin (1956) divided the Gunflint formation into the five following members, from bottom to top: basal conglomerate, algal chert, shale, taconite, and upper limestone. The five members are found twice in the geological record and are separated by an argillaceous unit. He interpreted this as a cyclic deposition and divided the formation into an upper and lower Gunflint. More recently Shegelski (1982) suggested that the Gunflint facies are lensoidal in shape and interfinger, inferring a more complex stratigraphy than presented by Goodwin. The upper limestone unit has a gradational contact with the overlying Rove Formation.

The Rove Formation in the Thunder Bay area consists of grey to black pyritic argillite with a thickness of up to 600 m. Morey (1969) divided the Rove Formation into three facies, from bottom to top: basal black pyritic shale, transitional interbedded argillite and greywacke, and a top of quartz-rich greywacke with minor interbedded argillite. The Rove Formation shows some primary structures such as cross bedding and graded beds.

Shegelski (1982) noted that the Rove Formation may be the lateral equivalent to the Gunflint Formation, as

well as lying stratigraphically above it. So the contact between the Rove and the Gunflint Formation is very gradational. The interfingering of the various lithologies results in very rapid lateral facies changes. Morey (1969, 1972) noted that the paleocurrent directions for both the Rove and the Gunflint Formations indicate that the source area was the Archean terrane to the north.

The Animikie Group in the Thunder Bay District has undergone various methods of radiometric age determinations. The Rb-Sr and K-Ar ages cluster around 1.6 Ga (Peterman, 1966 , Franklin, 1978 , Hurley *et al.*, 1962, Kovach & Faure, 1969). This age probably represents a mild deformation and metamorphism that occurred around 1.6 - 1.7 Ga (Morey, 1972). During this event the Rb-Sr and the K-Ar systems were reset and give the age of metamorphism. The Sm-Nd technique provide a older age of 2.08 ± 0.25 Ga (Stille & Clauer, 1986). This is considered to be much closer to the true age of the Animikie Group than the 1.6 Ga ages. The relative immobility of REE under metamorphic conditions, allowed the Sm-Nd method to approach the true age of the Animikie Group, while Rb-Sr and K-Ar methods date a later metamorphic event (Table 1-1).

The Paleohelikian terrane is made up of the Sibley Group. The Sibley Group unconformably overlies the Rove Formation and, in places, the Archean basement. Franklin

(1970) presented a Rb-Sr age for the Sibley Group of 1.345 ± 0.033 Ga. This Group is made up by the Pass Lake, Rossport, and Kama Hill Formations. These formations consist of red bed sequences that were deposited under hypersaline conditions and are believed to occupy the failed arm of the Keweenaw intracratonic rift system (Franklin et al., 1980). The Keweenaw rift was initiated as a series of axial faults, which focussed local sedimentation and magmatic activity.

The Neohelikian terrane is made up of the Osler Group and various basic intrusions. The Osler Group is a series of subaerial volcanic rocks with minor interlayered sediments. These volcanics are continental tholeiitic flood basalts, displaying features of subaerial eruption (Wallace, 1981). The flows average 25 m thick but attain thicknesses of 75 m.

Intruded contemporaneously with the Osler Group's deposition are the Logan sills, Pine River-Mount Mollie gabbro, and the Pigeon River dikes. The Logan sills are typically 10-25 m thick in the Thunder Bay area, but they reach thicknesses of over 50 m in the Lake Nipigon area (Franklin et al., 1986). The composition of the Logan sills is quartz tholeiitic; however, many sills have a granophyre phase near the upper contact of the sill and the host. The granophyre phase has been attributed to assimilation of

underlying granitic material (Blackadar, 1956). The Logan sills are characterized by their reversed magnetic polarity (DuBois, 1962). The Osler Group and associated intrusives have several radiometric ages. The results indicate that the Logan sills were intruded at approximately 1 Ga (Davis and Sutcliffe, 1984; Table 1-1).

The Pigeon River dikes are a series of northeast-trending dikes, which are seen to cross cut the Logan sills. They are characterized by normal magnetic polarity (DuBois, 1962). The Pine River-Mount Mollie gabbro consists of dikes and a funnel-shaped intrusion at Crystal Lake. This is the youngest of the intrusions, and the dikes are east-trending anorthositic to quartz gabbro in composition. The Pine River-Mount Mollie gabbro, as with the Pigeon River dikes, has a normal magnetic polarity (DuBois, 1962).

The Proterozoic sequence north of Lake Superior has undergone very little deformation in its history. The Animikie Group has gentle dips of 2°-10° towards the axis of the Keweenawan Synclinorium (fig 1-1; Franklin, 1982). The Animikie Group is cut by two groups of arcuate, northeasterly trending faults. The northern group of faults host the Mainland Belt of silver veins, and the southern group hosts the Island Belt of veins. These are listric, normal faults related to the development of the Keweenawan

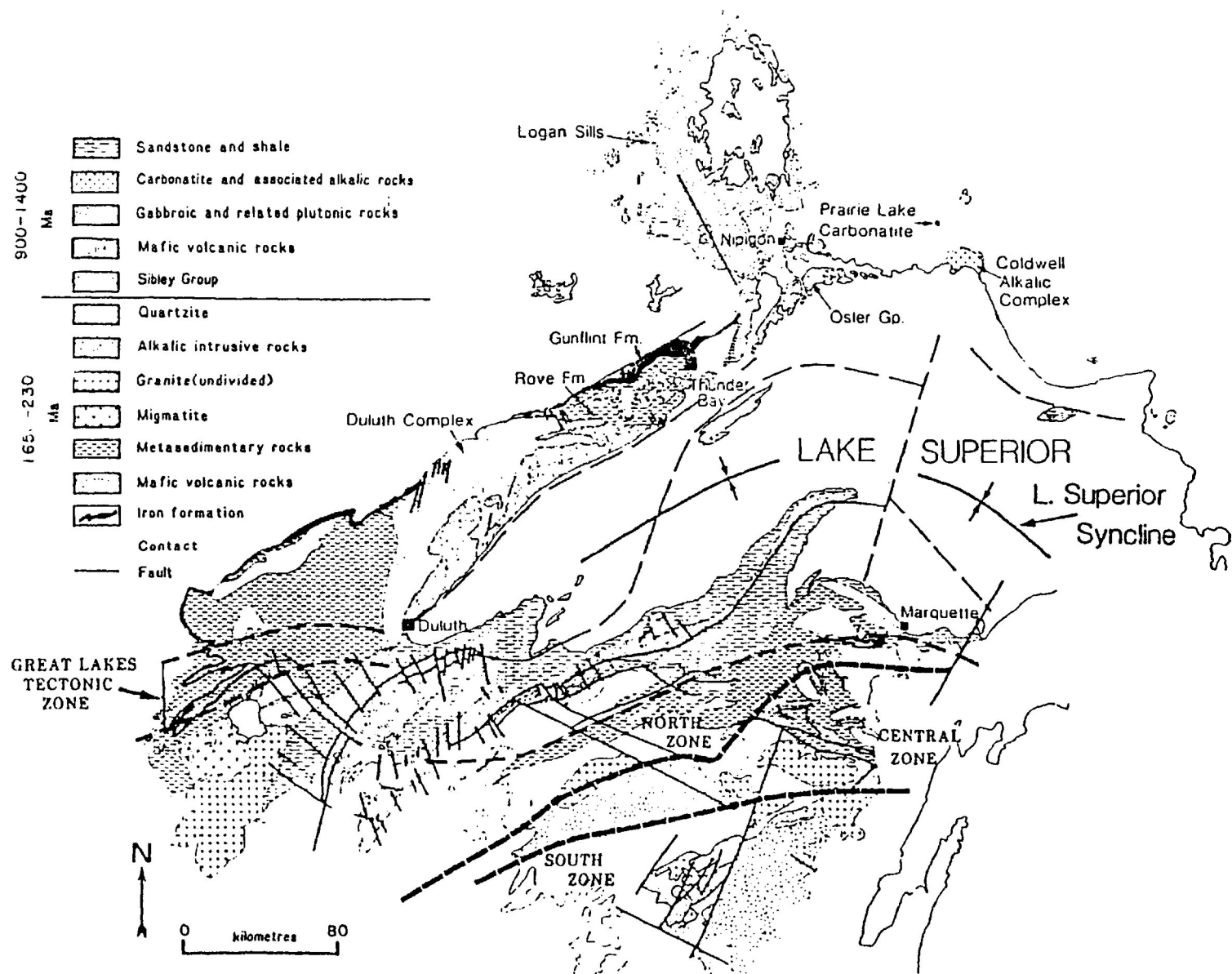


Figure 1-1. Geology of the Lake Superior Syncline
(from Franklin, 1982)

rift basin (Franklin et al., 1986). These faults were initially extensional normal faults formed by the development of the Keweenaw Rift Basin. After formation, the basin underwent slight compression, which resulted in the faults being reactivated as reverse faults (Franklin et al., 1982). It is these faults that host the silver veins and channeled diabasic and gabbroic hypabyssal intrusions.

Thunder Bay Silver District

The Thunder Bay silver district is divided into three distinct zones, the Port Coldwell veins, the Island Belt, and the Mainland Belt (fig. 1-2; Franklin et al., 1986).

Port Coldwell veins

The Port Coldwell veins are located in the Abitibi-Wawa Subprovince of the Superior structural province. The host rocks are metavolcanic - metasedimentary sequences with intrusive metagabbros. These rocks are cut by intrusions such as the Terrace Bay Batholith, Coldwell Alkaline Complex and various diabase dikes. Kissin and McCuaig (1988) have suggested, based on a recent fluid inclusion and stable isotope study, that the Dead Horse Creek North and South and the Morley High Grade occurrences

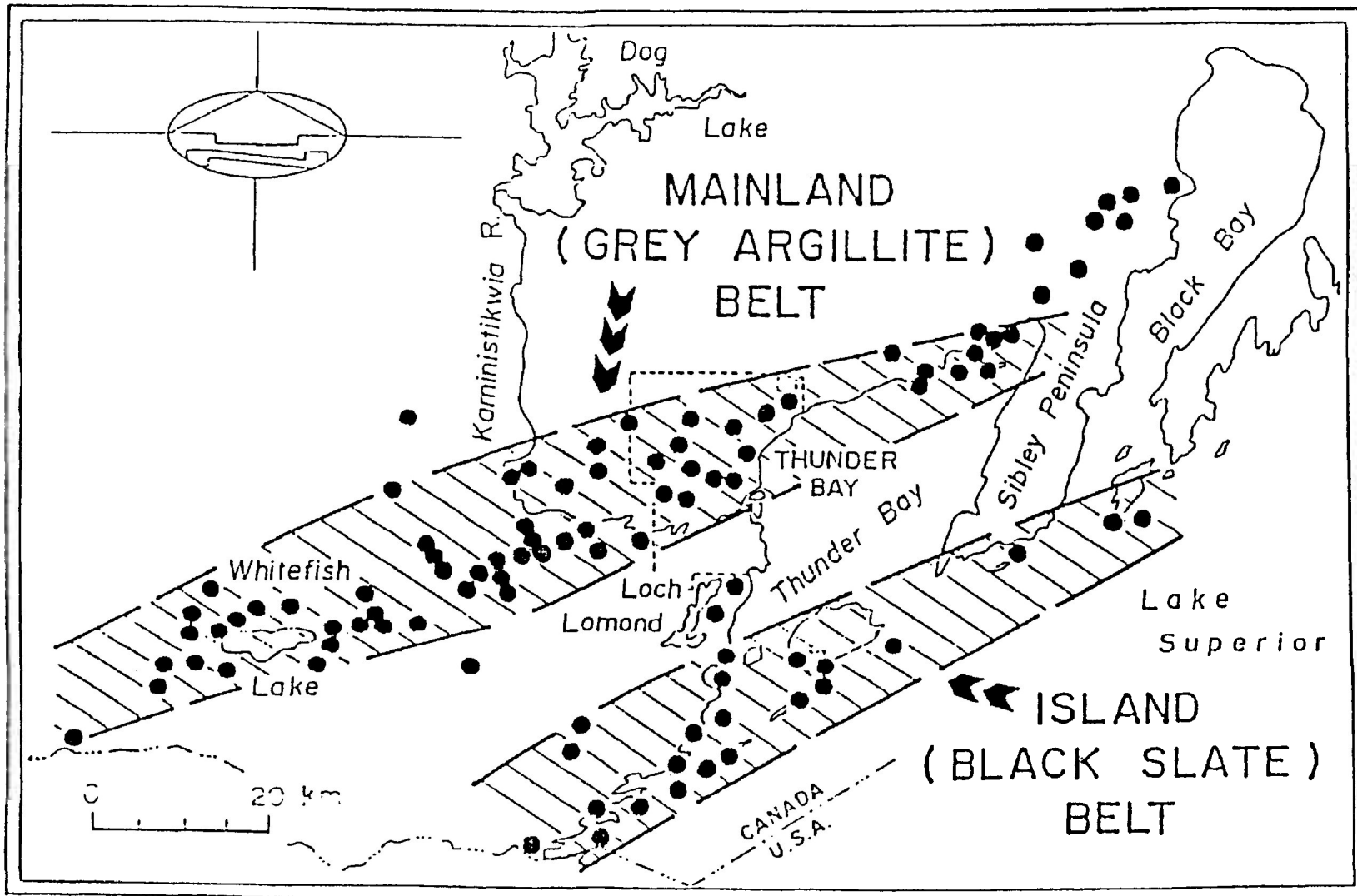


Figure 1-2. Two belts of silver veins according to Oja (1967) and Bowen (1911, in parentheses). Dots indicate vein locations after Tanton (1931)

are genetically related to the Proterozoic veins of the Thunder Bay area.

Island Group

The Island Belt of veins are spatially associated with a northeasterly trending swarm of Pigeon River dikes. These dikes form a broadly linear belt from the tip of Sibley Peninsula to the Pigeon River. The Island Belt veins are hosted in the Rove Formation, as well as in the local mafic intrusions. The veins of the Island Belt were most productive, if they were hosted by gabbroic dikes (Franklin et al., 1986).

The mineralogy of the Island Belt is quite complex. The vein mineralogy varies between simple, barren, base-metal veins to very complex five-element suites (Ag-Bi-Ni-Co-As) as found at Silver Islet (Smyk, 1984).

The country rock into which the Pigeon River dikes were intruded has been intensely metamorphosed. Large xenoliths of shale have been rafted into the gabbro (up to 15 m in length and 2 m in width). The shale adjacent to the dikes has been metamorphosed to pyroxene-hornfels and for up to tens of meters to hornblende-hornfels (Franklin, 1970).

Mainland Group

The Mainland Group of veins, the largest of the three groups, occupies a northeasterly trending series of normal faults. The veins are found cutting all the rocks of the local Proterozoic sequence; however, significant silver values are found only within the upper thirty meters of the Rove Formation. The veins are widest and carry the greatest silver values when they are hosted in the Rove shale immediately underlying a diabase sill. Outside this zone veins often lose their tenor. Three of the veins extend for significant distances into the Archean terrane (Tanton, 1931), but they are narrow and barren at depth.

The mineralogy of the Mainland Belt is generally quite simple. The mineralogy ranges from base metal-silver veins to barren veins with only trace amounts of sulfides. No veins of the five-element assemblage have been found in the Mainland Belt, although arsenides are found in the Beaver Junior Mine (Cole, 1978), and cobalt-bearing minerals were reported by Tanton (1931).

The veins are generally hosted in the Rove shale, but in some instances the veins extend upwards into the diabase. In these cases the veins narrow and pinch out within several meters of entering the sill. Alteration of the host rock is dominantly silicification of the host

shale. The silicification of the host rock generally is restricted to half the vein's width. Where the vein is hosted by diabase the alteration has been restricted to several centimeters and consists of chloritization of pyroxenes, and saussuritization of feldspars (Franklin et al., 1986). The effect of contact metamorphism from the Logan sills is much less than the effect on the Island Belt. Adjacent to the diabase intrusives illite has been metamorphosed from 1 m to 2 m, and pyrite has been metamorphosed to pyrrhotite (Franklin, 1970).

The vein systems occupy extensional normal faults. Hydrofracturing resulting in large horizons of country rock being rafted into the vein gangue is very common but restricted to the early phase of vein material. Deformation in the country rock is minor, restricted to drag folds found in the Porcupine Mine (Franklin et al., 1986). The faulting is not limited to one event. Many of the veins show evidence of multiple fracturing and renewed deposition of vein material (Jennings, 1986).

Proposal

The purpose of this study is to examine several of the Mainland veins in detail. The veins studied occur at the Shuniah Mine, the Porcupine Mine and the Keystone Mine (fig. 1-3). These veins were selected because of available drill core. With this core, the third dimension to the system will be observed and hopefully provide some insight on vein genesis. The Thunder Bay Mine was also included in the study due to its proximity to the Shuniah. The work on the Thunder Bay Mine involved only surface samples.

The study involves fluid inclusion analysis with close attention to the vein paragenesis. This will allow the thermal and chemical evolution of the vein-forming fluid to be described both with paragenesis and with depth. A stable isotope study will define the probable origin of the vein fluids and their constituents. Using all the information obtained a genetic model for the formation of the silver veins will be proposed.

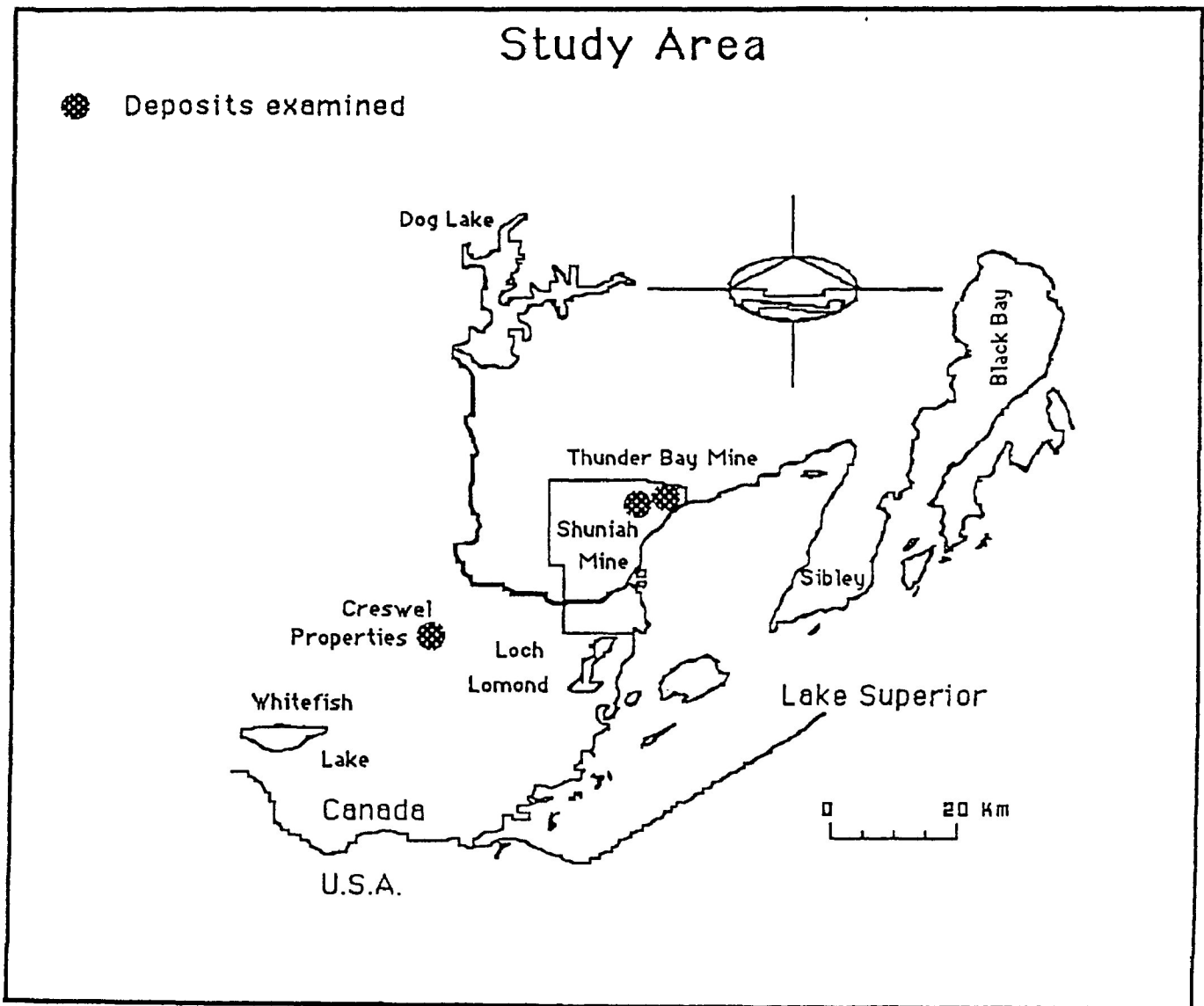


Figure 1-3. Study area showing the mines examined. The Porcupine and the Keystone Mines are located in the area labeled Creswel Properties.

Methodology

Fluid Inclusion Study

Double polished sections used in this fluid inclusion study were prepared at Lakehead University. A cold mounting technique (Appendix Two) was used to minimize heating of the sample during preparation. The technique prevents samples from being heated above 30°C, thus preserving the integrity of the fluid inclusion.

The fluid inclusion study was carried out at Lakehead University using an U.S.G.S. gas flow heating/freezing stage, mounted on a Leitz Orthoplan polarizing microscope. Heating and freezing runs were conducted by passing heated or cooled nitrogen gas over the sample. Heating of the nitrogen gas was achieved by passing the gas through a heating coil mounted in a quartz tube. Temperature control was achieved by a rheostat which controlled the current flow through the coil. Cooling of the nitrogen gas was achieved by bubbling the gas through liquid nitrogen. This system gives the microthermometric stage a range of -180°C to 600°C.

Temperature measurements were made by a thermocouple placed on the sample near the inclusion of

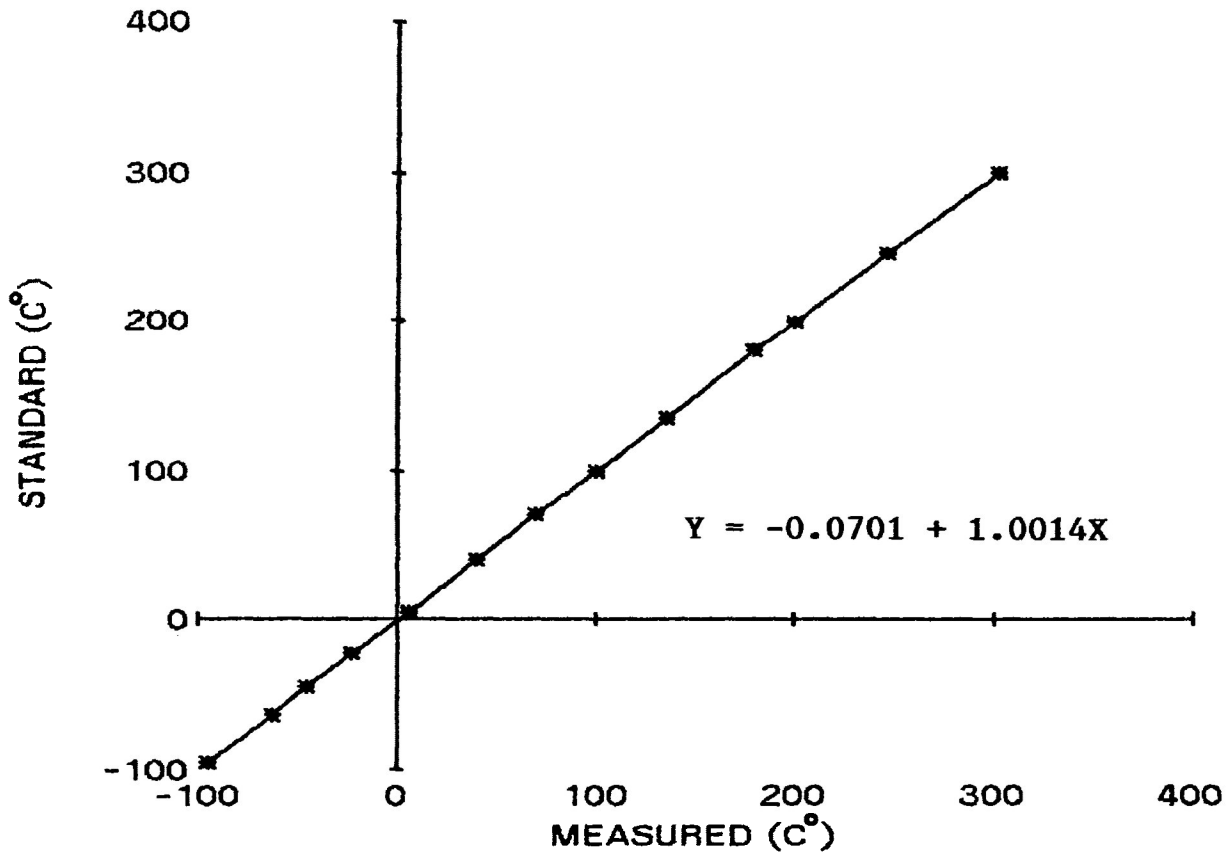
interest. Calibrations of the thermocouple were made by heating/freezing materials with precisely known melting and freezing points. Two calibrations were completed during the course of this study, one in January 1988, and the other in September 1988. The calibration curves presented in figure 2-1 and 2-2 show that instrumental error in the data is less than 2°C and generally less than 0.5°C with the error randomly distributed in the temperature range.

Initially, freezing runs were performed to avoid stretching or otherwise damaging the inclusion during homogenization, which would lead to invalidation of subsequent freezing data. Generally, the inclusions were supercooled before they would freeze. The inclusions were then heated until a first melt was observed in the inclusion. This temperature indicates the eutectic temperature for the fluid. The inclusions were further heated until all the ice melted. This temperature was recorded, and using the equations from Potter et al. (1978), the salinity in equivalent weight percent NaCl was calculated.

The inclusions were heated until they homogenized to a single phase, either a liquid or a vapor. This is the temperature of homogenization of the inclusion.

CALIBRATION JANUARY 1988

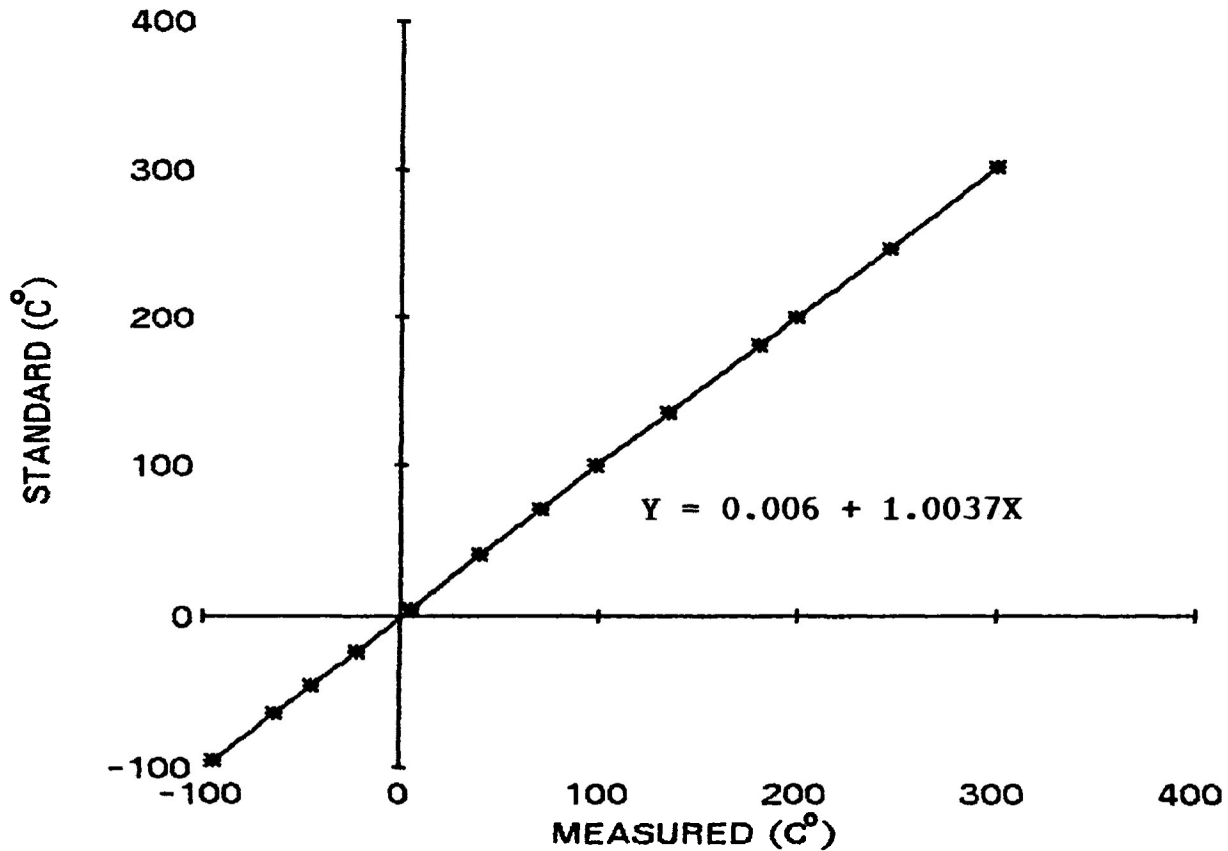
Figure 2-1



<u>Calibration Standard</u>	<u>Standard (C°)</u>	<u>Measured (C°)</u>
Toluene	-95.0	-94.9
Chloroform	-63.5	-63.0
Chlorobenzene	-45.6	-45.6
Carbon Tetrachloride	-23.0	-23.0
Benzene	5.0	5.5
Merck 9640	40.0	39.9
Merck 9670	70.0	69.5
Merck 9700	100.0	99.5
Merck 9735	135.0	135.6
Merck 9780	180.0	179.7
Merck 9800	200.0	200.0
Merck 9840	247.0	246.1
Omegalag	302.0	302.0

CALIBRATION SEPTEMBER 1988

Figure 2-2



<u>Calibration Standard</u>	<u>Standard (C°)</u>	<u>Measured (C°)</u>
Toluene	-95.0	-94.4
Chloroform	-63.5	-63.4
Chlorobenzene	-45.6	-45.5
Carbon Tetrachloride	-23.0	-22.7
Benzene	5.0	5.1
Merck 9640	40.0	39.9
Merck 9670	70.0	70.1
Merck 9700	100.0	97.8
Merck 9735	135.0	134.8
Merck 9780	180.0	180.1
Merck 9800	200.0	198.9
Merck 9847	247.0	246.5
Omegalaq	302.0	300.7

Only primary inclusions were tested in this study. If the inclusion showed evidence of being secondary or pseudosecondary (Roedder, 1984), the inclusions were not used. Also, if the inclusion showed evidence of fracturing or necking down, it was ignored.

Quite often a section would have several usable inclusions. Usable inclusions were two-phase inclusions larger than 0.01 mm with good, clear observation qualities. In sections with numerous inclusions the section could be heated only once to its homogenization temperature. Otherwise, there was a danger of stretching or decrepitating the inclusions. However, often several inclusions were observed in one field of view, allowing for several homogenization temperatures to be obtained during one heating run.

The stretching behavior of inclusions in the various host minerals was tested during this study in order to test the validity of the experimental procedure. Fluid inclusions in calcite, fluorite and quartz were heated 50 % past their homogenization temperatures. The inclusions were then cooled until the vapor bubble reformed, then they were reheated. The inclusions in quartz showed little change in homogenization temperature indicating little effect of stretching. The inclusions in calcite and fluorite showed an average of 15 % increase in homogenization temperature. This

indicates a strong effect of stretching due to overheating on the inclusions hosted in calcite or fluorite.

The rate of heating of the sample was about 1-2°C per minute. This allowed for accurate measurements, and it allowed the sample to thermally equilibrate with nitrogen gas.

Stable Isotopes

The stable isotope analyses were conducted by Kreuger Enterprises Inc., Geochron Laboratories Division, Cambridge, Massachusetts. Fourteen samples of calcite were analyzed for both $\delta^{13}\text{C}$ and $\delta^{18}\text{O}$, and one sample of quartz was analyzed for $\delta^{18}\text{O}$. Two samples of illite were analyzed for $\delta^{18}\text{O}$ and δD . Four samples of graphite were analyzed for $\delta^{13}\text{C}$. For each of the samples a fluid inclusion homogenization temperature was obtained.

The homogenization temperature allowed the fractionation factors to be calculated between for the mineral and vein-forming fluids. The fractionation factor is expressed as

$$1000 \ln \alpha_{A-B} = \Delta_{A-B} = \delta_A - \delta_B$$

where $\Delta_{A-B} = R_A/R_B$ R is the ratio of heavy (rare) to light (common) stable isotopes (Kyser 1987).

The fractionation factor between calcite and water that was applied in this study is a revised version of O'Neil et al. (1969) reported by Changkakoti et al., (1986 a). This takes into account the revised equilibrium constant between CO₂ and H₂O and is expressed as:

$$1000 \ln \alpha_{\text{calcite-water}} = 2.78(10^6/T^2) - 2.89$$

Application of this equation indicates the value of $\delta^{18}\text{O}$ for the water from which calcite precipitated. Similarly the Deines et al. (1974) equation:

$$1000 \ln \alpha_{\text{calcite-HCO}_3} = 0.095(10^6/T^2) + 0.9$$

calculates $\delta^{13}\text{C}$ for the aqueous carbon species HCO₃⁻. An additional fractionation factor was used for dolomite-water.

$$1000 \ln \alpha_{\text{dolomite-water}} = 3.06(10^6/T^2) - 3.24$$

(Matthews and Katz, 1977)

To calculate the fractionation between quartz and water the equation of Clayton et al. (1972) was used:

$$1000 \ln \alpha_{\text{quartz-water}} = 3.38(10^6/T^2) - 3.4$$

To calculate the deuterium fractionation between water and illite, the illite-water fractionation was assumed to be the equivalent of the fractionation between smectite and water, as described by Kyser (1987). The fractionation is:

$$1000 \ln \alpha_{\text{illite-water}} = -19.6(10^3/T) + 25$$

Yeh (1980)

The oxygen fractionation between illite and water is described by Eslinger & Savin (1973) as:

$$1000 \ln \alpha_{\text{illite-water}} = 2.43(10^6/T^2) - 4.8$$

Solution composition can have an effect upon the mineral-water fractionation (Taylor, 1967; Truesdell, 1974). Saline hydrothermal waters are generally depleted in D and ^{18}O . This is caused by the tendency of some cations to hydrate in solution with the isotopically heavier water molecules, which leaves the free water that equilibrates with the minerals depleted in D and ^{18}O (Field and Fifarek, 1985). However the mineral-brine fractionations are uncertain, and the brines in this study are mixed solutions of NaCl, MgCl₂ and CaCl₂, for which no studies has been done. For these reasons no correction for any solute effects was considered.

Four sample of graphite were analysed for $\delta^{13}\text{C}$, two from the Thunder Bay Mine area and two from Silver Islet

grab samples. One sample was from the Thunder Bay Mine wallrock, and the other was from the Rove Shale-diabase contact, which was isolated from any hydrothermal activity. Two samples of graphite from Silver Islet grab samples were also analyzed. The objective of this was to determine the origin of the graphite and to see if the graphitic wall rock could have acted as a source for the carbon in the carbonate.

X-Ray Diffraction Techniques

X-ray diffraction techniques were used to quantitatively identify unknown minerals. On a sample from the Silver Mountain Mine a pinhole X-ray photograph was made. The sample was powdered and mounted on a cellophane sheet. The sample was then exposed to $\text{CuK}\alpha$ radiation ($\lambda = 1.54178 \text{ \AA}$) using a nickel filter. The pattern obtained indicated that the sample was 2 M illite.

A Gandolfi and a pinhole X-ray photograph were made of a mineral collected from the Shuniah vein system. The pinhole technique was applied first, as described above. This indicated that the sample is possibly wavellite, but the camera's resolution of the smaller d-spacings was insufficient for complete identification. A Gandolfi camera x-ray photograph was then made of the sample. The sample was

mounted on a glass fiber and placed in a small (28.65 mm) camera. A fine (0.4 mm) collimator was used to minimize background radiation. The sample was exposed for 6 hours to CuK α radiation ($\lambda = 1.54178 \text{ \AA}$). The negative was developed, and the spectrum was measured using a KD-540 microphotometer optical film measuring device. The d-spacings were calculated and compared to the standards (Selected Powder Diffraction Data for Minerals Search Manual, Joint Committee on Powder Diffraction Standards, 1974). The sample was tentatively identified as wavellite; all d-spacings are tabulated in appendix three.

Port Arthur Group

(map 3-1)

Shuniah Mine

History

The history of the Shuniah Mine is summarized from Ingall, (1888) and Tanton, (1931) unless otherwise referenced. The vein system that makes up the Shuniah Mine was discovered in May of 1867 by George McVicar. During the following winter the vein was exposed by trenching performed by the Thunder Bay Company. Two shafts were sunk, one to forty feet and one to sixty feet; the latter shaft had a cross-cut to the vein. The mine had yielded up to this point several barrels of rich ore; however, due to disagreements within the company the mine was closed down.

In 1870, an American company purchased the mine for \$ 75 000, and the mine was reopened. The new owners sank the main shaft to 135 feet and drove an exploratory cross cut south for approximately 100 feet in hope of intersecting another vein system. In the summer of 1873, the mine was again closed down.

In November of 1873, the mine was reopened under the name of the Duncan Mine. Development of the mine continued more or less continuously until 1881. This period of operation included further underground development, the construction of a ten-stamp mill and four Frue vanners. A

map 3-1

geology and location map for the
Port Arthur Group

new technology at the time was diamond drilling, and a drilling program was started for the Duncan Mine. The resulting core from the project is the oldest known in Canada. By the time the mine closed in 1881, the shaft and underground development totaled 2500 to 3000 feet (Resident Geologist M.N.D.M. files, updated 1986) and diamond drilling resulted in 4884 feet of core (fig. 3-1 and 3-2).

In 1921 and 1922 attempts to reopen the mine occurred. Eleven cross cutting trenches were dug following the vein for a quarter of a mile east of the main workings. No additional ore was recovered. The property has lain idle since. Presently the property is patented land for both surface and mining rights and is owned by the City of Thunder Bay (Resident Geologist M.N.D.M. files, updated 1986).

The Shuniah Mine was not a very profitable undertaking, as no silver ore was found below the upper seventy feet of the workings. However, as is typical of these deposits, the ore when it was found was extremely rich, but the cost of the development far exceeded the value of the ore obtained. It is reported that the ore averaged two hundred to three hundred ounces per ton of silver, and the total production amounted to \$ 50 000 with silver valued at one dollar per ounce (Resident Geologist M.N.D.M. files, updated 1986). The total cost of development was \$500 000.

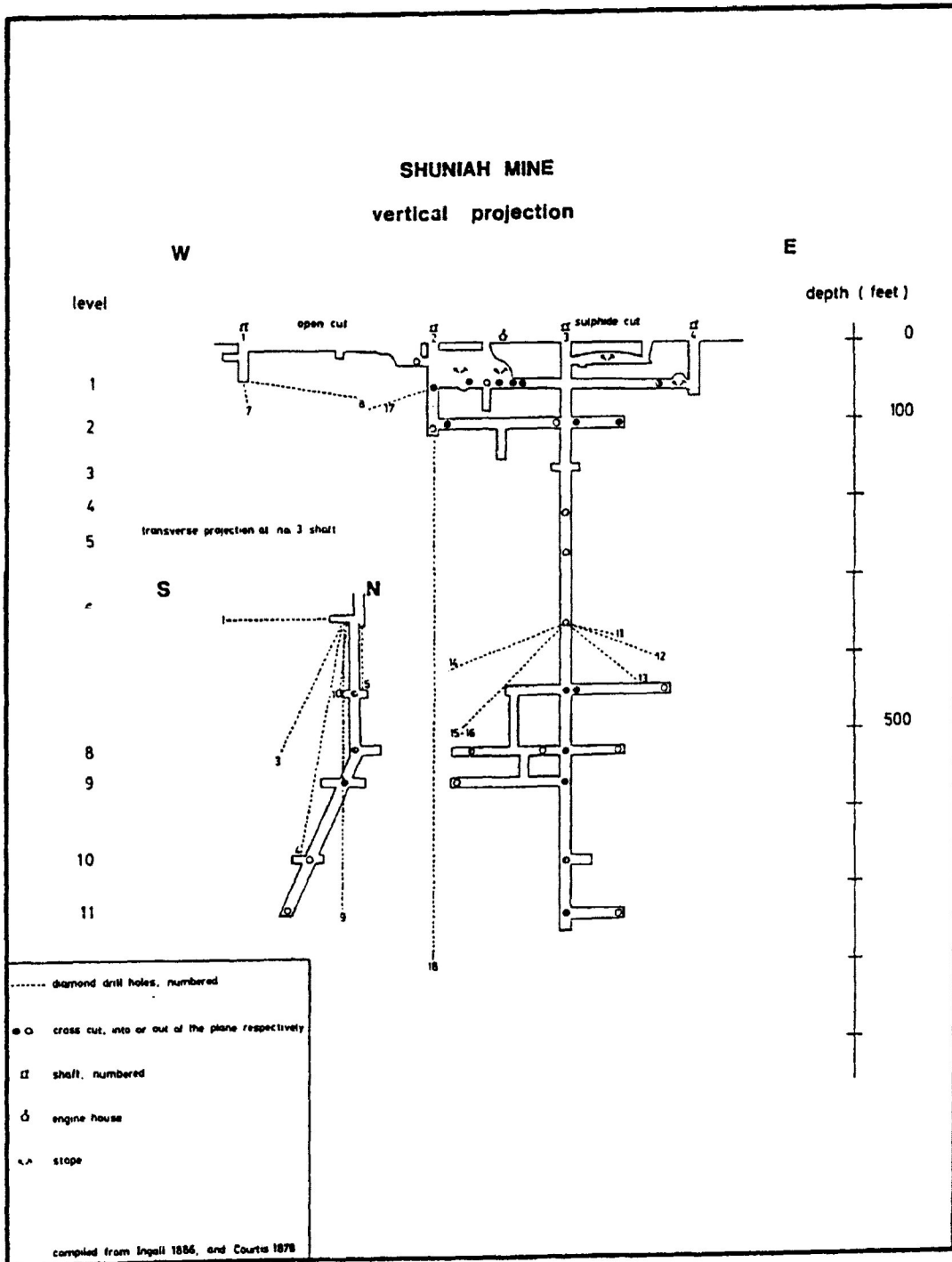


Figure 3-1. Vertical projection of the Shuniah Mine, showing the orientation of the diamond drill holes.

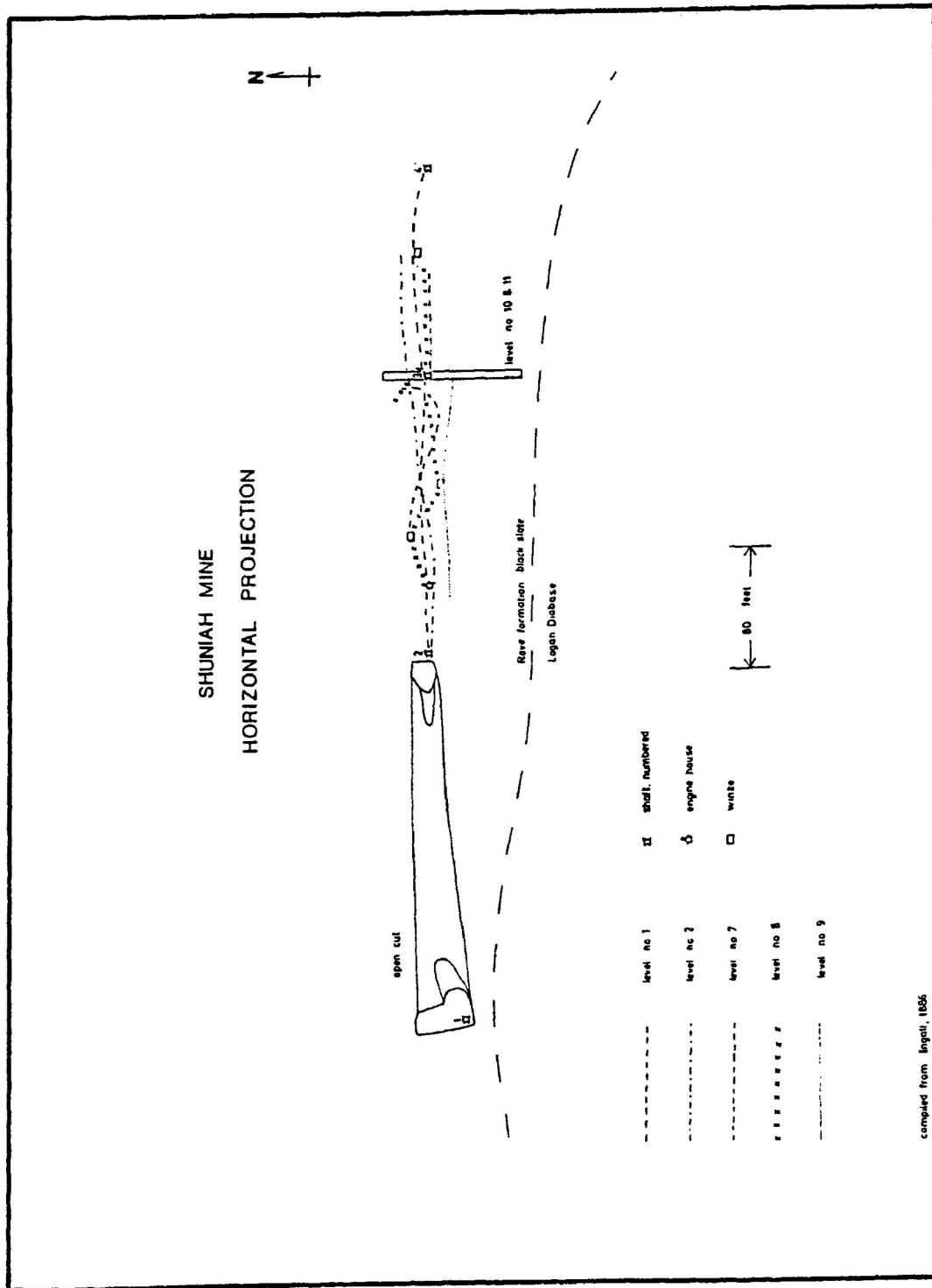


Figure 3-2. Horizontal projection of the Shuniah Mine

Geology

Much of the geological data of the Shuniah Mine comes from the efforts of W.M. Curtis who was the mine manager for a period of time. It was his instigation that led to exploration by diamond drilling, and it was also due to his foresight that the core was sampled for future work. The core that is available is not complete it is only samples of the core. For this reason it was not possible to log the core and the geology of the mine must be taken from previous workers. Most of the geology reported by Ingall (1888) is from the previous work of Curtis.

The Shuniah vein strikes east west and has a subvertical dip to the south. The width of the main vein is 20 to 30 feet with numerous stringers originating from the footwall and striking parallel to the vein. The smaller fissures appear to have an anastomosing nature with the main or Champion vein. The smaller fissures are anywhere from a few inches to several feet in width. It is these smaller veins that carry the bulk of the silver ore (fig. 3-3). The main vein contains silver values only where the smaller veins intersect it (Curtis, 1887).

The silver ore is very localized, occurring in pods with barren ground between the ore zones. The veins have a very brecciated nature and contain numerous horses of country rock. In this brecciated zone, silver is often found

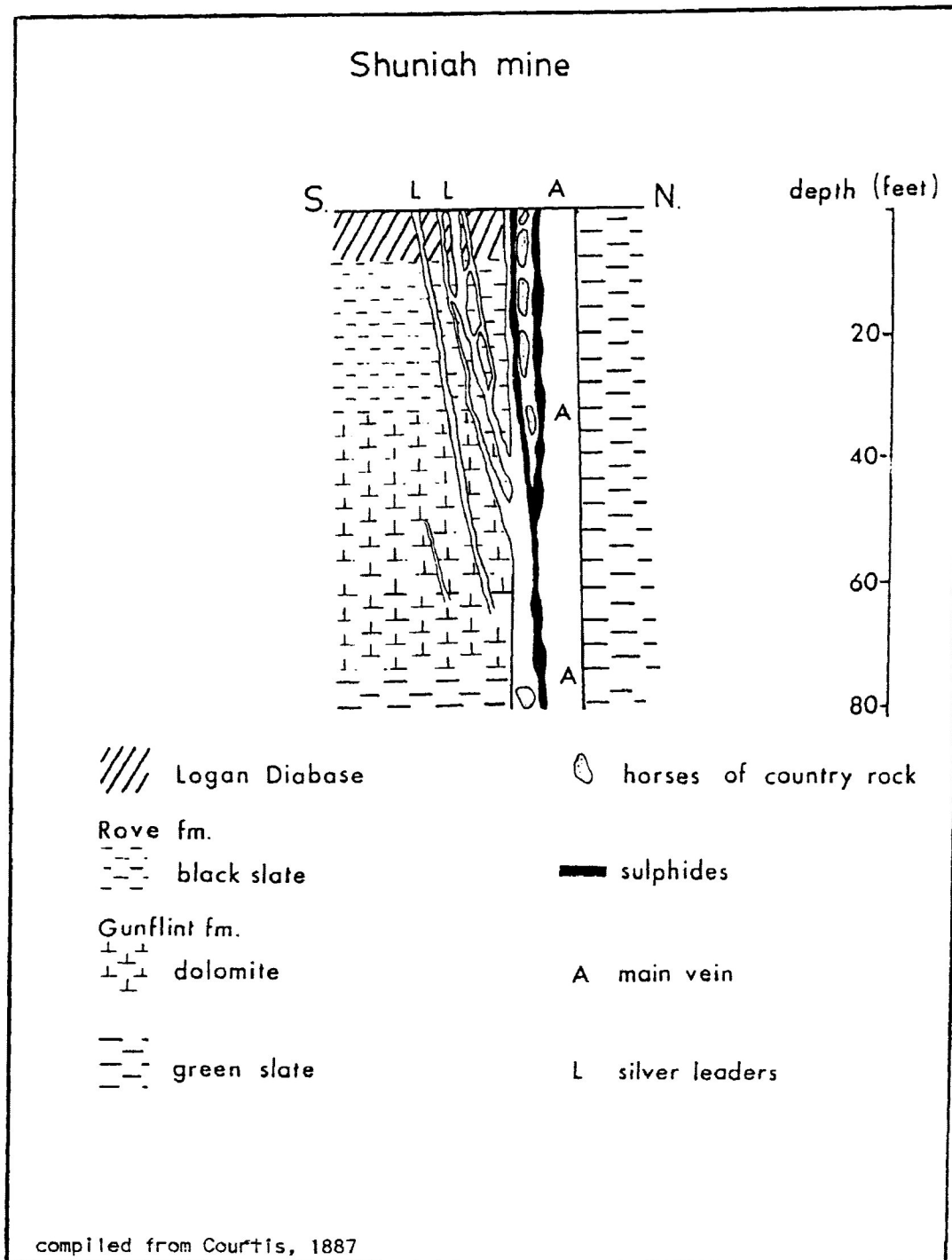


Figure 3-3. Generalized cross section of the upper portions of the Shuniah Mine. Shows the anastomosing relationship of the ore bearing leaders with the main vein.

as argentite or in its native form. The brecciated country rock has been heavily silicified, even though the bulk of the vein is composed of carbonate. In the areas of the Shuniah Mine where the country rock is carbonaceous, rich pods of silver ore are invariably found.

The Shuniah vein is dominantly hosted within the Gunflint Formation. As shown in the cross section (fig. 3-4), the footwall is composed of Logan diabase overlying the Rove shale. The diabase forms the footwall at the No. 2 shaft down to the first level (eighty feet; Ingall, 1888). The underlying Rove shale is only approximately forty feet thick in this area. The strata of the Gunflint Formation then form the wallrock for four hundred eighty feet. The vein then enters the Archean terrane. The vein was sampled to one thousand feet by diamond drilling and found to be continuous and contain sulfides but no silver. The main difference found in the vein at depth, besides the lack of silver, is the change in the gangue mineralogy. The near-surface gangue is dominantly calcite with minor fluorite and quartz; below two hundred feet as estimated from core samples, the dominate gangue mineral is quartz.

The Shuniah vein occupies a normal fault, with an offset of one hundred feet, north side up (Courtis, 1887). The present investigation of the vein showed at least two, possibly three or more episodes of movement along the fault. This movement resulted in brecciation of the vein material

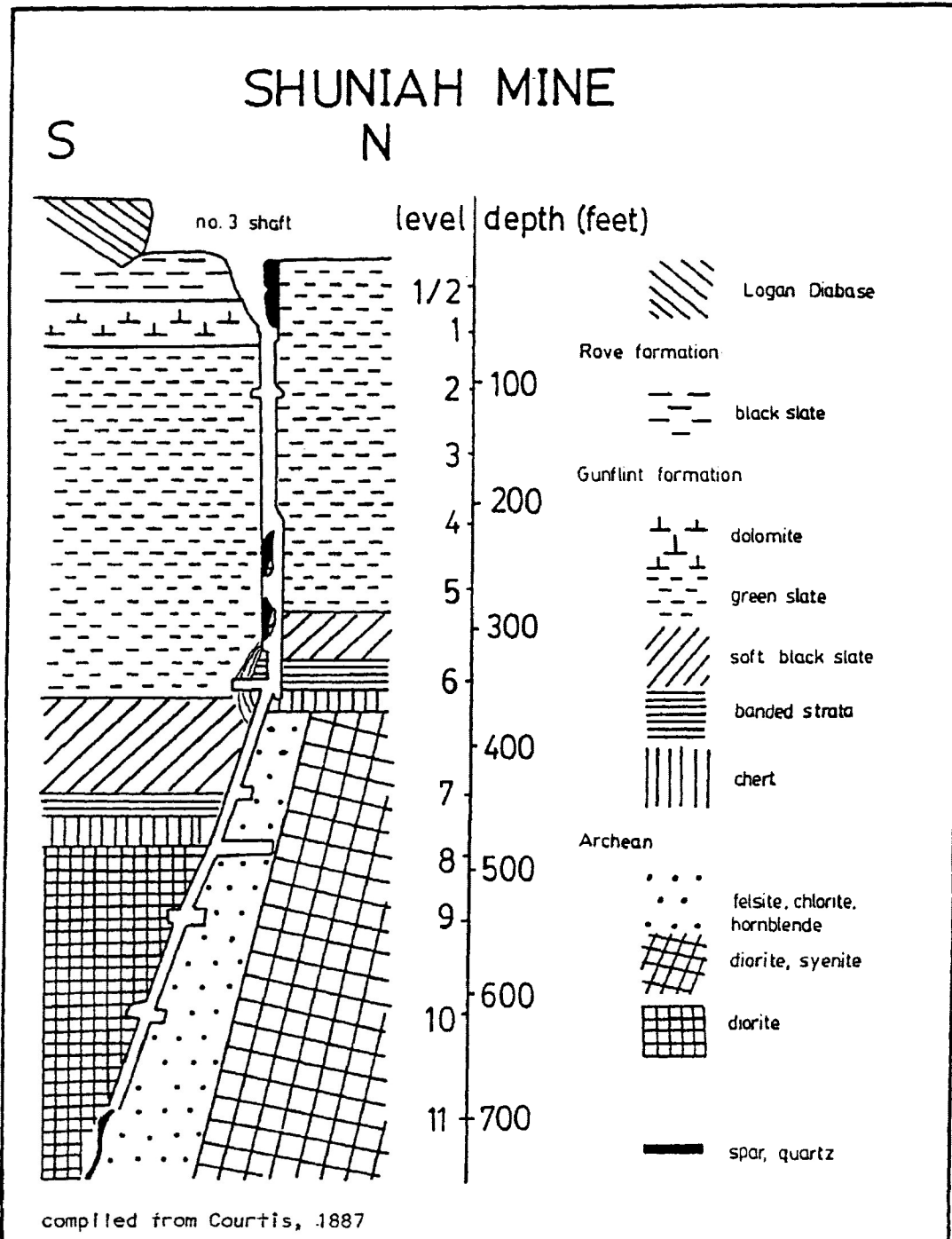


Figure 3-4. Cross section of the Shuniah Mine at shaft number three, shows the lithologies of the wall rocks.

and renewed hydrothermal activity. The host rocks were undeformed by the faulting, and the only effect the vein emplacement had on the surrounding rocks was intense silicification of the shale.

Thunder Bay Mine

(map 3-1)

History

The history of the Thunder Bay Mine is summarized from Ingall, (1888) and Tanton, (1931) unless otherwise referenced. The Thunder Bay Mine was discovered in the fall of 1866 by Peter McKellar and worked continuously until 1869, when it was closed. The work consisted of sinking four shafts, two to seventy feet, one to thirty-five feet and one to twenty-five feet. A cross-cut was driven northwest from the second shaft at the sixty foot level. In addition a road was built, for three miles down to the shore of Thunder Bay, where a stamp mill was constructed. The total production of the property was 3 294 lbs of ore valued at \$2 592.

In 1874, the mine was reopened for six months, with work performed on a subparallel vein to the southeast. This vein proved to be barren, and the mine has lain idle since that time. Presently, the property is patented land for both surface and mining rights and is owned by the City of Thunder Bay (Resident Geologist M.N.D.M. files, updated 1986).

Geology

The Thunder Bay vein is a network of anastomosing veinlets. Each veinlet is less than one foot wide, but the entire network is about ten feet wide. The vein system strikes 34° and dips steeply to the northwest. The vein material is mainly quartz with minor calcite, native silver, argentite, galena, pyrite and sphalerite. The silver ore is localized in streaks three to eighteen inches thick and six to forty feet in length (Tanton, 1931).

A second subparallel vein is located about twenty feet southeast of the silver-bearing zone. This vein averages between six and twelve feet wide and is composed mainly of coarse calcite (Tanton, 1931). Due to lack of outcrop this vein was not investigated during this project. This vein probably occupies the main fault zone, whereas the second, economic vein occupies a subparallel fracture system.

The host rock is diabase capping a sequence of black shale, impure dolomite and argillite. Interlayered with the sedimentary strata are small, subhorizontal layers of diabase (Ingall, 1888).

Joint Set Study

In November, 1987, a study of joint sets in the area around the Shuniah and the Thunder Bay Mines was undertaken. In this area (fig. 3-5) one hundred thirteen joint directions were measured from forty-four outcrops surrounding the Shuniah Mine.

Compilation of the data on a rose diagram (fig. 3-6) shows a wide scatter of data. When the data were plotted with respect to lithologies, pre- and post-diabase joint sets can be distinguished. Joint directions in the 280° to 290° and in the 30° to 40° ranges are well developed in the Animikie sedimentary rocks but are not developed in the diabase. These are interpreted as pre-diabase joint sets. The joint directions that range from 300° to 20° and 70° to 90° are well developed in both the diabase and the Animikie sediments. These joint directions are interpreted as post-diabase joint sets.

Although the data can be divided in this fashion, a wide scatter of the joint directions is still apparent. This indicates that the study area was not one continuous tectonic block; rather it was a series of smaller blocks that were rotated with respect to each other. The data can be divided and grouped geographically to delineate the tectonic blocks. It is assumed in this method that each individual block should have fairly consistent joint

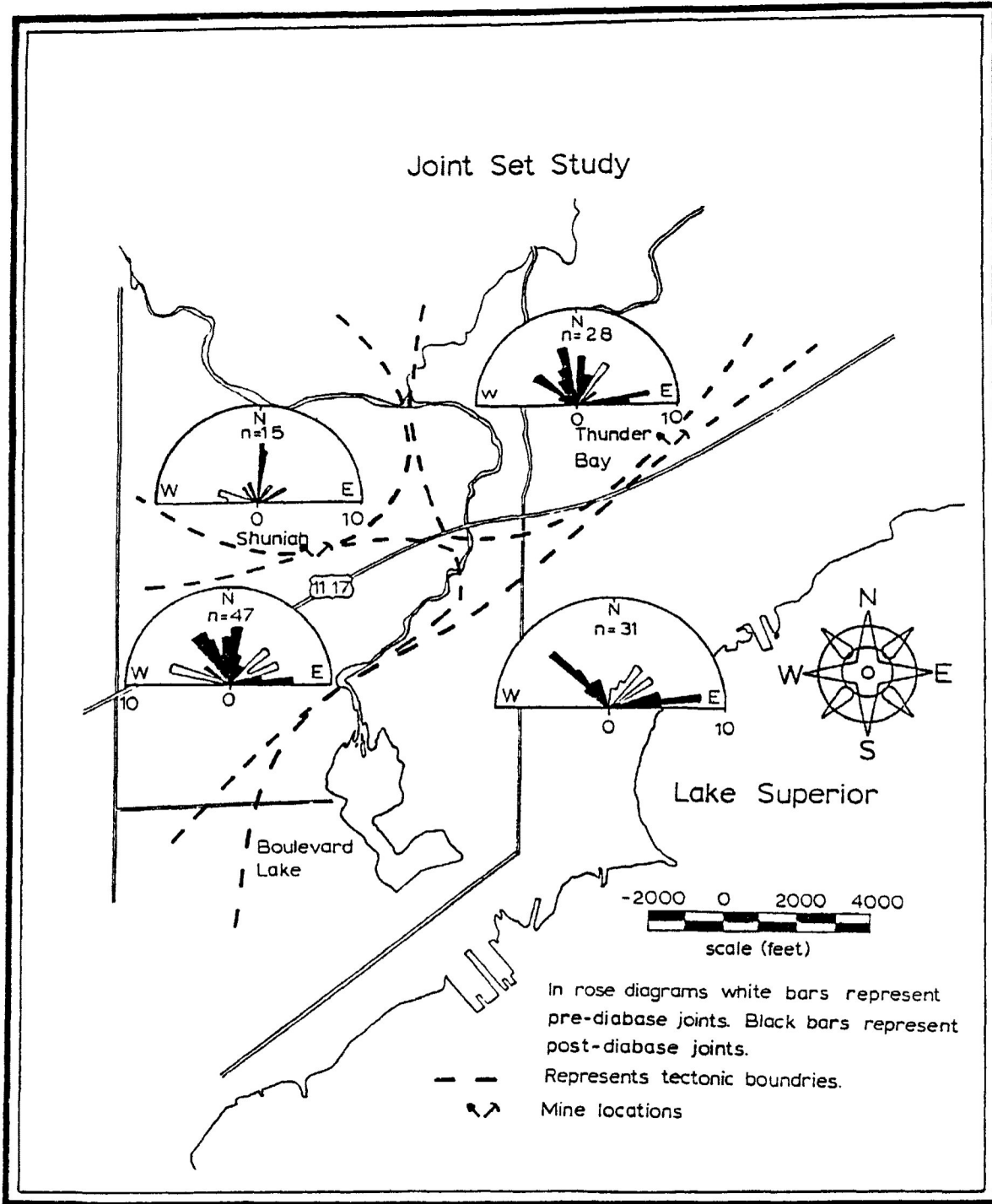


Figure 3-5. Area over which the joint set study was undertaken. Also shows the division of the study area into four tectonic blocks based on joint set analysis.

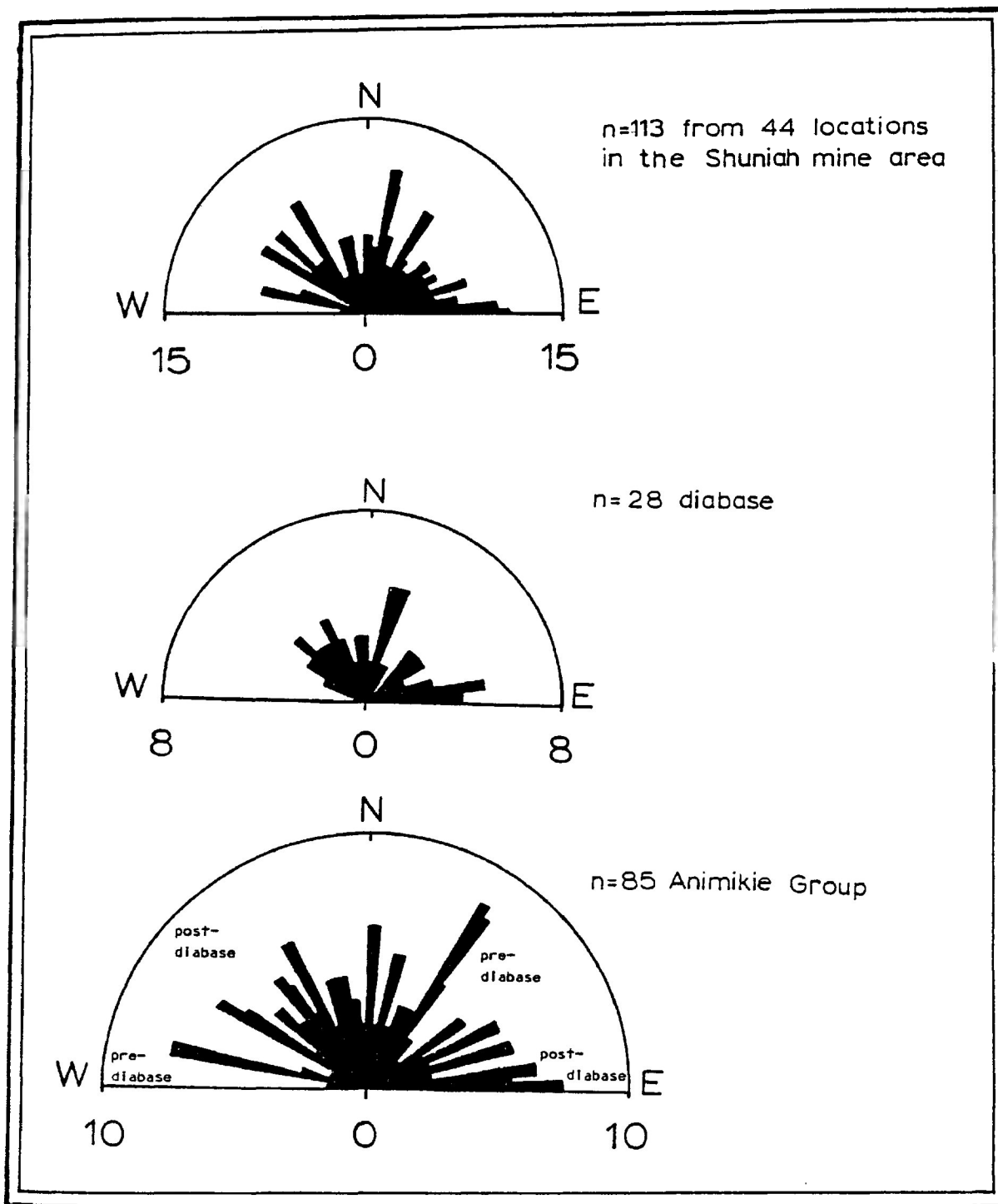


Figure 3-6. Compilation of joint set data from the Shuniah Mine area. Shows the division of the joint set data into pre- and post-diabase intrusion joint directions.

directions, but adjacent blocks will have different joint orientations due to differential rotation of the blocks. When the data were grouped by geography, four blocks were outlined within the study area (fig. 3-5).

An interesting observation is that both the Shuniah and the Thunder Bay Mines are located on the intersection of two blocks. In the other areas where the blocks intersect, veining is observed. This is not surprising, since the blocks must be fault-bounded, and the faults acted as conduits for vein fluids. This has interesting implications for prospecting; locating the block's boundaries with greater precision would identify excellent prospecting targets.

This study was hampered by a lack of outcrop in some areas. For a future project I would recommend that more joint measurements be taken and compiled with the existing data in order to further define the block margins.

Fluid Inclusion Study

Shuniah Mine

Fluid inclusion analysis were carried out on two hundred and fifteen inclusions hosted in quartz, calcite, sphalerite, and fluorite from the Shuniah vein, in both core and surface samples. The core that is available was donated to the Geological Survey of Canada by Curtis and is a condensed suite of representative samples. Samples of the vein cross section were collected during this study. Sample descriptions and core logs are compiled in Appendix Four.

Eutectic Temperatures

The results of the eutectic temperature determinations (fig. 3-7) indicate a peak at -44°C , corresponding to a metastable NaCl-MgCl_2 eutectic (-44°C ; Davis *et al.*, 1988). There is also a peak at -48°C , which corresponds to a stable CaCl_2 eutectic (-49.8°C ; Crawford, 1981). There are lesser peaks that correspond to NaCl-CaCl_2 (-52°C) and $\text{NaCl-CaCl}_2\text{-MgCl}_2$ (-58°C) eutectic (Crawford, 1981).

There is scatter in the data that is probably in part due to observational error. The eutectic temperature was determined by the observation of the onset of melting in the frozen inclusions. If the observational qualities of the

SHUNIAH MINE FLUID INCLUSION DATA

EUTECTIC TEMPERATURES

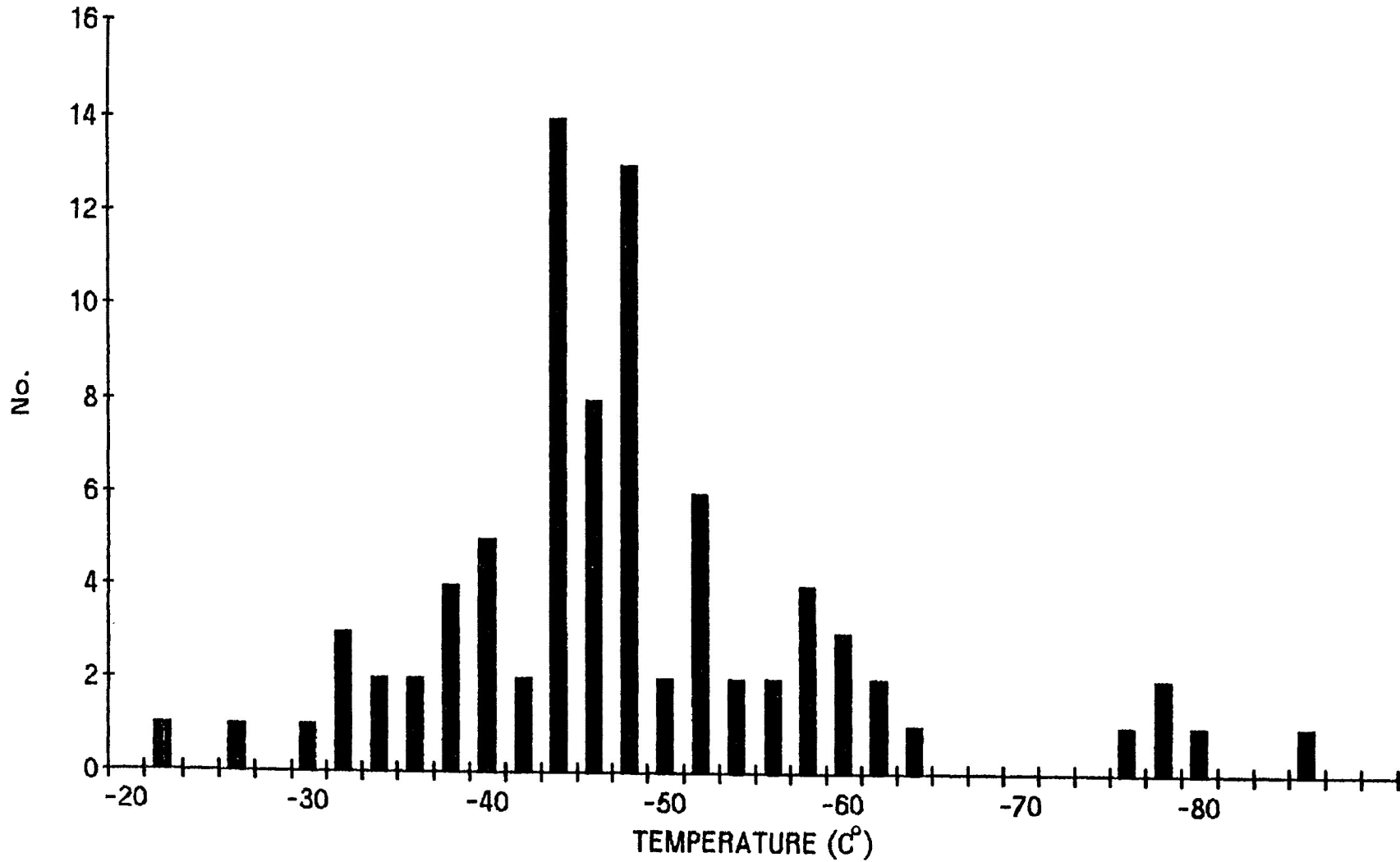


Figure 3-7. Histogram of the eutectic temperature for 83 fluid inclusions hosted in the Shuniah Mine vein.

inclusions were not excellent it was possible to miss the onset of melting. This results in recorded eutectic temperatures that were several degrees higher than the actual eutectic temperature. This would skew the histogram to slightly higher temperatures. It is also possible that the inclusions were heated too rapidly to remain in thermal equilibrium with the heating gas. This would also cause the histogram to be skewed to higher temperatures. Another possibility is that there are additional cations within the solution that increase the eutectic temperatures for the solutions.

The eutectic data were unsuccessfully analyzed for trends. There was no apparent trend in eutectic temperature with depth, paragenesis or mineralogy of the host rock. The scatter of the data indicate that on a local scale the fluid composition was variable, but the overall bulk composition of the fluid was dominated by Na, Mg and Ca chloride solutions. There is some evidence of CO₂-rich solutions that are characterized by eutectic temperatures lower than -75°C. These CO₂-rich inclusions are restricted to the final phase of calcite (fig. 3-9).

Salinity

The salinity of the inclusions, in terms of equivalent weight percent NaCl, was calculated from the final melting temperature of ice in the inclusions, using

SHUNIAH MINE FLUID INCLUSION DATA

SALINITY WT% NaCl EQUIVALENT N = 76

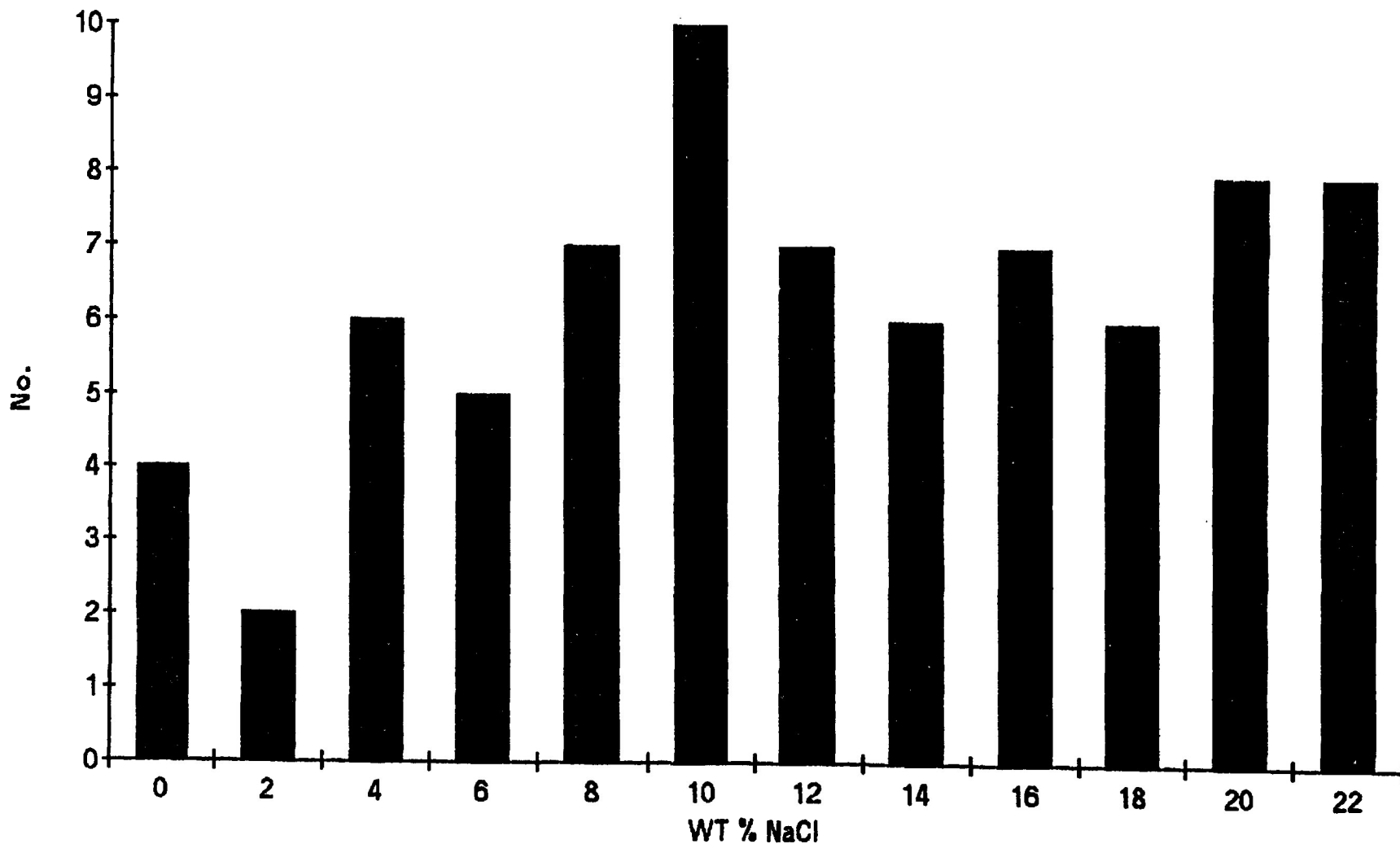


Figure 3-8. Histogram of salinity values, expressed as equivalent weight percent NaCl, for the Shuniah Mine. The salinity values were calculated using the final melting temperature and the equations of Potter *et al.*, (1978).

the equation of Potter et al. (1978). The histogram of these values (fig. 3-8) shows no peaks. This is probably the result of fluid mixing combined with boiling. This would give the fluids a very heterogeneous salinity. As with the eutectic temperature data, no trends were found in salinity with depth or paragenesis.

It is interesting that the histogram indicates a number of inclusions are approaching saturation with NaCl. However, no inclusions with NaCl daughter crystals were observed. Only one daughter crystal was observed, but it was prismatic and birefringent (photo 3-1) and was not identified.

Paragenesis

The paragenesis diagram of the Shuniah Mine (fig. 3-9) is quite complex. Examination of paragenesis along with fluid inclusion homogenization temperatures indicates characteristic trends. The paragenesis is dominated by three fracturing events. After each fracturing event a hot, boiling fluid was injected into the fault. The injection of boiling fluid was not a single event; in one crystal several episodes of boiling are observed (photo 3-3). Quartz was always the initial mineral precipitating from the boiling solution.

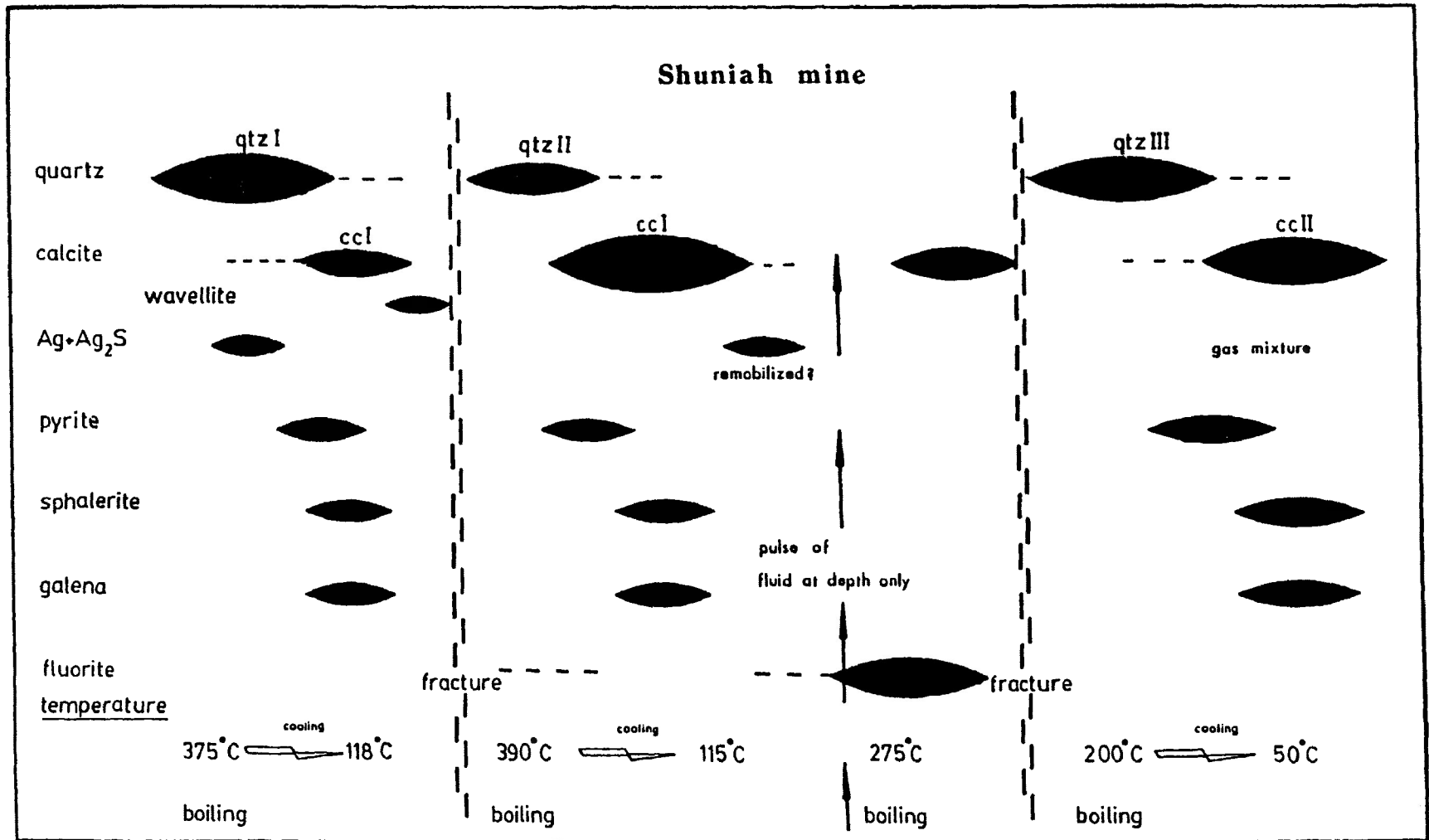


Figure 3-9. Paragenetic diagram for the Shuniah Mine.

Photograph 3-1. Fluid inclusion hosted in sample SHA-2
Homogenization temperature = 349.4°C to liquid
Eutectic temperature = -42.7°C
Salinity = 4.6 wt.% NaCl equivalent.

This inclusion is hosted in quartz and is typical of inclusions from zones that formed from a non-boiling fluid. Note the daughter crystal in the upper right hand corner of the inclusion. This crystal is prismatic and birefringent and was not identified.

Photograph 3-2. Fluid inclusions hosted in sample SH-10-1
Homogenization temperatures = 375.0°C to vapor
375.3°C to vapor
376.4°C to liquid
Eutectic temperature = -56.6°C
Salinity = 15.4 wt.% NaCl equivalent.

These fluid inclusions are hosted in quartz and are typical of inclusions from zones that formed from a boiling fluid. Note the variations in liquid/vapor ratios.

National Library
of Canada

Canadian Theses Service

Bibliothèque nationale
du Canada

Service des thèses canadiennes

NOTICE

THE QUALITY OF THIS MICROFICHE
IS HEAVILY DEPENDENT UPON THE
QUALITY OF THE THESIS SUBMITTED
FOR MICROFILMING.

UNFORTUNATELY THE COLOURED
ILLUSTRATIONS OF THIS THESIS
CAN ONLY YIELD DIFFERENT TONES
OF GREY.

AVIS

LA QUALITE DE CETTE MICROFICHE
DEPEND GRANDEMENT DE LA QUALITE DE LA
THESE SOUMISE AU MICROFILMAGE.

MALHEUREUSEMENT, LES DIFFERENTES
ILLUSTRATIONS EN COULEURS DE CETTE
THESE NE PEUVENT DONNER QUE DES
TEINTES DE GRIS.

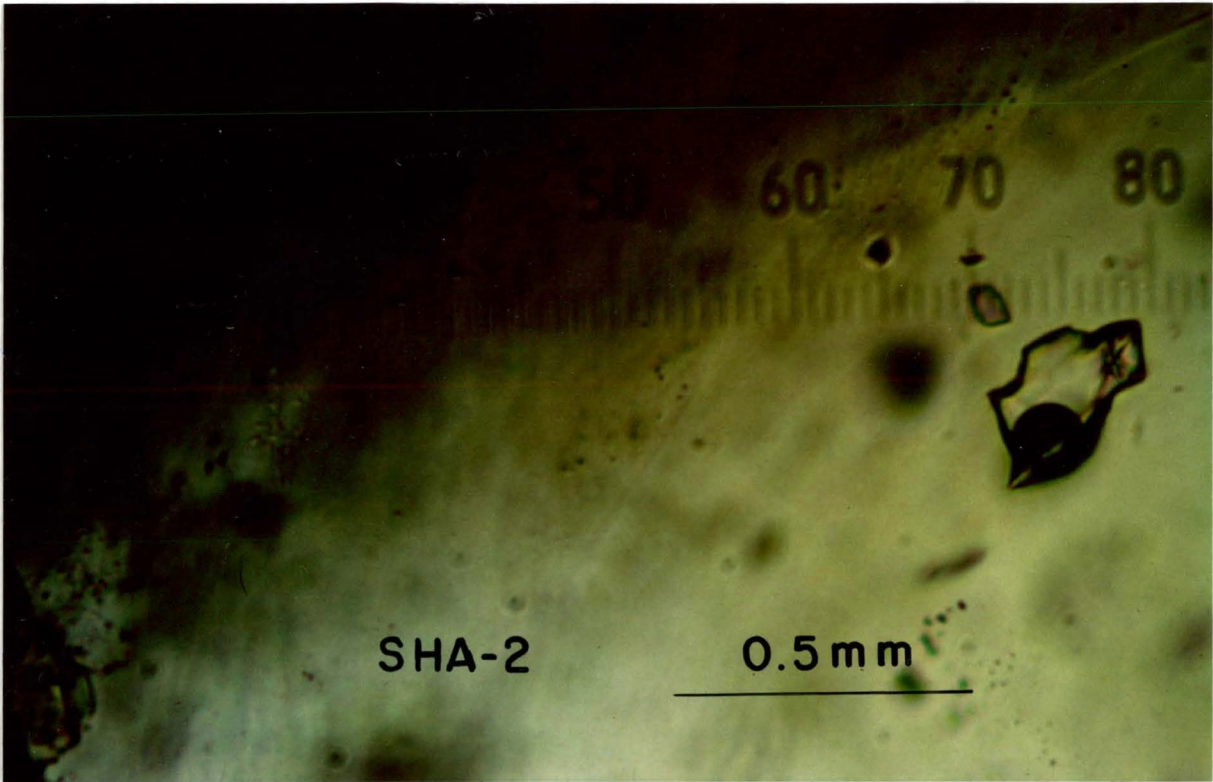


Photo 3-1

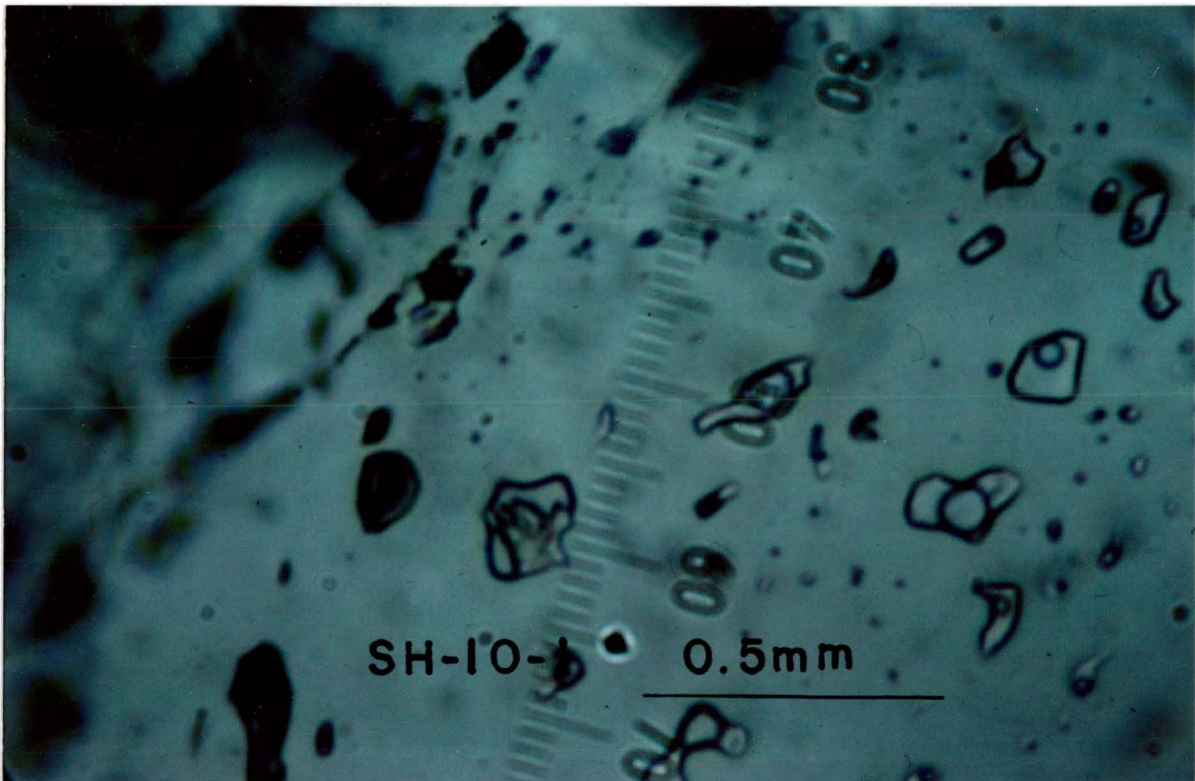
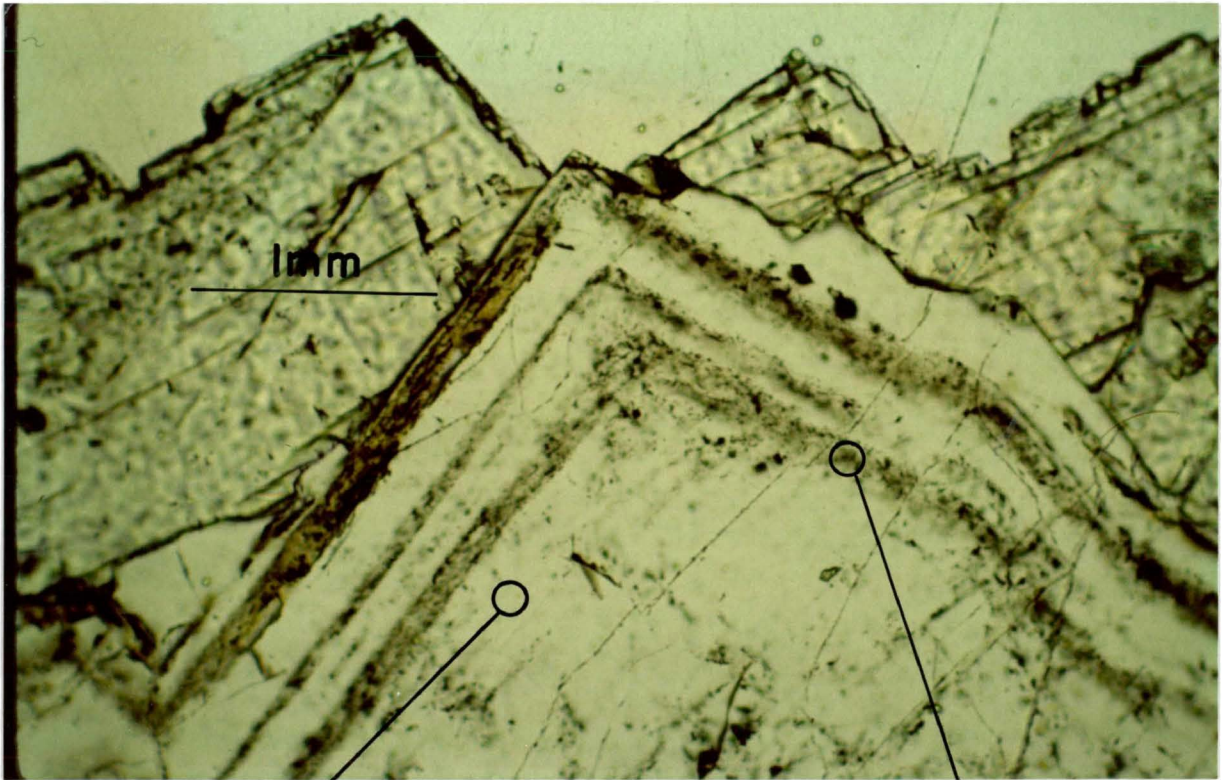


Photo 3-2

Photograph 3-3. Photograph from a hydrothermal quartz grain from the Thunder Bay Mine. This photograph shows zoning due to pulses of boiling fluid. The foggy areas, labeled boiling zone, are characterized by dense populations of fluid inclusion. A close up of this type of zone is shown in photo 3-2. These zones generally exhibit fluid inclusion homogenizations characteristic of boiling. These boiling zones are interspaced with zones of sparse fluid inclusions. These areas are labeled non-boiling zone. A close up of this type of zone is shown in photo 3-1. These zones do not show any evidence for boiling and they commonly have a lower homogenization temperature than the boiling zones. This difference in homogenization temperature is interpreted to be the temperature correction due to the effect of pressure.



non-boiling zone

boiling zone

Photo 3-3

The precipitation of quartz was followed by cooling of the solution, with small amounts of calcite precipitating. Once the solution temperature reached approximately 100°C, the bulk of the calcite precipitated along with sulfides and native silver.

The sulfides and the silver exhibit a characteristic sequence. The first metallic mineral to have precipitated is silver and argentite, followed by pyrite and then sphalerite and galena.

The injection of boiling fluid was not always accompanied by fracturing. In the Shuniah Mine (fig 3-9) fluorite was deposited from a boiling fluid at 275°C, but it has no associated fracturing event.

The characteristic paragenesis of high-temperature quartz followed by low-temperature calcite and sulfides was identified three times in the Shuniah Mine. Each sequence was separated by a fracturing event. The fracturing may have occurred during a hiatus in precipitation or during the precipitation of vein material.

Homogenization Temperatures

The calcite generally has large inclusions with excellent observation qualities (photo 3-4). Two distinct phases of calcite were identified, CC I and CC II. Graphs of

Photograph 3-4. Fluid inclusion hosted in sample SHA-6

Homogenization temperature = 97.6°C to liquid

Eutectic temperature = -43.8°C

Salinity = 10.2 wt.% NaCl equivalent

This inclusion is hosted in calcite and is typical of the inclusions that are found in calcite. Notice the small vapor bubble and the negative crystal faces.

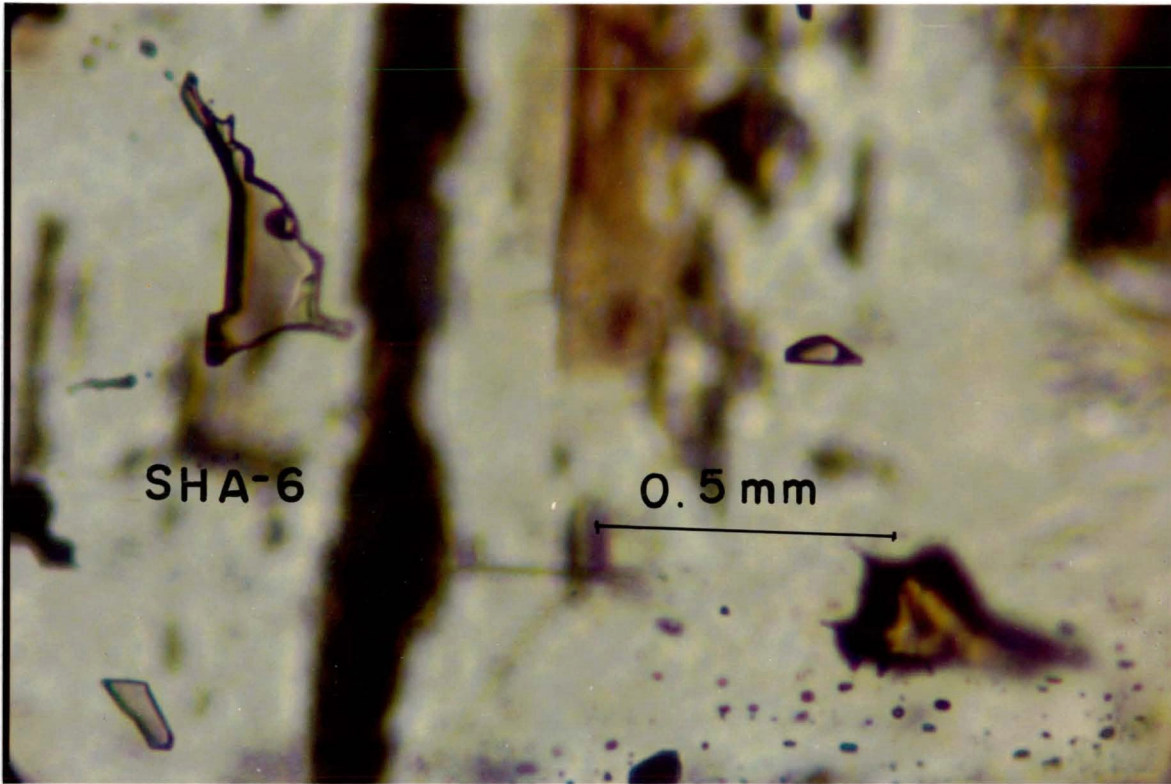


Photo 3-4

SHUNIAH MINE FLUID INCLUSION DATA
CALCITE I HOMOGENIZATION TEMPERATURE

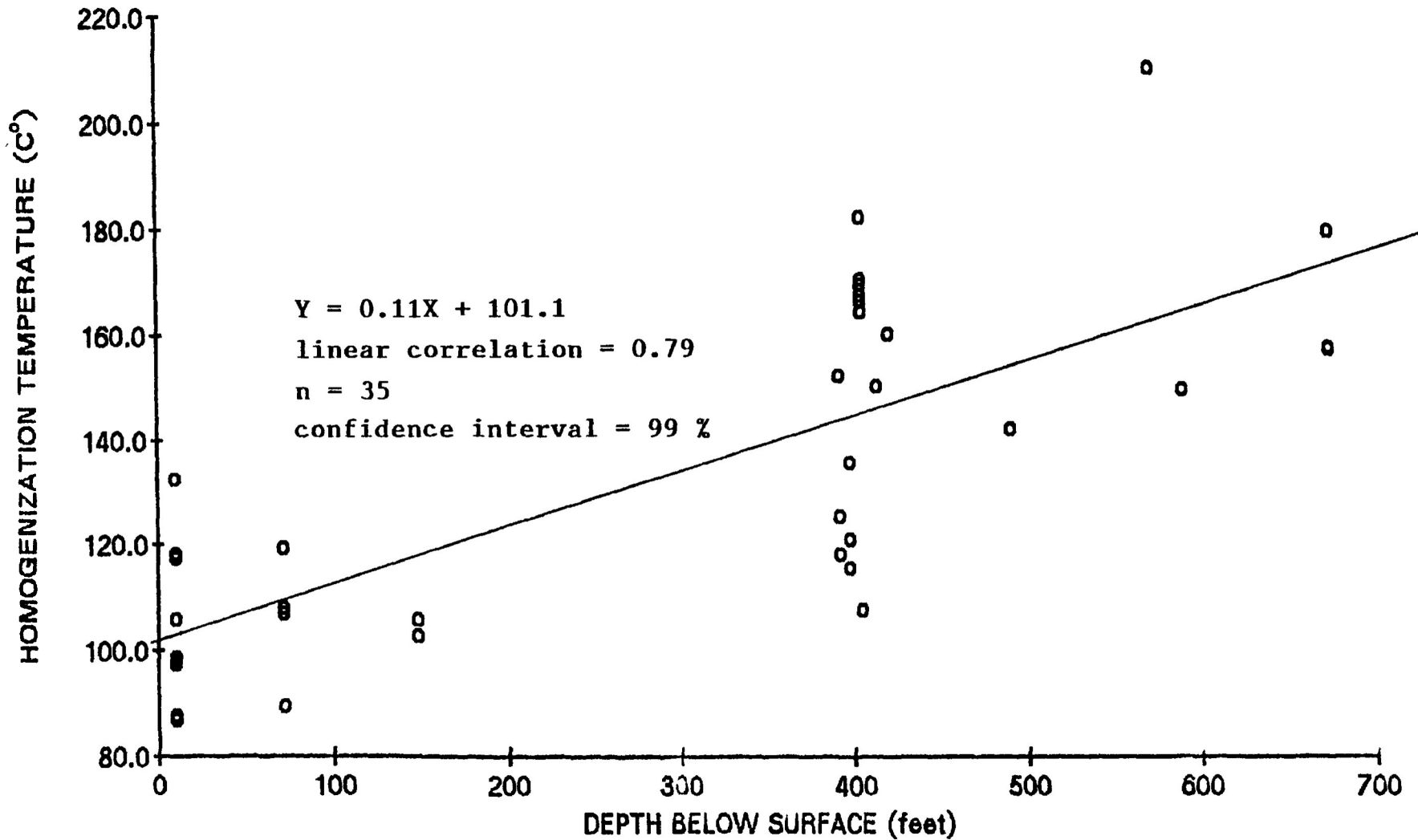


Figure 3-10. Graph of the homogenization temperatures of fluid inclusions hosted in calcite I as a function of depth.

SHUNIAH MINE FLUID INCLUSION DATA

CALCITE II HOMOGENIZATION TEMPERATURE

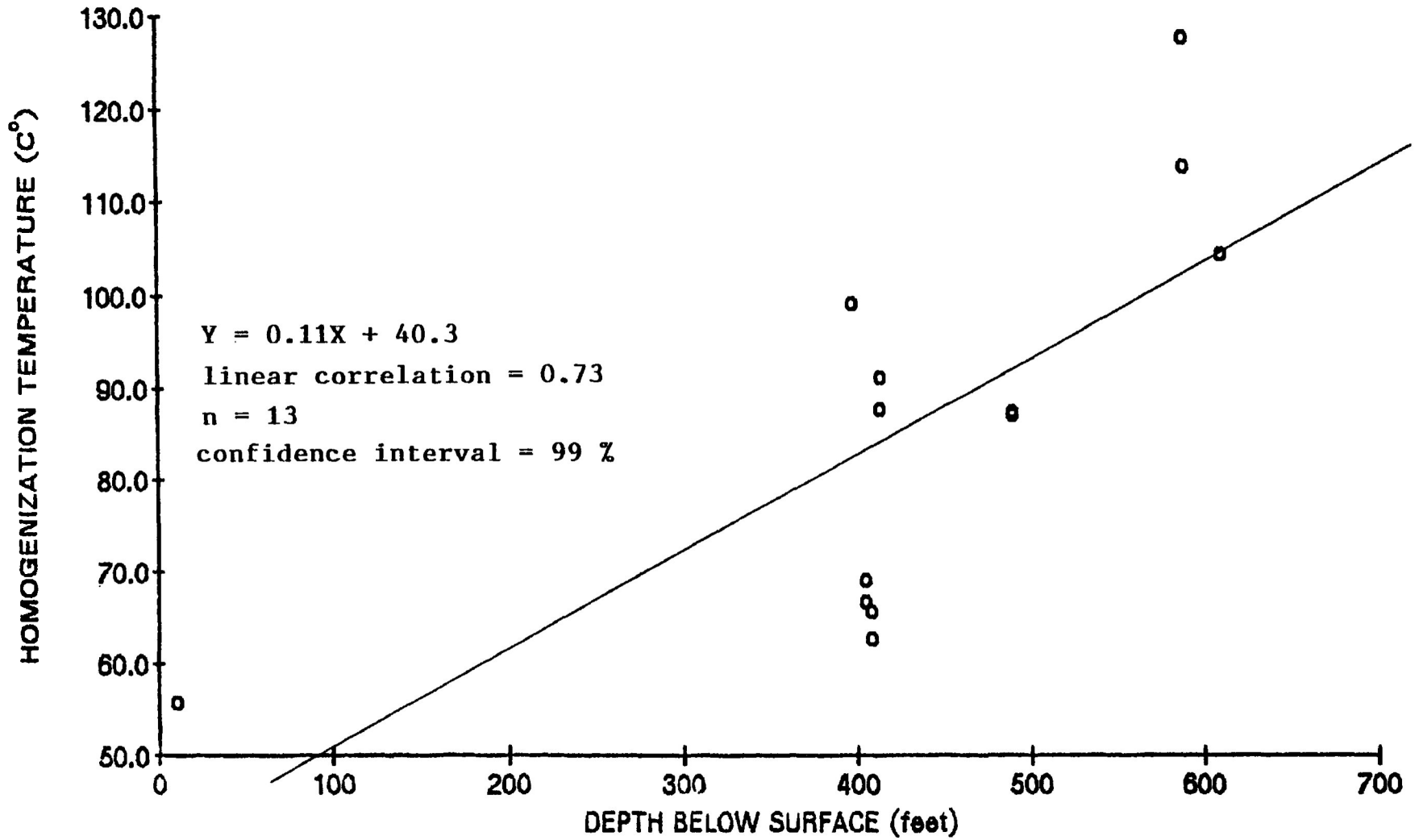


Figure 3-11. Graph of the homogenization temperatures of fluid inclusions hosted in calcite II as a function of depth.

homogenization temperature with depth show a strong trend for increasing temperature with depth (fig. 3-10, 3-11). This trend is apparent in both the quartz and the calcite.

The initial, high-temperature quartz shows evidence of precipitation from a boiling fluid. The episodes of boiling are seen in areas with very dense concentrations of fluid inclusions (photo 3-2 and 3-3). Within these zones the inclusions show a large variation in liquid/vapor ratios. When they are heated, adjacent inclusions homogenize to liquid and vapor. For example, sample SH-79 had one inclusion homogenized to liquid at 362.8°C and another inclusion homogenized to vapor at 359.8°C. This is interpreted as boiling of the solution at 360°C. Data such as these have allowed the definition of a boiling curve as a function of depth for two of the three phases of quartz identified (fig. 3-12, 3-13). These data are invaluable since they represent the true temperature of trapping. In a boiling solution, a temperature correction due to the effects of pressure is unnecessary because the ambient pressure is equal to the vapor pressure of the fluid (Roedder, 1984). One characteristic of each of the boiling temperature vs. depth curves is that the temperatures increase with depth. This has implications for the heat source that will be discussed latter.

SHUNIAH MINE FLUID INCLUSION DATA

HOMOGENIZATION TEMPERATURE QUARTZ I

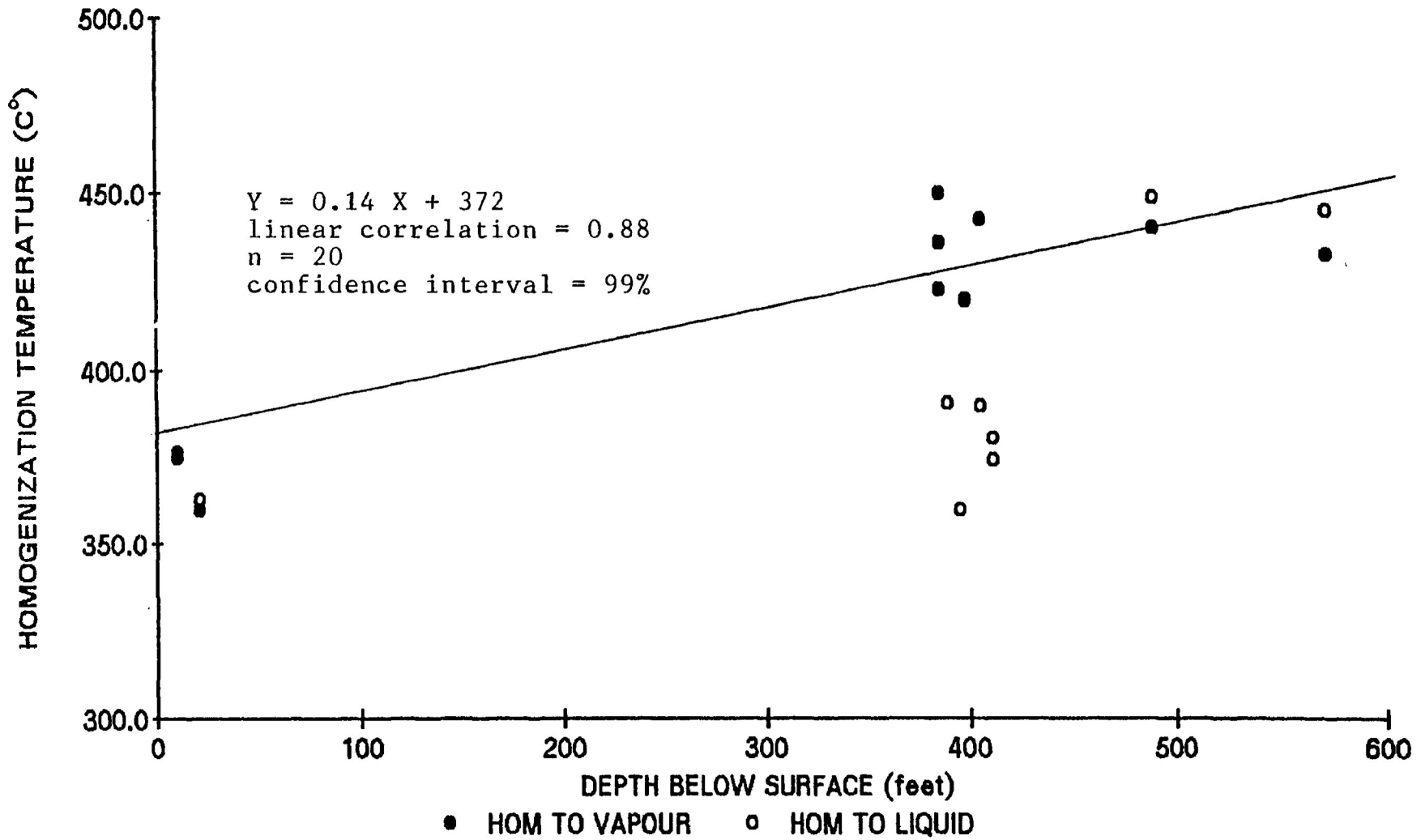


Figure 3-12. Graph of the boiling curve for fluid inclusions hosted in quartz I as a function of depth. The boiling temperature is the mean of the homogenization to liquid and to vapor temperatures.

SHUNIAH MINE FLUID INCLUSION DATA

HOMOGENIZATION TEMPERATURE QUARTZ II

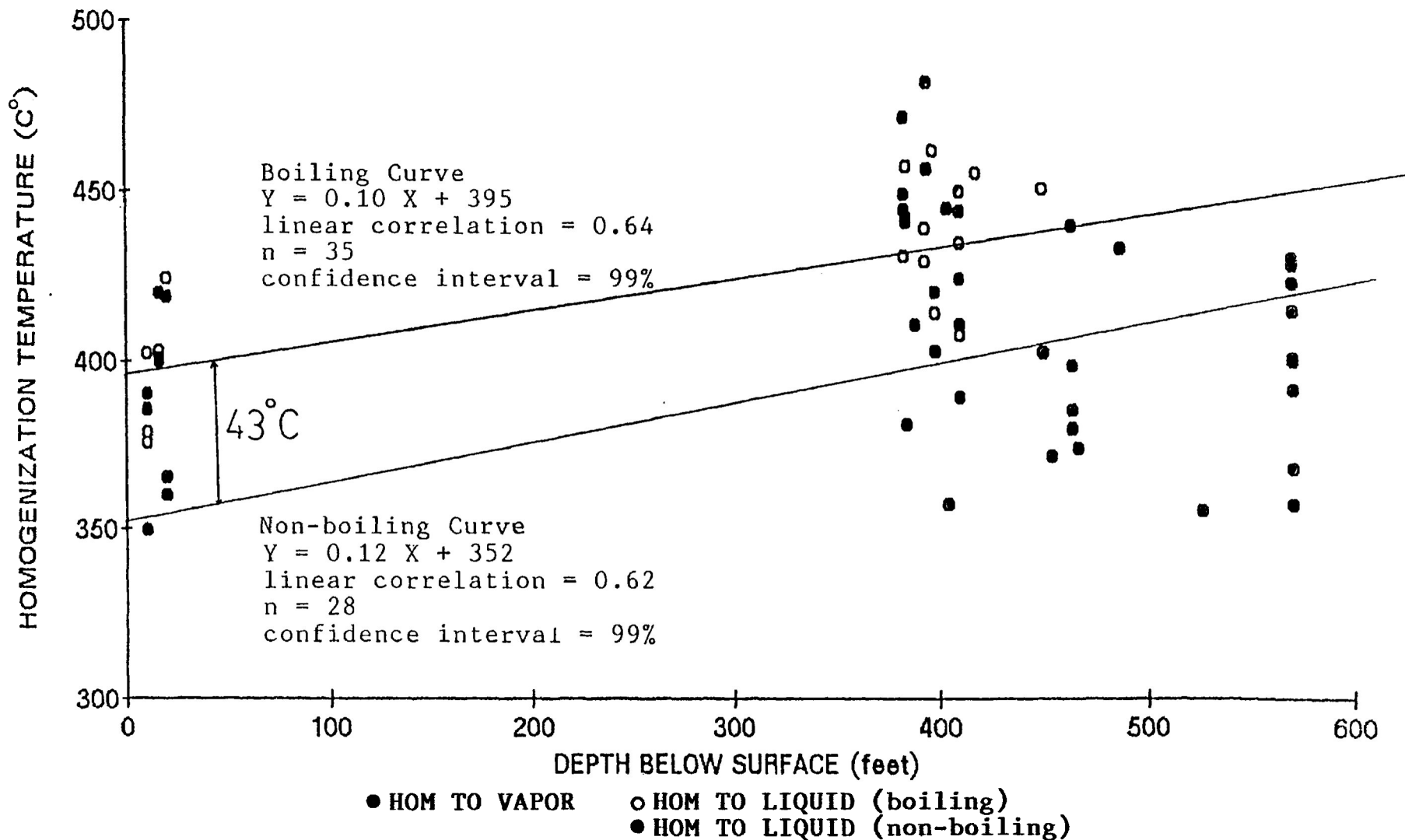


Figure 3-13. Graph of the boiling and non-boiling curves for fluid inclusions hosted in quartz II as a function of depth. The boiling temperature is the mean of the homogenization to liquid and to vapor temperatures.

In the crystals that host inclusions exhibiting boiling behavior, there are often zones that show no evidence of boiling (photo 3-1). These are zones of relatively clear quartz that do not have large concentrations of inclusions. The fluid inclusions within these zones, although rare, are often large and have excellent observation qualities. These inclusions, when homogenized, show no evidence of boiling, since they consistently homogenize to liquid. In two adjacent zones, one that shows boiling and one that shows non-boiling behavior (Photo 3-3) have a temperature difference. The data from Quartz II are plotted in fig 3-13. They show a boiling and a non boiling curve as a function of depth. The boiling temperature is consistently approximately 43° higher than the non boiling temperature. This has been interpreted to be the temperature correction due to the effect of pressure.

The boiling temperature can be used to determine the trapping pressure of the fluid inclusion. This is done and the implications of it is discussed in chapter five.

Thunder Bay Mine

Fluid inclusion analysis was carried out on fourteen inclusions. The samples were all in situ surface samples collected in the fall of 1987. Fluid inclusions were found hosted in quartz and calcite.

The histogram (fig. 3-14) of eutectic temperatures shows a strong peak at -47°C , which corresponds to a CaCl_2 solution. As with the Shuniah Mine data, the eutectic temperature peak is skewed to slightly higher temperatures due to error in determining the onset of melting.

The salinities of the fluid inclusions were calculated using the equation of Potter et al., (1978). The histogram (fig. 3-15) of the results indicate that the quartz precipitated out of a more saline solution than the calcite.

The paragenetic diagram (fig. 3-16) for the Thunder Bay Mine was based on fourteen fluid inclusion homogenization temperatures (fig. 3-17) and shows a good correlation with the Shuniah paragenesis. The Thunder Bay vein, unlike the Shuniah vein, has only an initial fracturing event. The initial mineral is quartz, which precipitated out of a boiling solution. As the solution cooled, there was precipitation of small amounts of calcite and silver. When the solution's temperature reached

approximately 100°C, the bulk of the calcite, sulfides and native silver precipitated. The metallic minerals also have a similar paragenetic sequence to the Shuniah Mine. Silver and argentite were the first metallic minerals to form, followed by pyrite and then sphalerite and galena.

As with the Shuniah Mine a boiling temperature is found, which allows the trapping pressure of the fluid inclusion to be found. The implications of this are discussed in chapter five.

THUNDER BAY MINE FLUID INCLUSION DATA

EUTECTIC TEMPERATURES

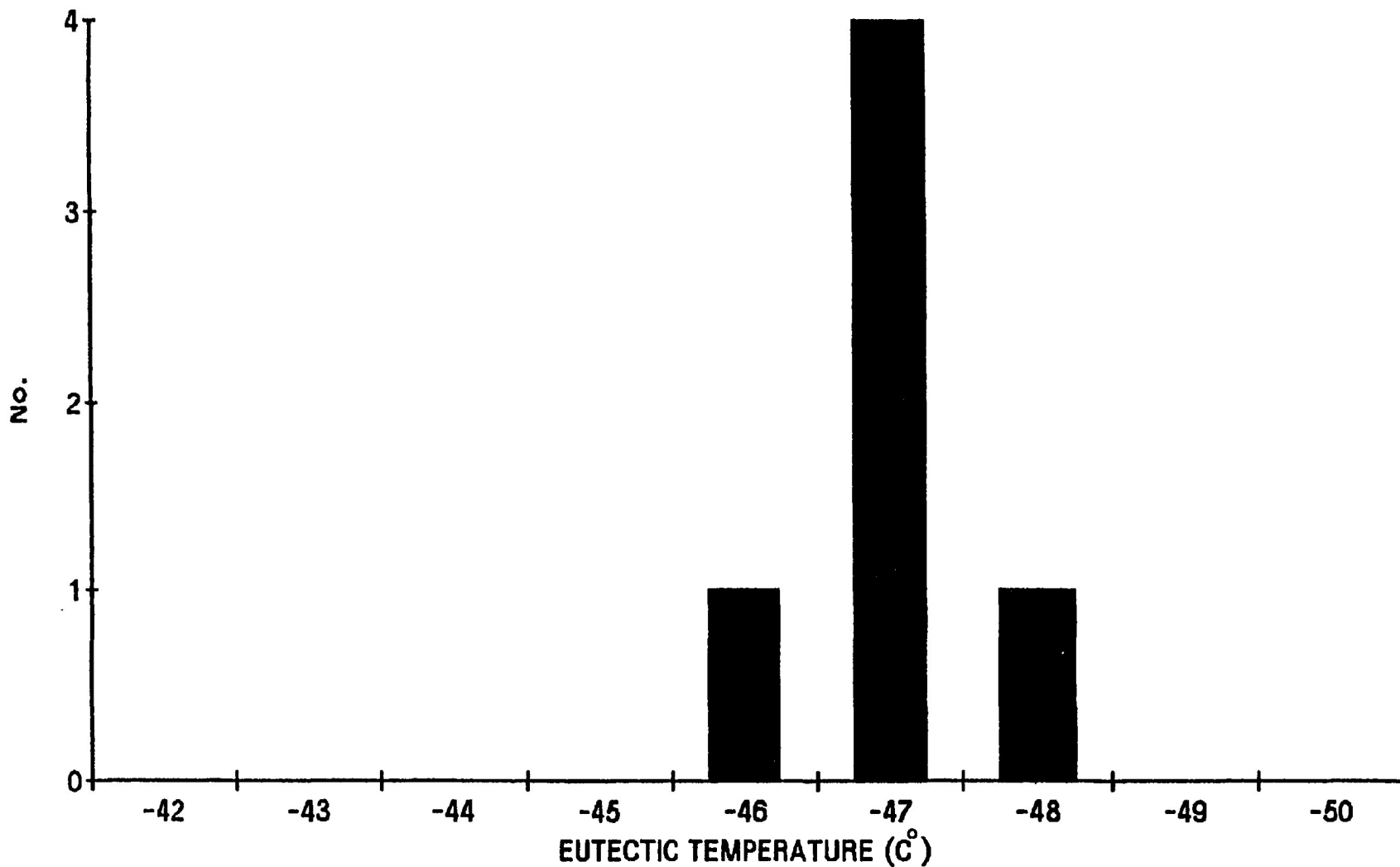


Figure 3-14. Histogram of the eutectic temperature for six fluid inclusions hosted in samples of the Thunder Bay Mine vein.

THUNDER BAY MINE FLUID INCLUSION DATA

SALINITY

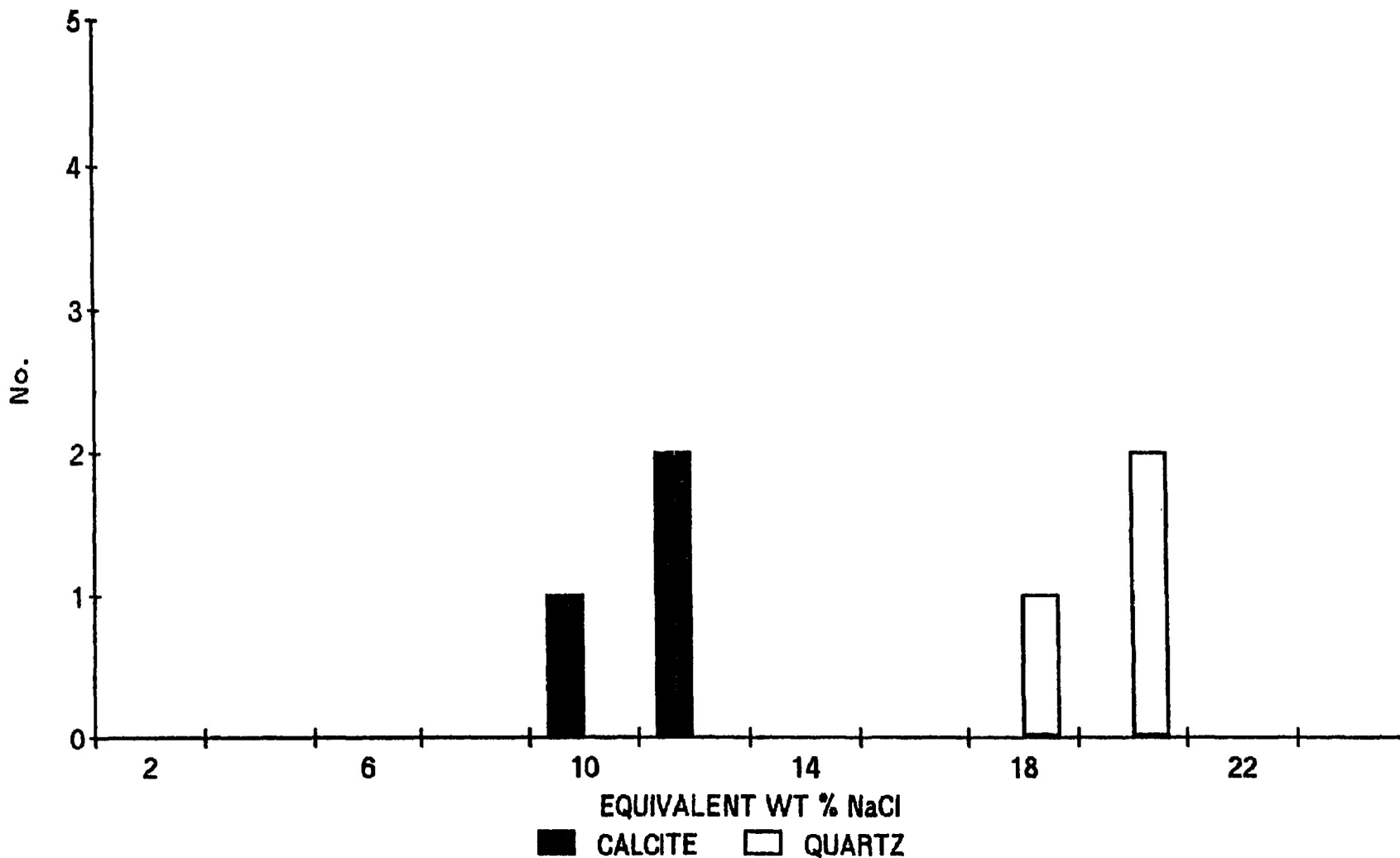


Figure 3-15. Histogram of salinity values, expressed as equivalent weight percent NaCl, for the Thunder Bay Mine. The salinity values were calculated using the fluid inclusion's final melting temperature and the equations of Potter et al., (1978).

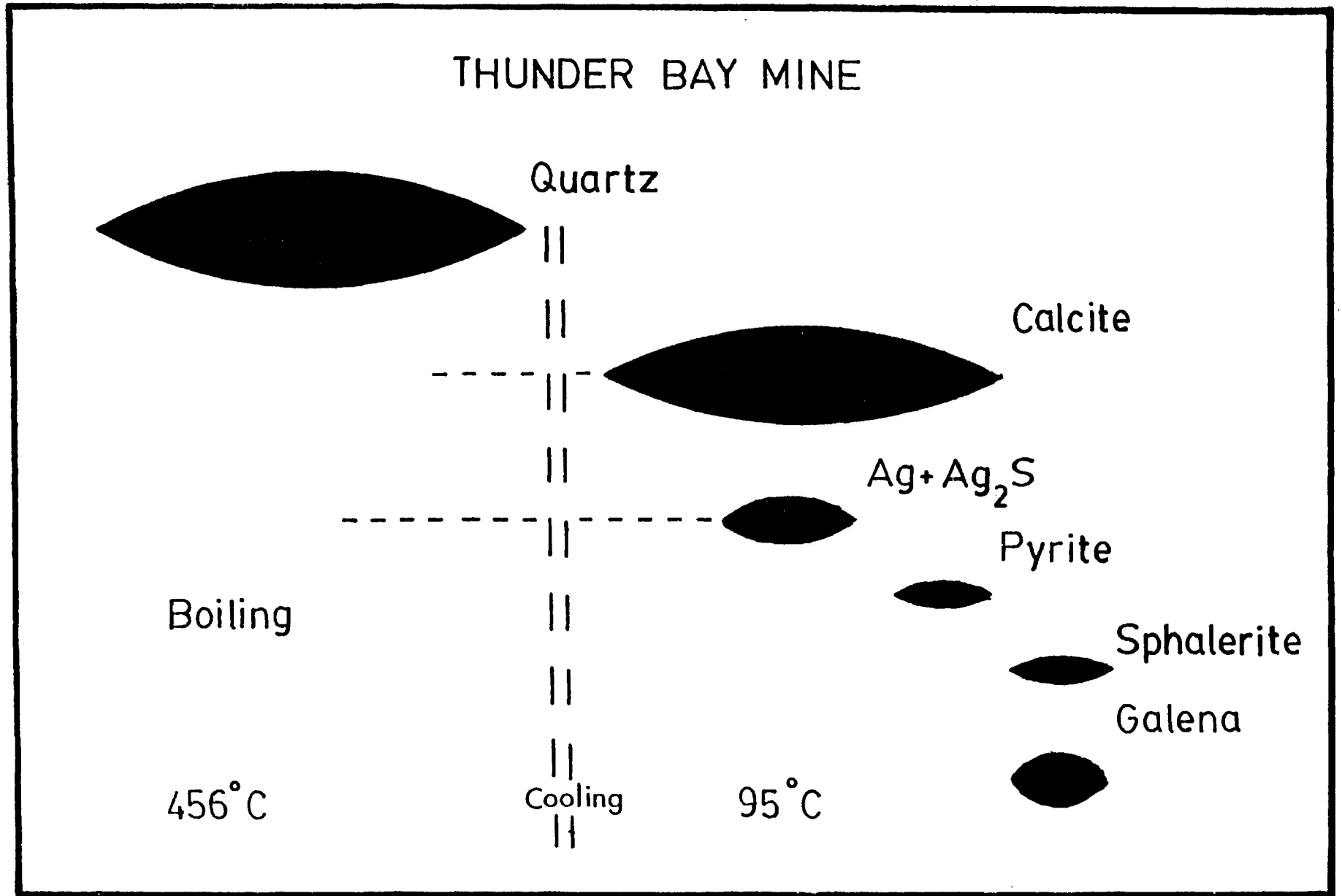


Figure 3-16. Paragenetic diagram for the Thunder Bay Mine, based on fourteen fluid inclusion homogenization temperatures and examination of the vein cross section.

THUNDER BAY MINE FLUID INCLUSION DATA HOMOGENIZATION TEMPERATURES

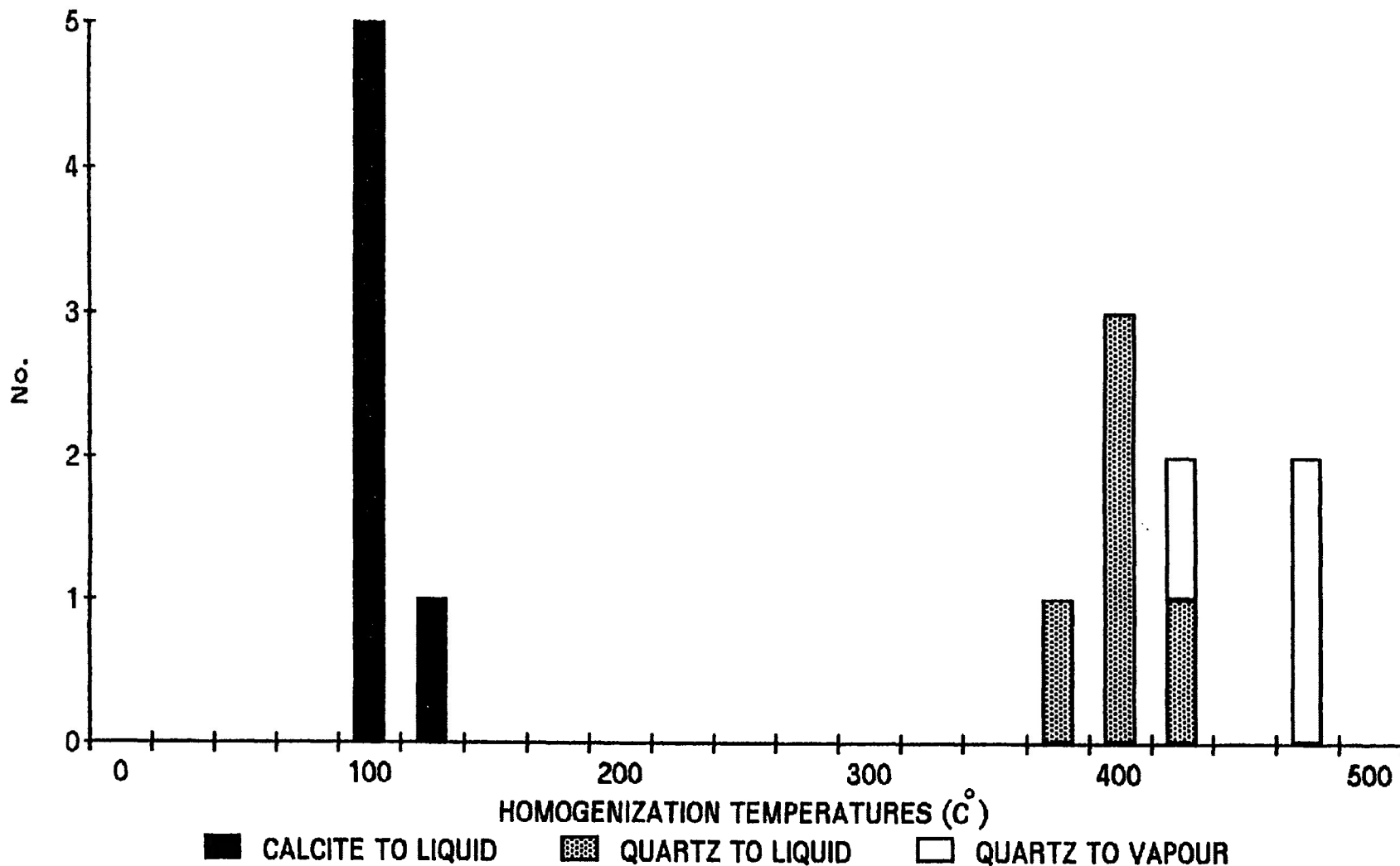


Figure 3-17. Histogram of the homogenization temperatures of fourteen fluid inclusions hosted in the Thunder Bay Mine.

Stable Isotope Data

Shuniah Mine

Six samples of calcite were analyzed for carbon and oxygen isotope ratios from the Shuniah Mine, and one sample of quartz was analysed for oxygen ratios. The samples were selected to give a profile of variations in stable isotope data with depth. The maximum depth from which the samples were obtained was 754 feet. Each sample had a fluid inclusion homogenization temperature, so fractionation factors for calcite-H₂O, calcite-HCO₃⁻, and quartz-H₂O were calculated (table 3-1).

The plot of $\delta^{18}\text{O}$ with depth for the samples of calcite shows a strong trend for increasingly positive ratios with depth (fig. 3-18). The oxygen signature of the quartz shows a positive $\delta^{18}\text{O}$, similar to the deep samples of calcite. The calcite is low temperature and late in the paragenesis, while the quartz is high temperature and early in the paragenesis. This indicates that the water's oxygen ratio tended to become progressively lighter as the fluid migrated upwards. This could be the result of mixing of the two types of fluids, which cooled the fluid. The isotopic signature of the most pristine fluid is given by the isotopic values for the deepest sample, or of the early, high-temperature quartz. These samples would precipitate from a fluid that has undergone the least amount of

Table 3-1

SHUNIAH MINE STABLE ISOTOPE DATA

CARBONATE OXYGEN AND CARBON ISOTOPE RATIOS

<u>SAMPLE No.</u>	<u>DEPTH (feet)</u>	<u>TEMP.(C°)</u>	<u>$\delta^{18}O_{cc}(\text{‰})$</u>	<u>$\delta^{18}O_{WATER}(\text{‰})$</u>
SHA-3	10	92.7	12.5	-5.4
SH-154	72	106.4	12.0	-4.4
SH-156	148	104.5	11.4	-5.2
SH-29	421	160.4	18.9	7.0
SH-48	674	158.0	18.0	5.9
SH-190	754	295.7	18.5	12.8

<u>SAMPLE No.</u>	<u>DEPTH (feet)</u>	<u>TEMP.(C°)</u>	<u>$\delta^{13}C_{cc}(\text{‰})$</u>	<u>$\delta^{13}C_{CHCO_3}(\text{‰})$</u>
SHA-3	10	92.7	-5.7	-5.9
SH-154	72	106.4	-6.2	-6.8
SH-156	148	104.5	-6.1	-5.9
SH-29	421	160.4	-1.0	0.6
SH-48	674	158.0	-13.3	-12.9
SH-190	754	295.7	-1.7	-1.1

QUARTZ OXYGEN ISOTOPE RATIOS

<u>SAMPLE No.</u>	<u>DEPTH (feet)</u>	<u>TEMP.(C°)</u>	<u>$\delta^{18}O_{qtz}(\text{‰})$</u>	<u>$\delta^{18}O_{WATER}(\text{‰})$</u>
SHA-6	10	375.0	16.4	11.8
SHA-6	10	375.0	15.8	11.2

THUNDER BAY MINE STABLE ISOTOPE DATA

CARBONATE OXYGEN AND CARBON ISOTOPE RATIOS

<u>SAMPLE No.</u>	<u>DEPTH (feet)</u>	<u>TEMP.(C°)</u>	<u>$\delta^{18}O_{cc}(\text{‰})$</u>	<u>$\delta^{18}O_{WATER}(\text{‰})$</u>
TB-5	0	95.0	13.1	-4.0

<u>SAMPLE No.</u>	<u>DEPTH (feet)</u>	<u>TEMP.(C°)</u>	<u>$\delta^{13}C_{cc}(\text{‰})$</u>	<u>$\delta^{13}C_{CHCO_3}(\text{‰})$</u>
TB-5	0	95.0	-5.8	-5.6

TABLE 3-1 (continued)

ELEMENTAL CARBON STABLE ISOTOPE DATA

<u>SAMPLE No.</u>	<u>LOCATION</u>	<u>$\delta^{13}\text{C}(\text{‰})$</u>
RS87-TB2	FROM THUNDER BAY MINE WALL ROCK	-31.9
RS86-43	FROM ROVE FORMATION AT SHALE DIABASE CONTACT. LOCATION # 43 IN DIABASE QUARRY	-31.1
SI	SILVER ISLET GRAB SAMPLE	-33.3
SI-27	SILVER ISLET GRAB SAMPLE	-34.8

SILVER ISLET STABLE ISOTOPE DATA

CARBONATE OXYGEN AND CARBON ISOTOPE RATIOS

<u>SAMPLE No.</u>	<u>TEMP. (C°)</u>	<u>$\delta^{18}\text{O}_{\text{CC}}(\text{‰})$</u>	<u>$\delta^{18}\text{O}_{\text{WATER}}(\text{‰})$</u>
SI	177.5	20.4	8.6

<u>SAMPLE No.</u>	<u>TEMP. (C°)</u>	<u>$\delta^{13}\text{C}_{\text{dol}}(\text{‰})$</u>	<u>$\delta^{13}\text{C}_{\text{HCO}_3}(\text{‰})$</u>
SI	177.5	-11.1	-10.6

OXYGEN ISOTOPE VARIATIONS WITH DEPTH

DATA FROM THE PORT ARTHUR GROUP

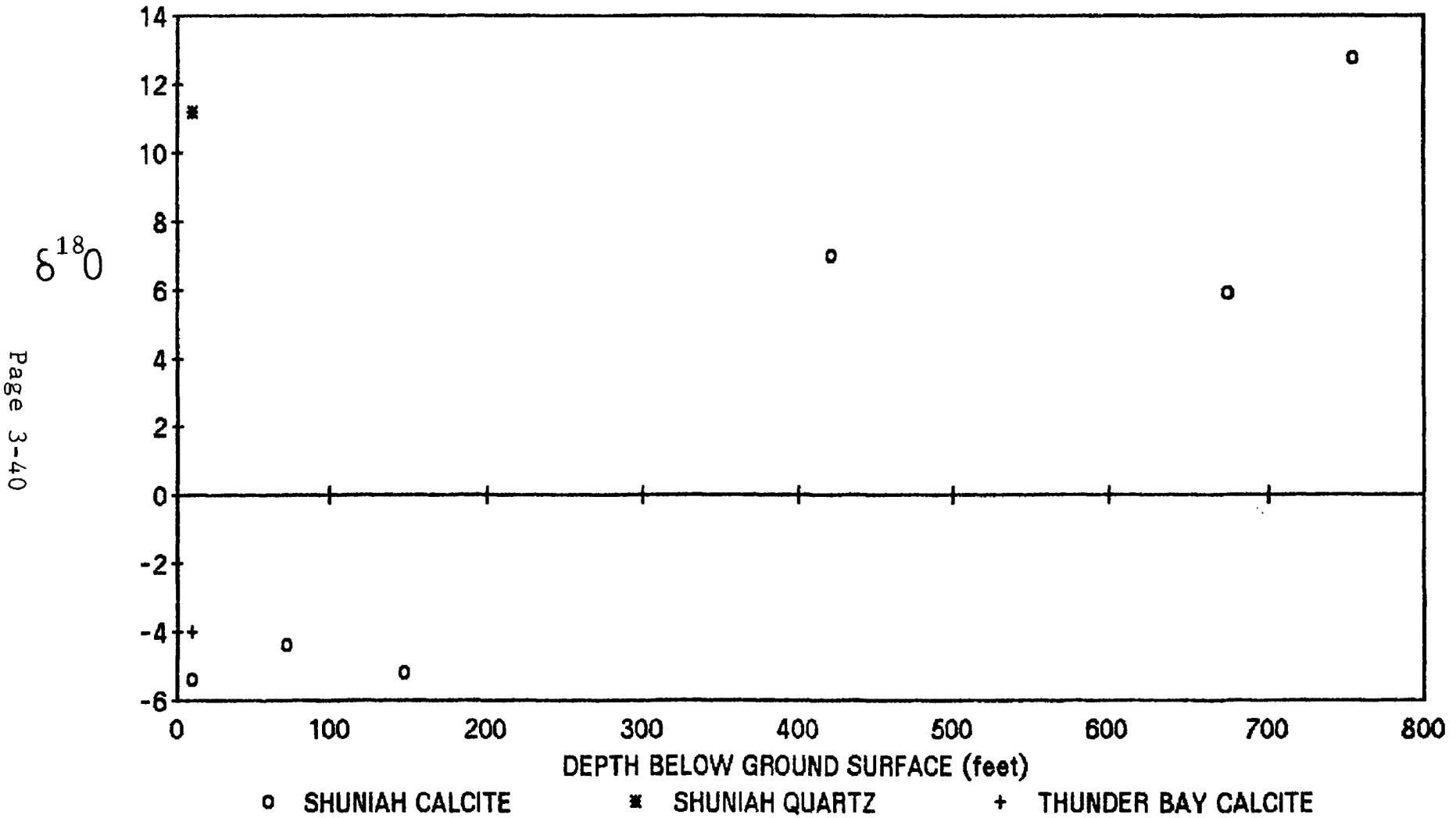


Figure 3-18. Graph of oxygen isotope variations as a function of depth. Data are from the Shuniah and Thunder Bay Mines, N=8

dilution. The data can be interpreted to indicate that the initial fluid had a oxygen isotope ratio of approximately 12‰.

The carbon isotope ratios (Table 3-1) are less clear; they tend to be variable but average -5.3 ‰. The deeper higher temperature samples (SH-29, SH-48, SH-190) demonstrate the greatest degree of scatter. These deep samples are also from vein material that is hosted within the Gunflint Formation. If the hydrothermal fluids scavenged the carbon from the wall rock, the Gunflint being dominantly chert would give a variable carbon source resulting in the scatter of data. However, the Rove shale would present a uniform carbon source, and samples hosted within the Rove would show consistent data. The trend in the carbon data is probably explained in this manner.

Thunder Bay Mine

From the Thunder Bay Mine wall rock a sample of graphite was taken and analyzed for carbon isotope ratios. A second sample of graphite was taken from the shale-diorite contact, removed from any hydrothermal activity; this was also analyzed for carbon isotope ratios. The results are almost identical with $\delta^{13}\text{C} = -31$ ‰. This is the value that is expected for metamorphosed, organic carbon (Schoell, 1984; summarized by Ohmoto, 1986). This indicates that the

graphite found in the wall rock is likely primary, recrystallized, organic carbon from the Rove shale.

From the Thunder Bay Mine a sample of calcite from a veinlet in contact with the graphitic wall-rock was separated and analyzed for carbon and oxygen isotope ratios. The results (Table 3-1) are similar to those found in the shallow depths of the Shuniah Mine. The object of this analysis was to determine if the graphitic wall rock could act as a source for the carbon in the carbonate. For the wall-rock graphite to act as a carbon source the fractionation between carbonate and the graphite would be 26.3‰ at 95.0°C.

Silver Islet Grab Sample

One grab sample from Silver Islet had graphite and dolomite occurring together. This sample was crushed, and the dolomite fraction was analyzed for carbon and oxygen isotope ratios and the graphitic fraction was analyzed for carbon isotope ratios (Table 3-1). The object of this analysis is to compare these results with the results of the carbonate-graphite pair from the Thunder Bay vein. The results are consistent; the Silver Islet sample indicates a fractionation of 22.2 ‰ at 177.5°C.

One other sample of elemental carbon was analyzed for carbon isotope ratios (Table 3-1). This sample was graphite from Silver Islet. The result is consistent with the earlier mentioned sample with $\delta^{13}\text{C} = -34.8$. This indicates that the graphite in the vein systems is recrystallized organic carbon (Schoell, 1984; summarized by Ohmoto, 1986).

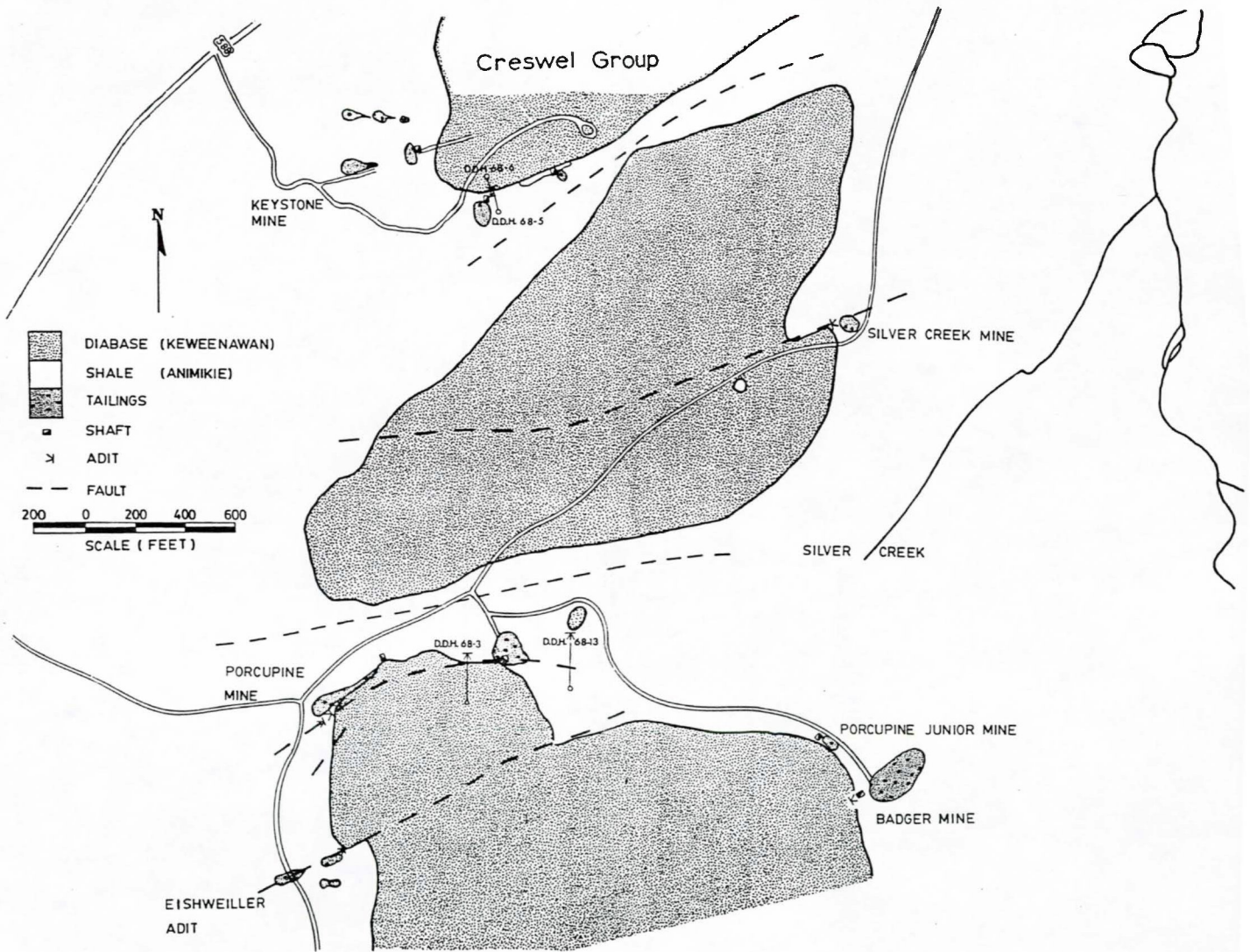
Creswel Group

(map 4-1)

The Creswel Group is a block of claims optioned and worked by the Creswel Mines Limited from 1965 to 1971. The Creswel Group includes the Badger Mine, Porcupine Mine, Porcupine Jr. Mine, Keystone veins, West Beaver Mine, Little Pig vein, Eischweiller vein and the Silver Creek Mine (Chambers, 1986). Since this project was undertaken to determine how the vein systems vary with depth, only veins with available drill core were studied. These veins are the Porcupine Mine (Creswel number eight vein) and the Keystone number three vein (Creswel number six vein). The history of the mines examined from the Creswel Group is summarized from Tanton (1931) and the Ontario Ministry of Northern Development and Mines, Resident Geologist Files, updated 1986; unless otherwise referenced.

Porcupine Mine History

The vein system of the Porcupine Mine was discovered in 1883 by Captain Daniel McPhee, Oliver Dounais and T.A. Keefer. The property was optioned to an American company called the Twin City Mining Corporation. In August of 1885 the option was dropped, and mineral rights reverted back to the original owners. The property was then worked by the owners intermittently until 1887. The work consisted of



driving four adits into the west side of the bluff and the sinking of a shaft to sixty feet. In October of 1887 the property was sold to a Detroit syndicate; at that time the total length of drifts was three hundred and ninety feet.

In June 1890, the Badger Mining Company held the property, and completed a south cross cut, which intersected a second vein system. The property was then sold to H.M. Nichol in 1891, at which time the shaft was one hundred and thirty feet deep, and drifting totaled one thousand three hundred five feet. There was little work done on the property after this time. The property went through a series of sales and options with only minimal work done.

Between 1928 and 1933, the property was held by Animikie Mines Limited. At this time the shaft was two hundred fifty feet deep, and a total of one thousand eight hundred ninety feet of drifting had been accomplished. In November, 1946, Climax Silver Mines Limited obtained the property. Airborne magnetic and electromagnetic surveys were done on the property in 1959. Climax Silver Mines Limited held the property until 1965, when it was optioned it to Creswel Mines Limited. The work done after 1965 is described in a later section.

Keystone Mine History

The Keystone vein system was discovered in 1891 by Peter Young. Between 1891 and 1892, development work on the property was done on two of the three veins. On the northern vein two adits were drifted along the vein, the upper one for eighty feet and a lower one for one thousand eight hundred nine feet with a shallow connecting winze. On the middle, or number two vein, two adits were driven along the vein, the upper for two hundred and ten feet and the lower for one hundred and thirty five feet.

Between 1911 and 1912, two shafts were sunk on the southern, or number three vein (Creswel vein number six), to depths of eighty and sixty-five feet. The mine then lay dormant until 1965, when several bulk samples of the tailings were taken. In 1965, the property was optioned to Creswel Mines Limited.

Creswel Mines Limited

The history of the Creswel Group is summarized from unpublished Creswel Mines Limited documents unless otherwise referenced. Much of the assessment work was completed by A.C.A. Howe consulting geologists.

In 1965, Creswel Mines Limited obtained fourteen unpatented mining claims, four patented mining claims and four patented lots. This block of land included the Porcupine, Keystone and Badger Mines. Between 1965 and 1971, Creswel Mines Limited conducted an extensive exploration program over the property including geological mapping, geochemical soil sampling, diamond drilling and surface trenching.

On the Porcupine vein system four diamond drill holes totaled one thousand one hundred thirty two feet. The Porcupine Mine was dewatered and sampled, and a twenty foot raise was put in two hundred twenty feet west of the shaft to provide a bulk sample.

On the Keystone vein system eight diamond drill holes totaled one thousand three hundred and fifty feet. The old workings were dewatered and mapped in detail. On the Badger Mine eight diamond drill holes were bored.

In 1971, Creswel Mines Limited dropped their option on the property. In 1974, Climax Mines Limited leased the land for ninety-nine years, and in 1975, three diamond drill holes were bored on the Badger property. The lease on the property was sold to Ruperta Dewhirst in 1978. Some attempt to reevaluate the property's potential has been

attempted recently, without promising results (Resident Geologist M.N.D.M Files, updated 1986).

Geology of the Creswel Property

Outcropping on the Creswel property are Logan diabase and Rove shale (map 4-1). The diabase caps the shale, forming large mesas that dominate the topography. The diabase was intruded as sills, which in the area are up to 13 m thick (Chambers, 1986). The Rove shale is typically black argillite and has been identified by Chambers (1986) as the lower argillite unit of Morey's (1972) divisions.

Diamond drilling has defined the subsurface geology. The Rove Formation is sixty-six meters thick and is intruded by a two meter thick diabase sill near its base. Underlying the diabase are three meters of Rove shale which are underlain by the Gunflint Formation.

The vein systems of the Creswel Group occupy extensional faults. These faults cut the diabase, so they must be post-or syn-Keweenawan. The faults are steeply dipping, normal fractures with offsets generally less than eight meters. As in all other Mainland veins, the veins are widest and carry good silver values only when they occupy the zone immediately underlying the diabase-shale contact.

The veins are found cutting the diabase, but they are narrow and barren.

There are eighty-four different veins exposed on the Creswel property (Miles, 1933). All the veins have similar gangue mineralogy and are genetically related. The gangue is calcite, white and amethystine quartz, green and purple fluorite, galena, sphalerite, argentite and native silver. The veins have been sampled by diamond drilling for over four hundred feet into the underlying Gunflint Formation. The veins were found to be continuous but considerably narrower than near the surface.

The Porcupine Mine consists of two groups of veins, the northern group, and a southern group (also called the Eisheweiller adit). The main working of the Porcupine Mine is located in the northern group (fig. 4-1) and is called the Creswel number eight vein. The northern group of workings consists of three adits and one shaft. The adits are located one above the other on the hillside sloping up to the diabase cap. There is a shaft of unknown depth sunk thirty meters to the north of the number eight vein. This is not connected to the main workings.

The vein occupies a fault zone that averages one meter wide and strikes eighty degrees with a subvertical dip. The total fault offset is four meters, north side up.

Porcupine Mine Cross Section

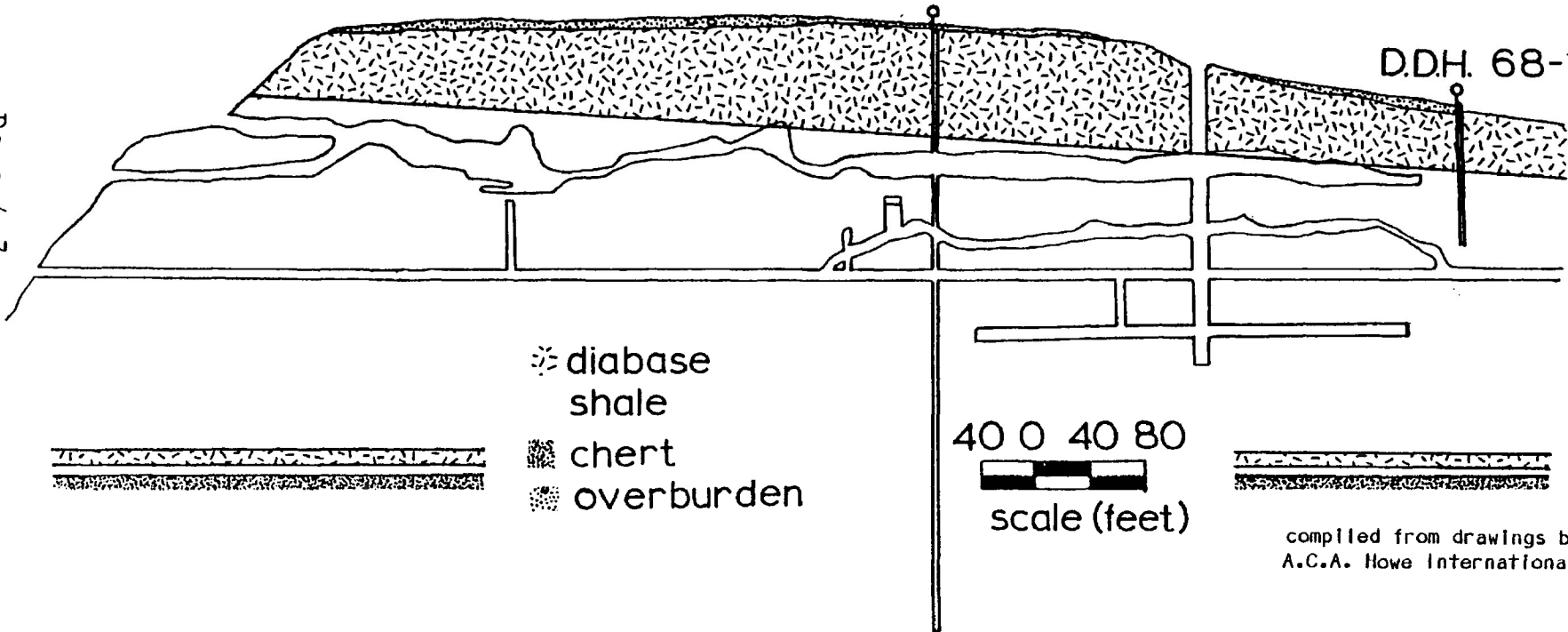
W

E

D.D.H. 68-3

D.D.H. 68-13

Page 4-7



- ⊗ diabase shale
- ▨ chert
- ⋯ overburden

40 0 40 80
scale (feet)

compiled from drawings by
A.C.A. Howe International LTD.

Figure 4-1. Porcupine Mine cross section, showing subsurface geology and the vertical projection of D.D.H. 68-13 and D.D.H. 68-3.

The movement was initially normal, but renewed activity reactivated the fault with reverse movement (Franklin, 1970). Two diamond drill holes, D.D.H. 68-3 and 68-13, were examined from the Creswel Mines Limited. These drill holes intersect the vein system at two points (fig. 4-2 and 4-3) and define the general stratigraphy of the area.

The Eischweiller workings are located about six hundred feet south of the main workings. The vein does extend into the diabase, but it quickly pinches out. Miles (1933) reported that small amounts of cobalt were found in the trenching at the Eischweiller vein.

The Keystone property encompasses six veins. Three of the veins underwent some development work besides from surface trenching. The vein examined in this study is vein number six, also termed vein number three in the older literature. This vein has two shafts sunk on it, one to sixty feet and one to eighty feet (fig. 4-4 and 4-5). The two shafts are joined by trenching.

The average vein width is four and a half feet, but it varies from eight inches to twenty feet (Miles, 1933). The vein occupies a fault zone striking 80° with a subvertical dip. This parallels a large fault indicated by a valley to the southeast of the vein.

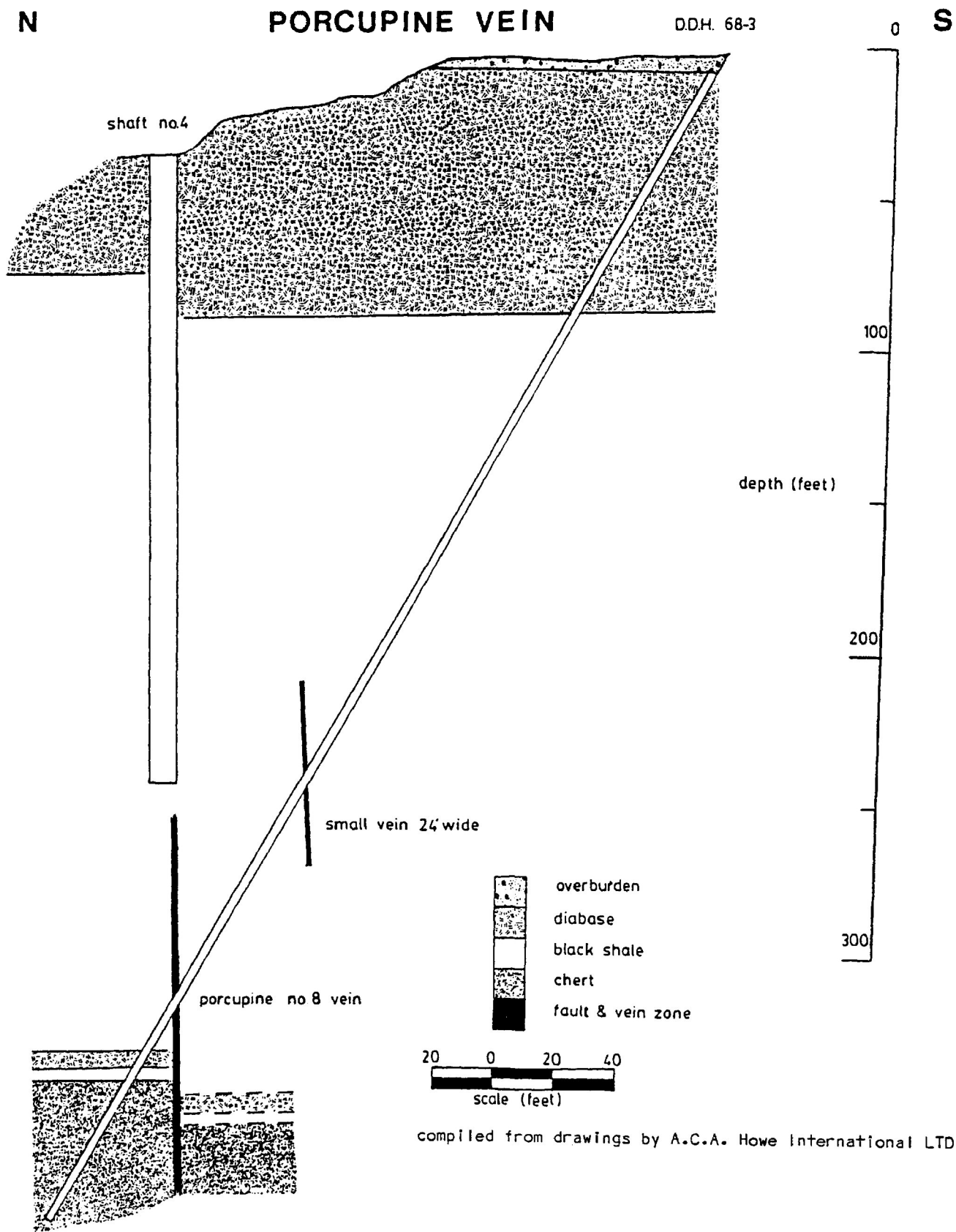


Figure 4-2. Cross section of the Porcupine number eight vein showing subsurface geology and the vertical projection of D.D.H. 68-3

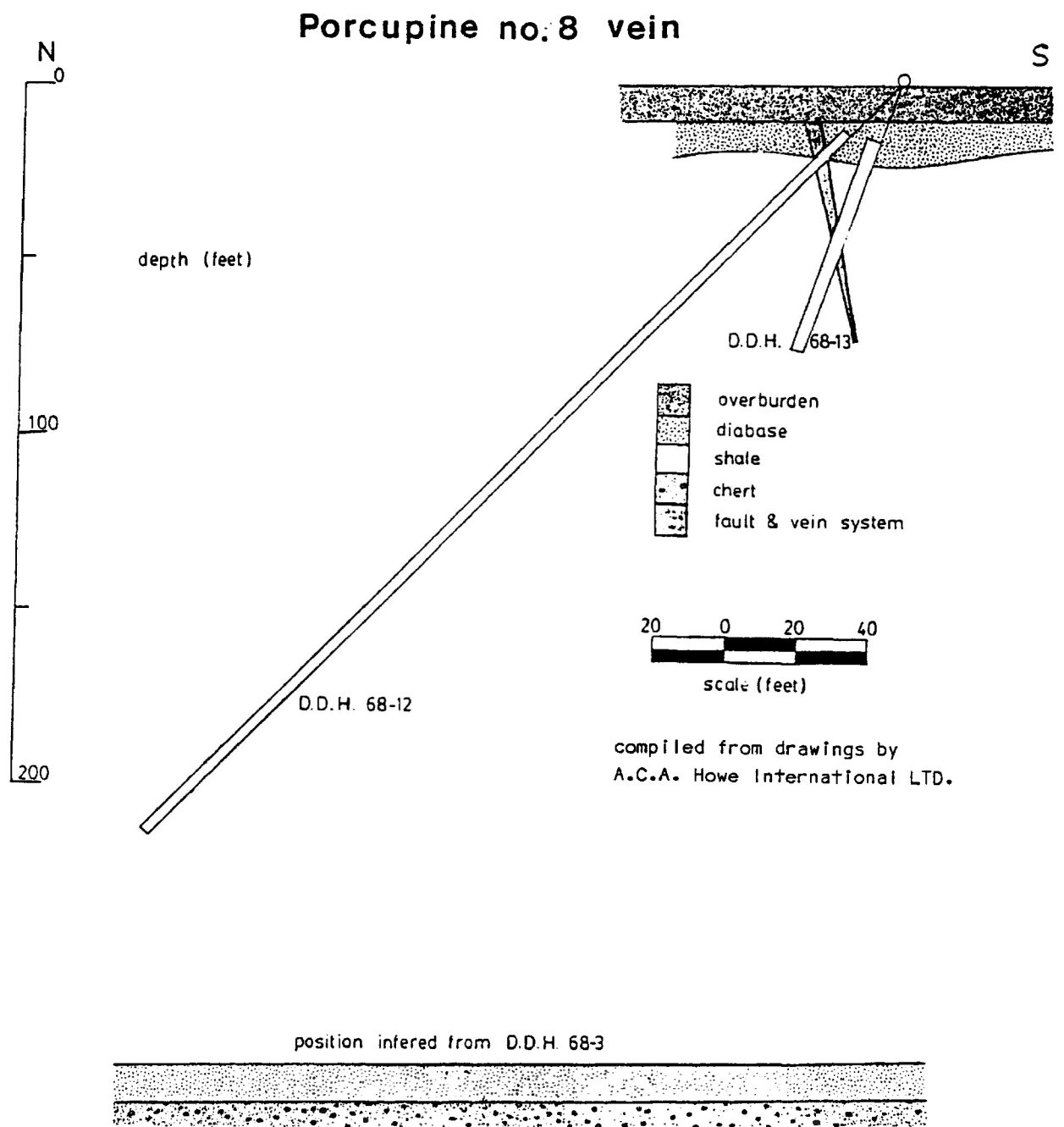
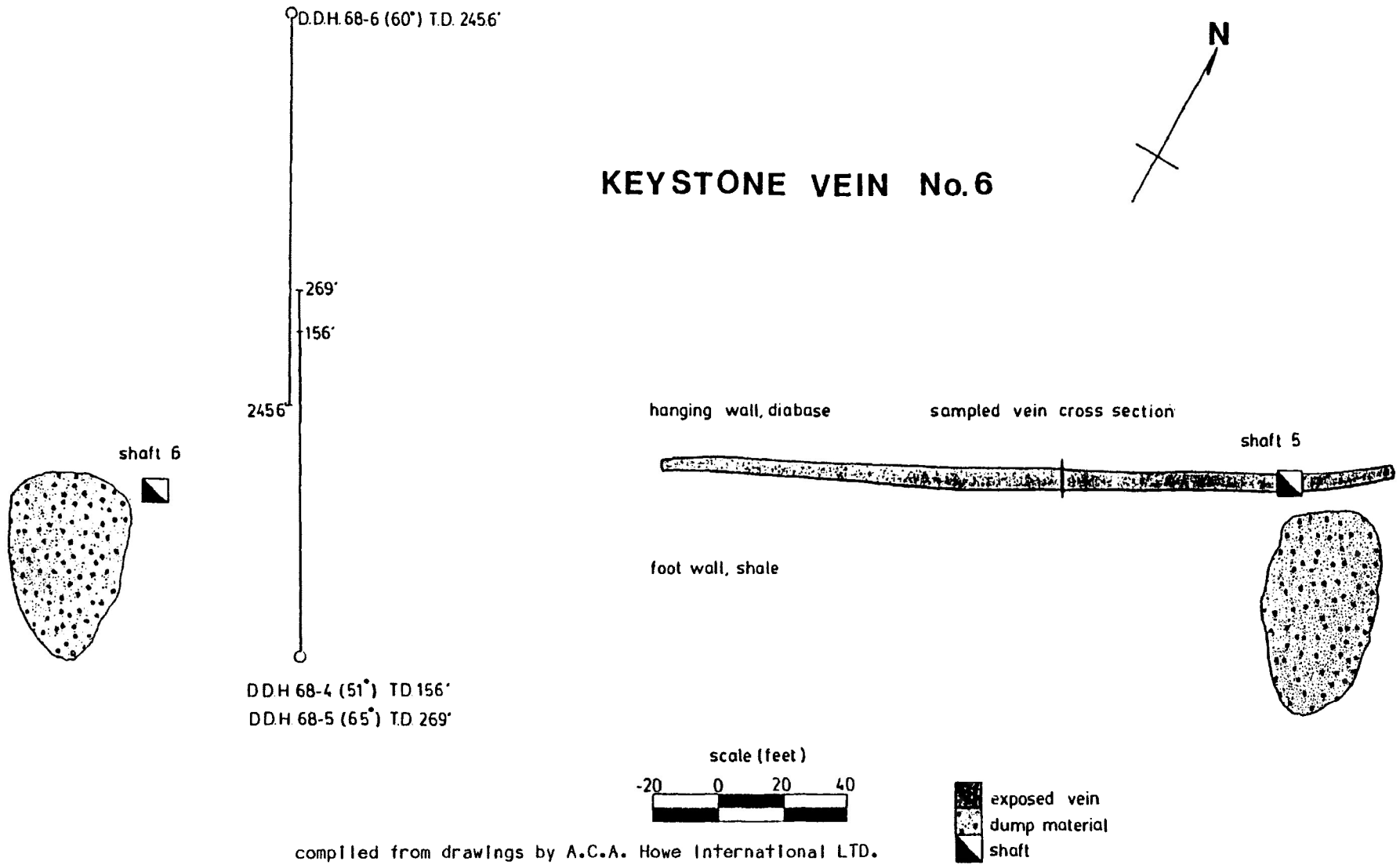


Figure 4-3. Cross section of the Porcupine number eight vein showing subsurface geology and the vertical projection of D.D.H. 68-13 and D.D.H. 68-12.

Two diamond drill holes, D.D.H. 68-5 and 68-6, from the Creswel number 6 vein were examined. These drill holes intersect the vein in two places (fig. 4-6) and define the subsurface geology.



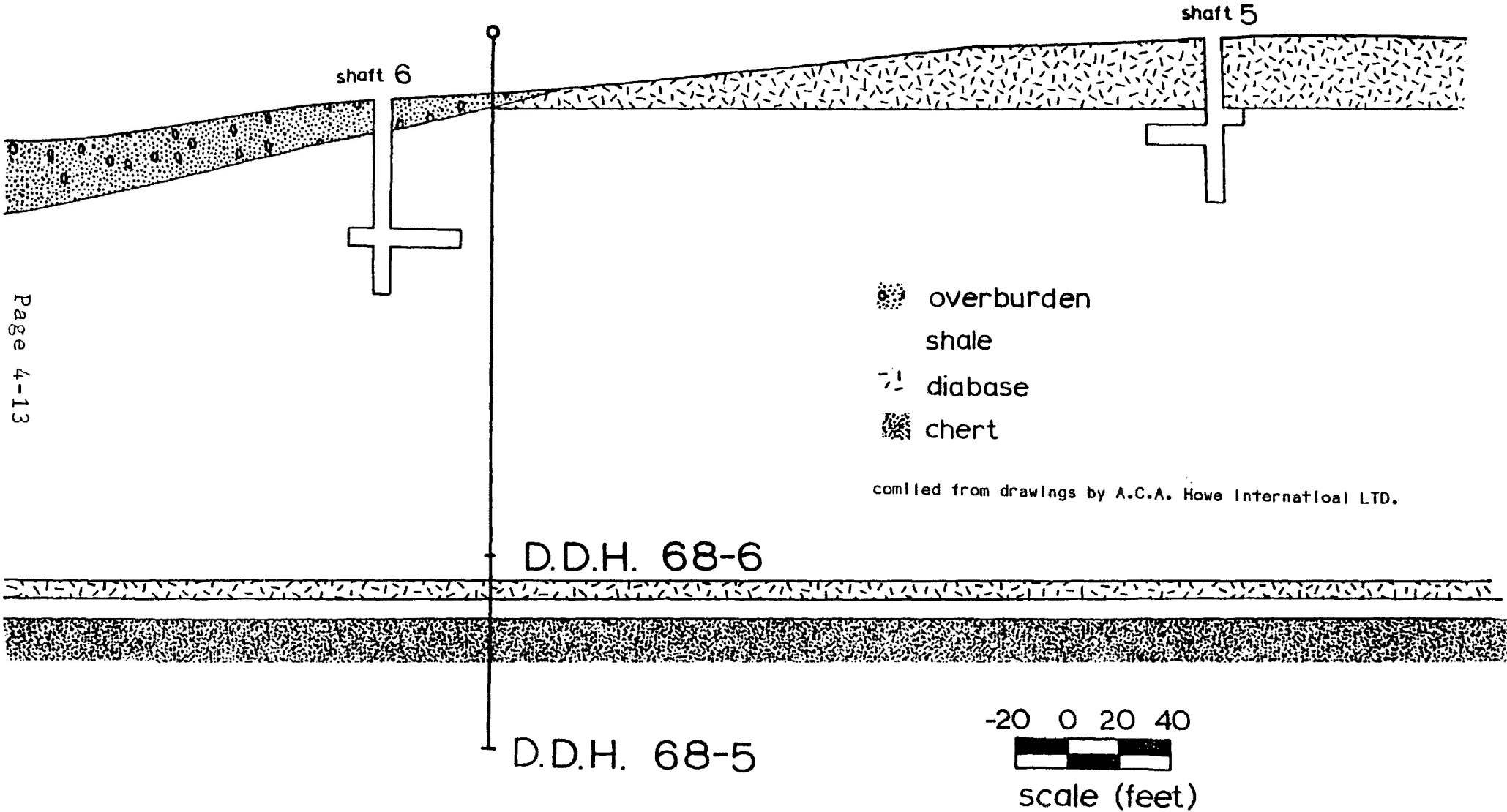
compiled from drawings by A.C.A. Howe International LTD.

Figure 4-4. Detailed map of Keystone number six vein, showing horizontal projection of D.D.H. 68-5 and D.D.H. 68-6.

SW

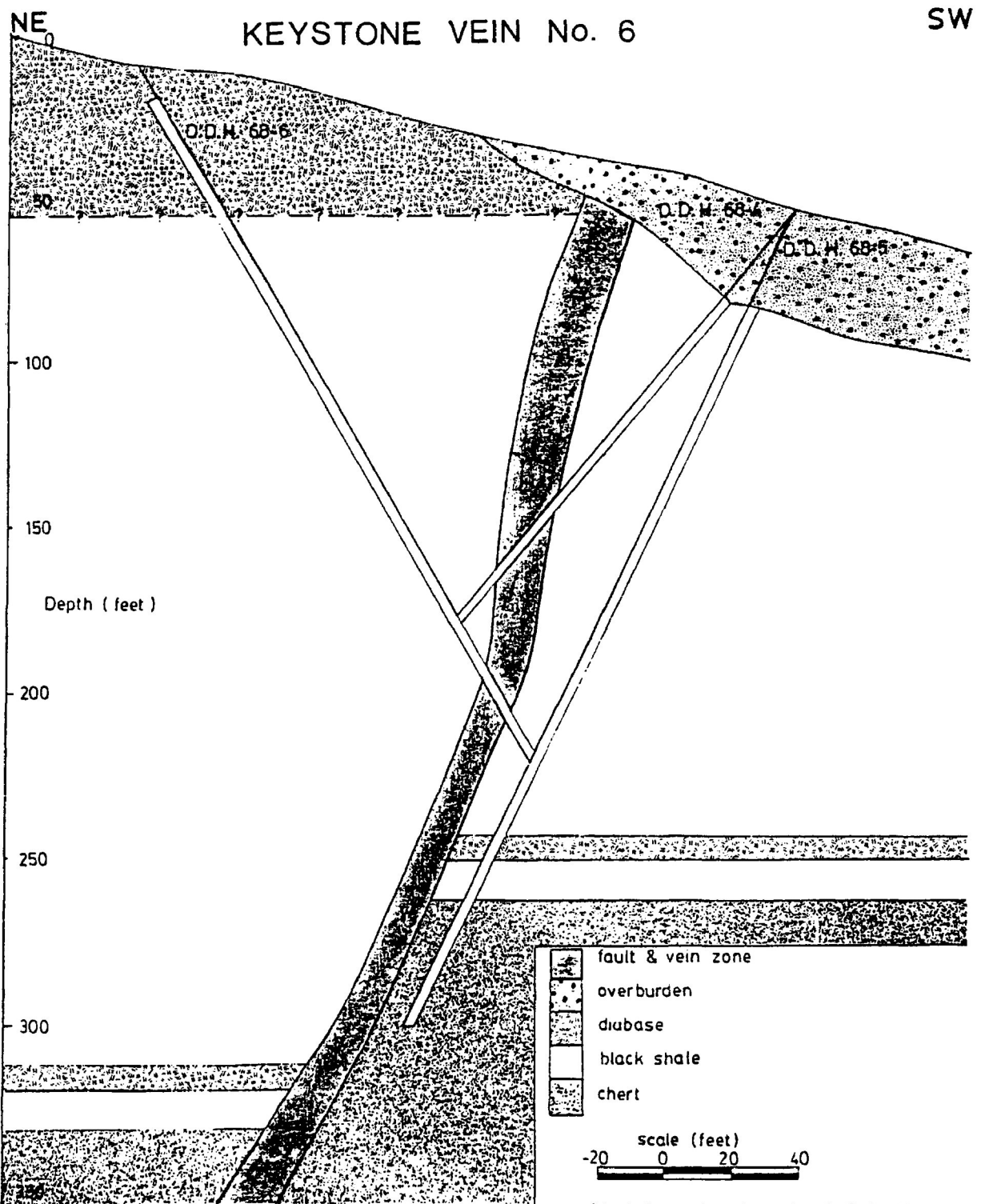
Keystone Mine cross section

NE



Page 4-13

Figure 4-5. Keystone Mine cross section at number six vein showing subsurface geology and vertical projection of D.D.H. 68-5 and D.D.H. 68-6.



compiled from drawings by A.C.A. Howe
International LTD.

Figure 4-6. Cross section of the Keystone Mine showing subsurface geology and the vertical projection of D.D.H. 68-4, 68-5 and 68-6

Fluid Inclusion Study

Fluid inclusion analysis were conducted for both surface and core samples from the Porcupine and Keystone veins. Fluid inclusions were found hosted in quartz, calcite, sphalerite and fluorite. There are four drill cores available from the Creswel Group, two from each of the Keystone and Porcupine Mines. Surface cross sections of the veins were also collected during this study. Sample descriptions are tabulated in Appendix Four.

Porcupine Mine

Eutectic temperatures

Initially, freezing runs were conducted on the fluid inclusions. The eutectic temperature was determined by the temperature of onset of melting in the inclusion.

The results are graphed (fig 4-7) and indicate temperature peaks at -36°C and -44°C . These temperatures correspond to a stable NaCl-MgCl_2 eutectic (-35°C ; Crawford, 1981) and a metastable NaCl-MgCl_2 eutectic (-44°C ; Davis *et al.*, 1988), respectively. There are smaller peaks that correspond to NaCl-CaCl_2 (-52.0°C) and MgCl_2 (-33.6°C) eutectics (Crawford, 1981). There is a peak at -38°C which may correspond to a metastable NaCl-KCl eutectic (-38°C ;

PORUPINE MINE FLUID INCLUSION DATA EUTECTIC TEMPERATURES

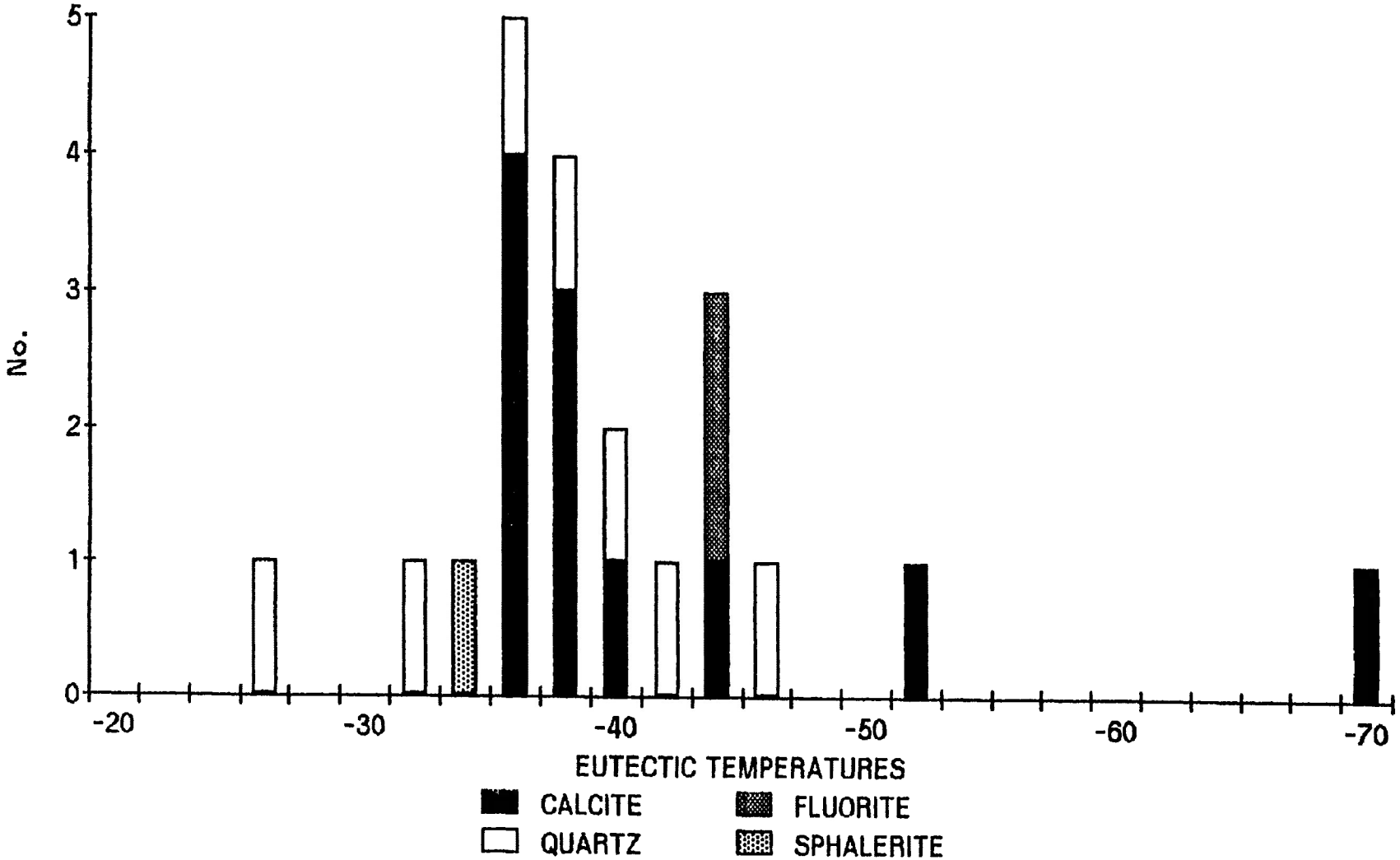


Figure 4-7. Histogram of the eutectic temperature for 21 fluid inclusions hosted in the Porcupine number eight vein.

Davis et al., 1988) or a NaCl-MgCl₂ eutectic (-35°C; Crawford, 1981). This peak is probably due to a NaCl-MgCl₂ eutectic since there is no evidence of a stable eutectic temperature for a NaCl-KCl solution (-22.9°C; Crawford, 1981).

There is some evidence for CO₂-H₂O fluids. One inclusion with a eutectic temperature of -69.5°C was observed. This inclusion was from calcite that formed in the final phase of vein formation.

There are no trends found in the eutectic temperature data either with depth in the vein or with paragenesis. The scatter of data indicates that the fluids were heterogeneous on a local scale, but the overall bulk composition of the fluid was mainly NaCl, MgCl₂ and to a lesser extent CaCl₂.

Salinity

The salinity of the solution is calculated using the final melting temperature and the equation from Potter et al., (1978). The results are presented the histogram 4-8. It shows a peak at 8 weight % NaCl, with a normal distribution around the peak, indicating the average salinity of the fluid. It is apparent that although the

PORCUPINE MINE FLUID INCLUSION DATA

SALINITY

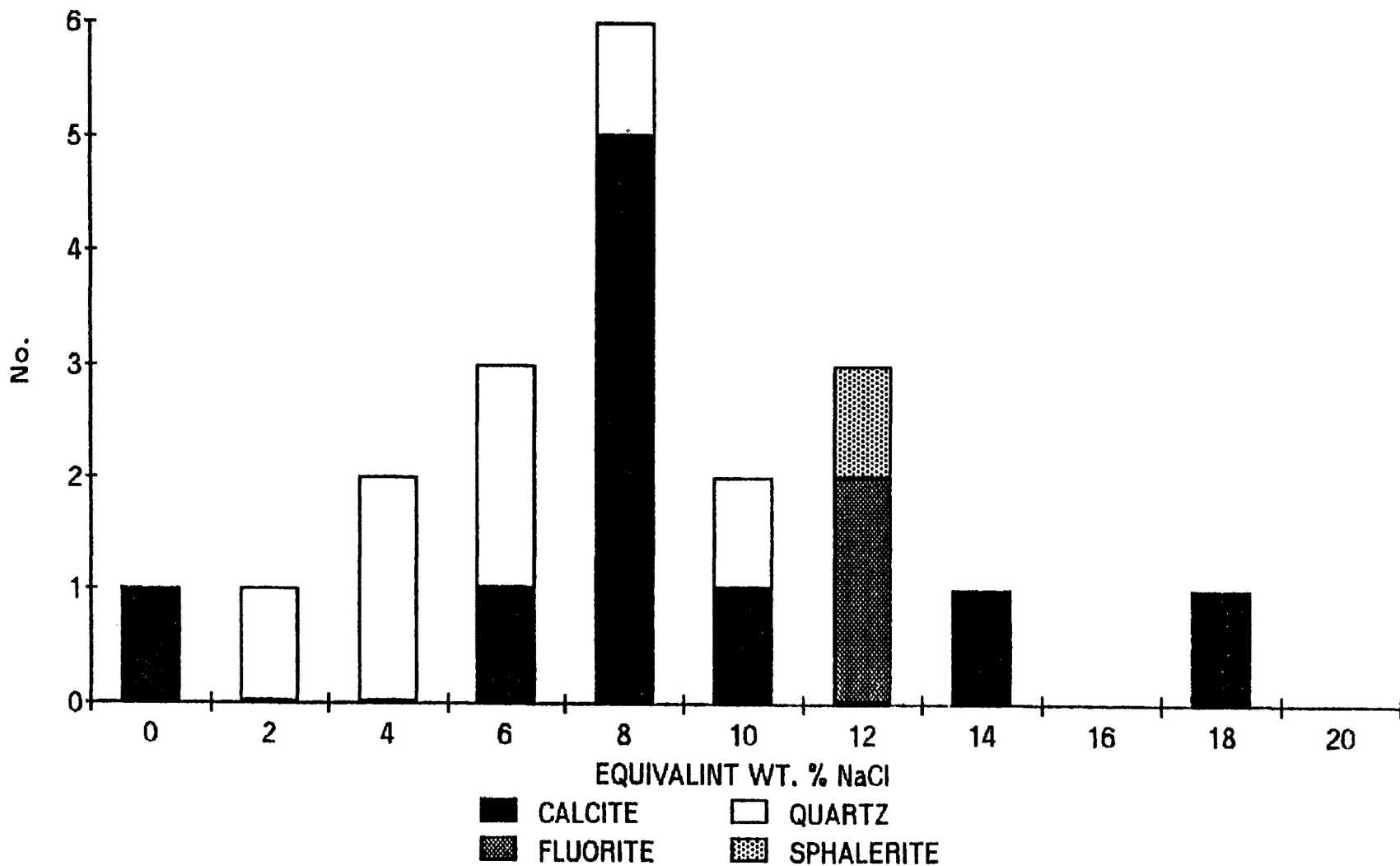


Figure 4-8. Histogram of salinity values, expressed as equivalent weight percent NaCl, for the Porcupine number eight vein. The salinity values were calculated using the final melting temperature and the equations of Potter *et al.*, (1978).

salinity is variable, it is still quite low. No daughter crystals were observed in any fluid inclusions suggesting that the fluids were unsaturated with respect to NaCl.

There does appear to be a trend for increasing salinity with paragenesis, which could be the result of boiling. The quartz is the initial phase to be precipitated from a boiling fluid. The boiling would concentrate the fluid, so that subsequent minerals to form would precipitate from a more saline fluid. These conclusions are based on only twenty freezing runs. As the stable isotope data will demonstrate, there was mixing of the fluids with depth in the system. The vein shows evidence of fracturing and renewed precipitation of gangue. This indicates that the vein fluid was likely a mixture of several generations of fluids. Thus, the salinity data should not be interpreted as the evolution of an isolated fluid.

Homogenization Temperatures

Homogenization temperatures are obtained from inclusions hosted in twenty-nine quartz samples. The results are graphed as a histogram (fig. 4-9). It indicates that quartz precipitated from a boiling fluid at 380, 300, 280 and 260°C. These temperatures correspond to discrete pulses of fluid that had no fracturing event separating the pulses.

PORCUPINE MINE FLUID INCLUSION DATA

QUARTZ HOMOGENIZATION TEMPERATURES

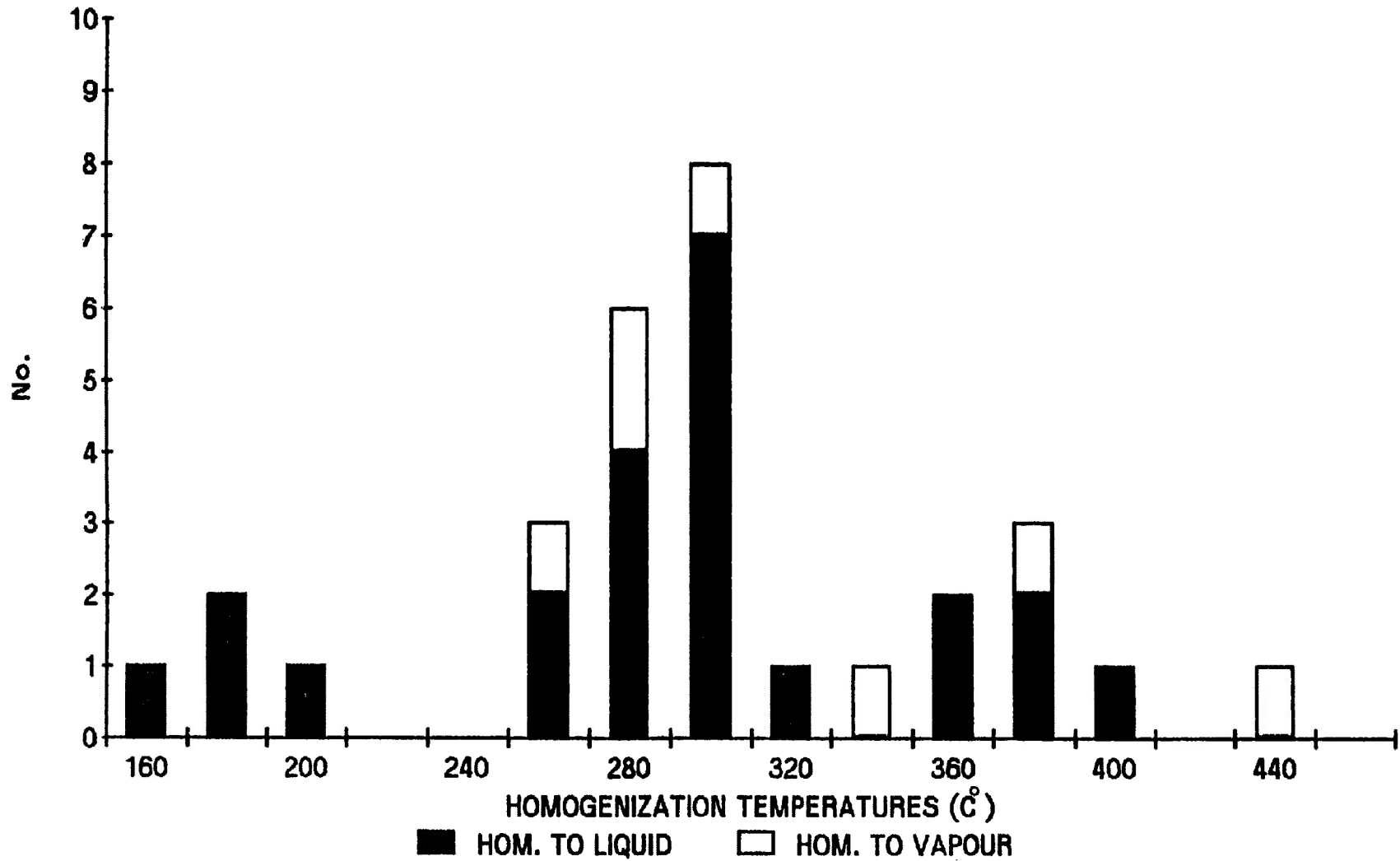


Figure 4-9. Histogram of twenty-nine homogenization temperatures for fluid inclusions hosted in quartz. Data are from the Porcupine number eight vein.

Homogenization temperatures are also obtained from twenty inclusions hosted in calcite. These temperatures indicate that calcite precipitated out of a non-boiling fluid at a fairly constant temperatures. The homogenization temperatures are plotted as a function of depth below ground level (fig. 4-10). This indicates a strong trend of increasing temperature with depth and is consistent with the results from the Shuniah Mine.

Paragenesis

The paragenetic diagram (fig. 4-11) is based on sixty-two fluid inclusion homogenization temperatures and examination of the vein cross section. The paragenesis shows that the initial mineral to precipitate was quartz from a boiling fluid. The fluid was injected as several pulses at various temperatures, as described in the Shuniah Mine. These pulses were not necessarily associated with a fracturing event. It is not possible to separate the pulses as was done with the Shuniah Mine data.

Following the formation of quartz was fluorite from a boiling fluid at 265°C. The fluid then cooled, and when it reached a temperature of approximately 80°C, calcite and the bulk of the sulfides precipitated. The metallic

**PORCUPINE MINE FLUID INCLUSION DATA
CALCITE HOMOGENIZATION TEMPERATURES**

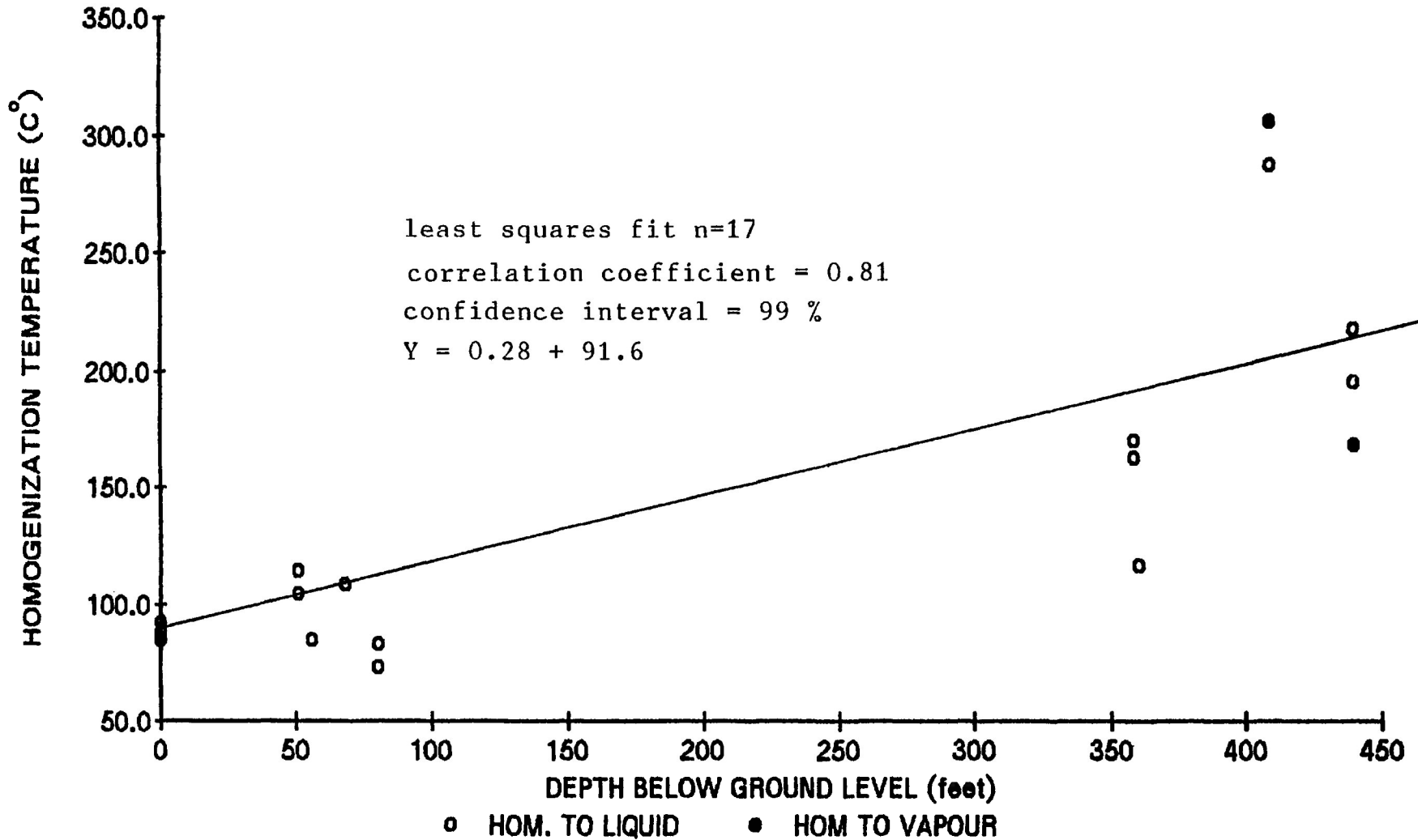
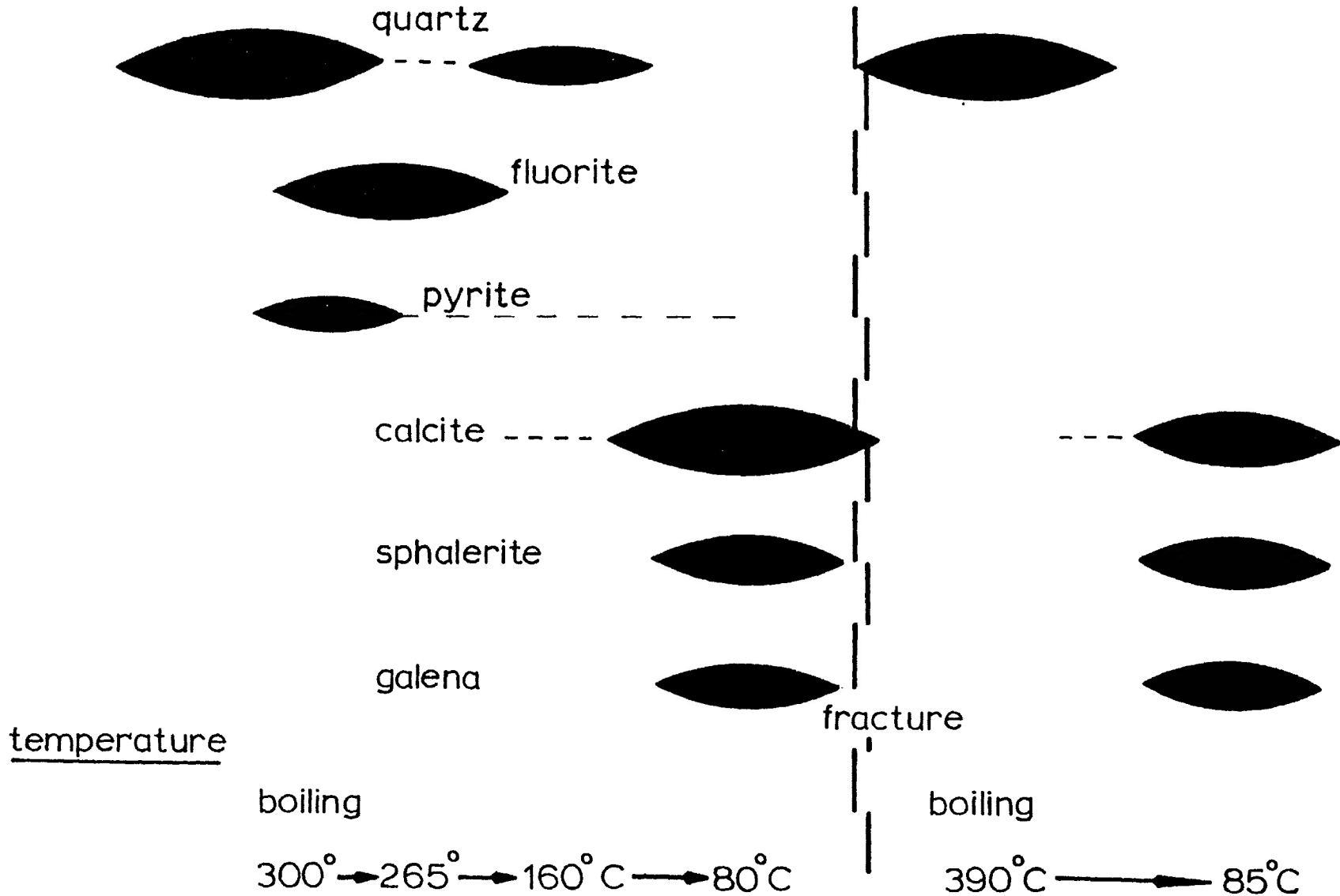


Figure 4-10. Graph of homogenization temperatures from fluid inclusions hosted in calcite as a function of depth. Data is from the Porcupine number eight vein.

Porcupine vein no. 8



Page 4-23

Figure 4-11. Paragenetic diagram for the Porcupine number eight vein.

minerals have a characteristic paragenesis, with pyrite initially precipitating followed by sphalerite and galena.

The vein shows evidence of a fracturing event. After the fracturing occurred, the vein was invaded by a boiling fluid, and the same paragenesis as the pre-fracture mineralization is found.

Keystone Mine

Eutectic Temperatures

The eutectic temperatures for the Keystone Mine were determined using seventeen samples of calcite, fluorite, quartz and sphalerite. The results are graphed in figure 4-12 and show a peak at -36°C , which corresponds to a NaCl-MgCl_2 eutectic (-35°C ; Crawford, 1981). There are also peaks at around -40°C , which probably corresponds to a metastable NaCl-MgCl_2 eutectic (-44°C ; Davis *et al.*, 1988). There is a peak at -48°C , which corresponds to a CaCl_2 eutectic (-48.9°C ; Crawford, 1981). The temperatures are skewed to slightly lower temperatures probably due to error in determining the onset of melting.

There is some evidence for a $\text{CO}_2\text{-H}_2\text{O}$ fluid suggested by an inclusion with the eutectic temperature of

KEYSTONE MINE FLUID INCLUSION DATA

EUTECTIC TEMPERATURES

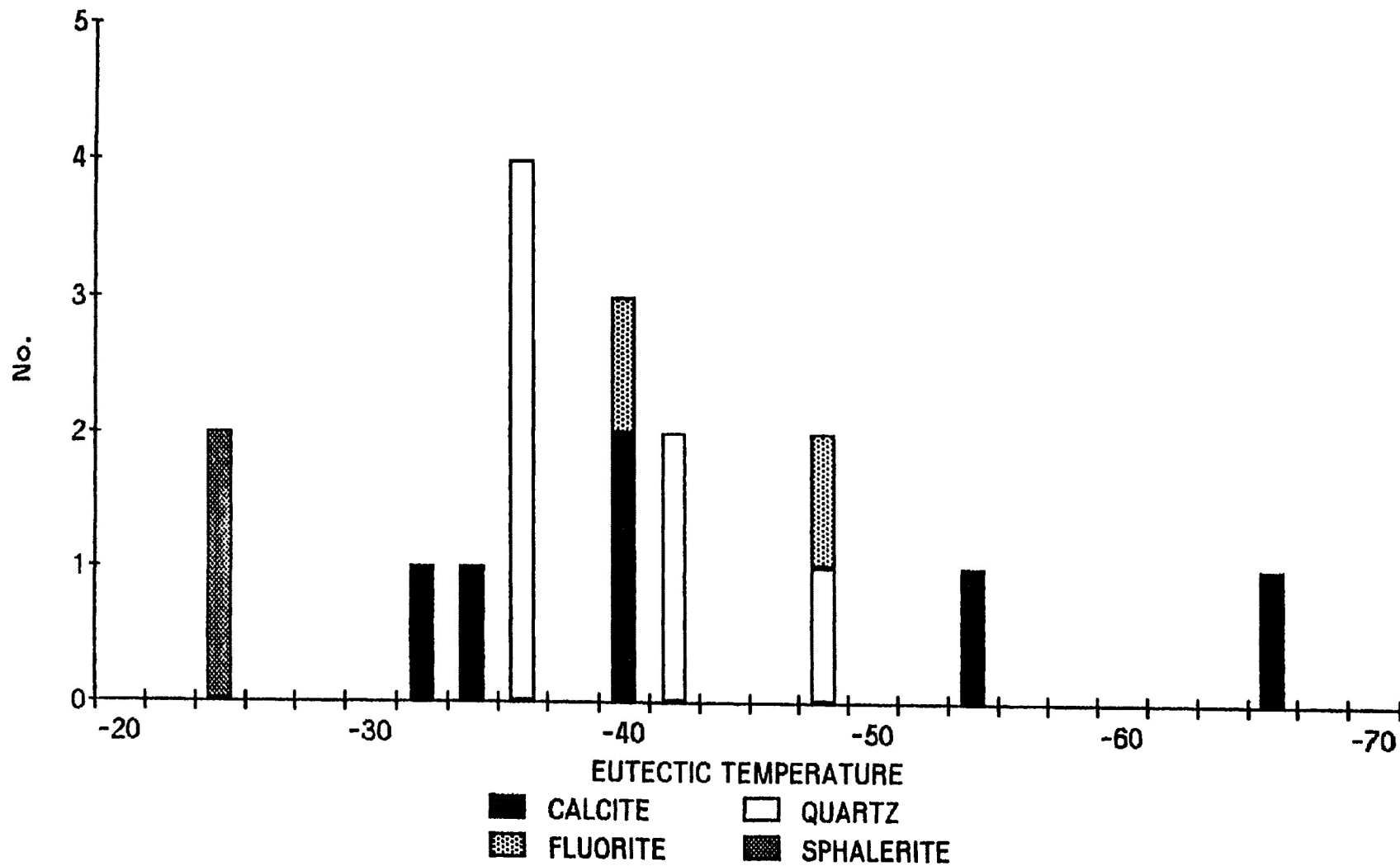


Figure 4-12. Histogram of the eutectic temperature for 17 fluid inclusions hosted in the Keystone number six vein.

-66.2°C. This is constrained to the last phase of calcite, and does not occur in any of the other phases.

There are no trends found in the eutectic temperature data either with depth in the vein or with paragenesis. The scatter of data indicates that the fluids were heterogeneous on a local scale, but the overall bulk composition of the fluid was mainly NaCl, MgCl₂ and to a lesser extent CaCl₂.

Salinity

The salinity data of the Keystone Mine were determined by the final melting temperature and using the equations of Potter et al., (1978) and are graphed in fig. 4-13. The histogram of the salinity does not show any peaks nor any trend with either host or depth. The data indicate that the salinity of the fluid was variable and is probably the result of boiling combined with fluid mixing. As with the Porcupine Mine the salinity data are variable but quite low. No daughter crystals were seen in any fluid inclusions examined, which suggests that the fluid was unsaturated with respect to NaCl.

KEYSTONE MINE FLUID INCLUSION DATA

SALINITY

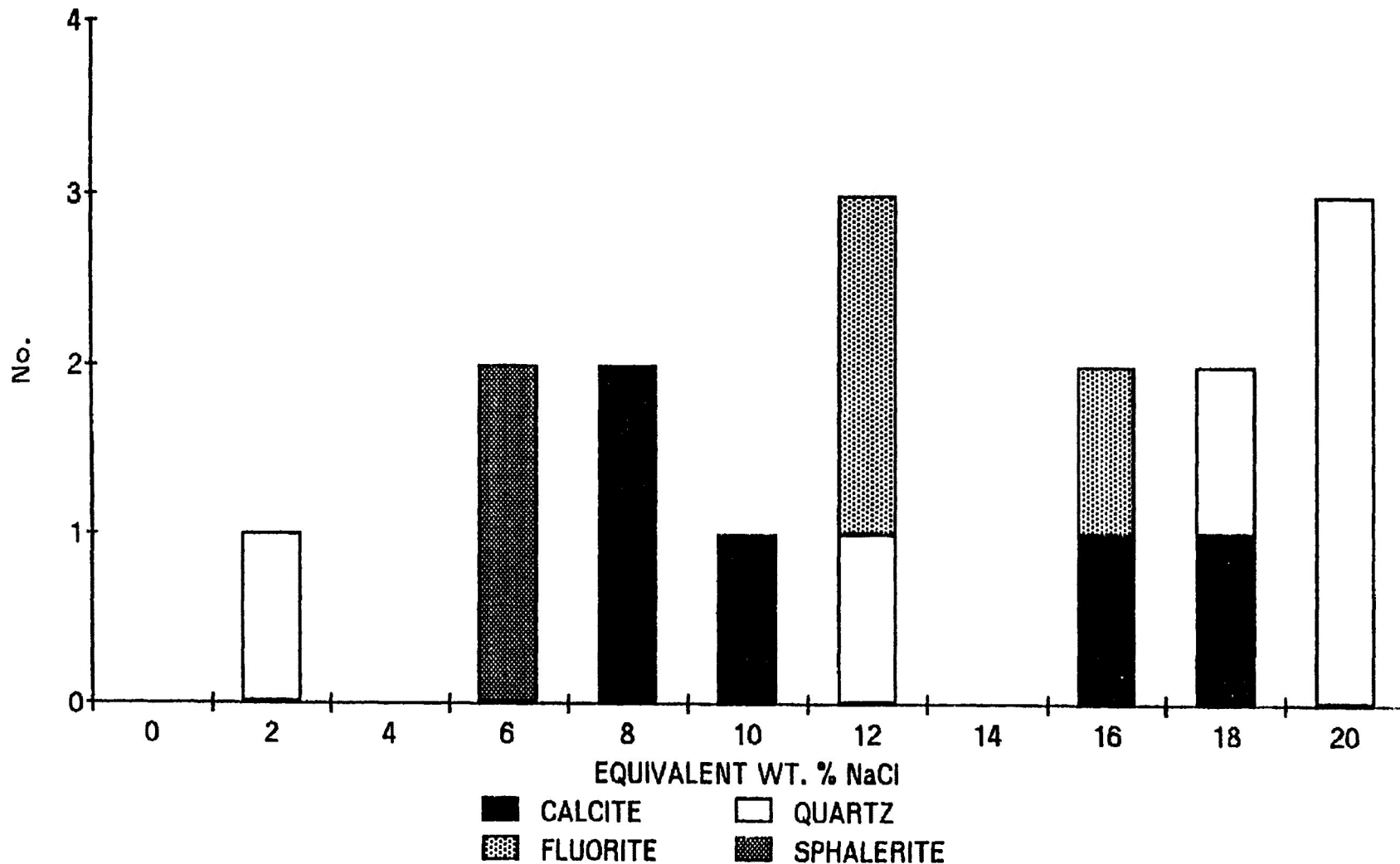


Figure 4-13. Histogram of salinity values, expressed as equivalent weight percent NaCl, for the Keystone number six vein. The salinity values were calculated using the final melting temperature and the equations of Potter *et al.*, (1978).

KEYSTONE MINE FLUID INCLUSION DATA

QUARTZ HOMOGENIZATION TEMPERATURES

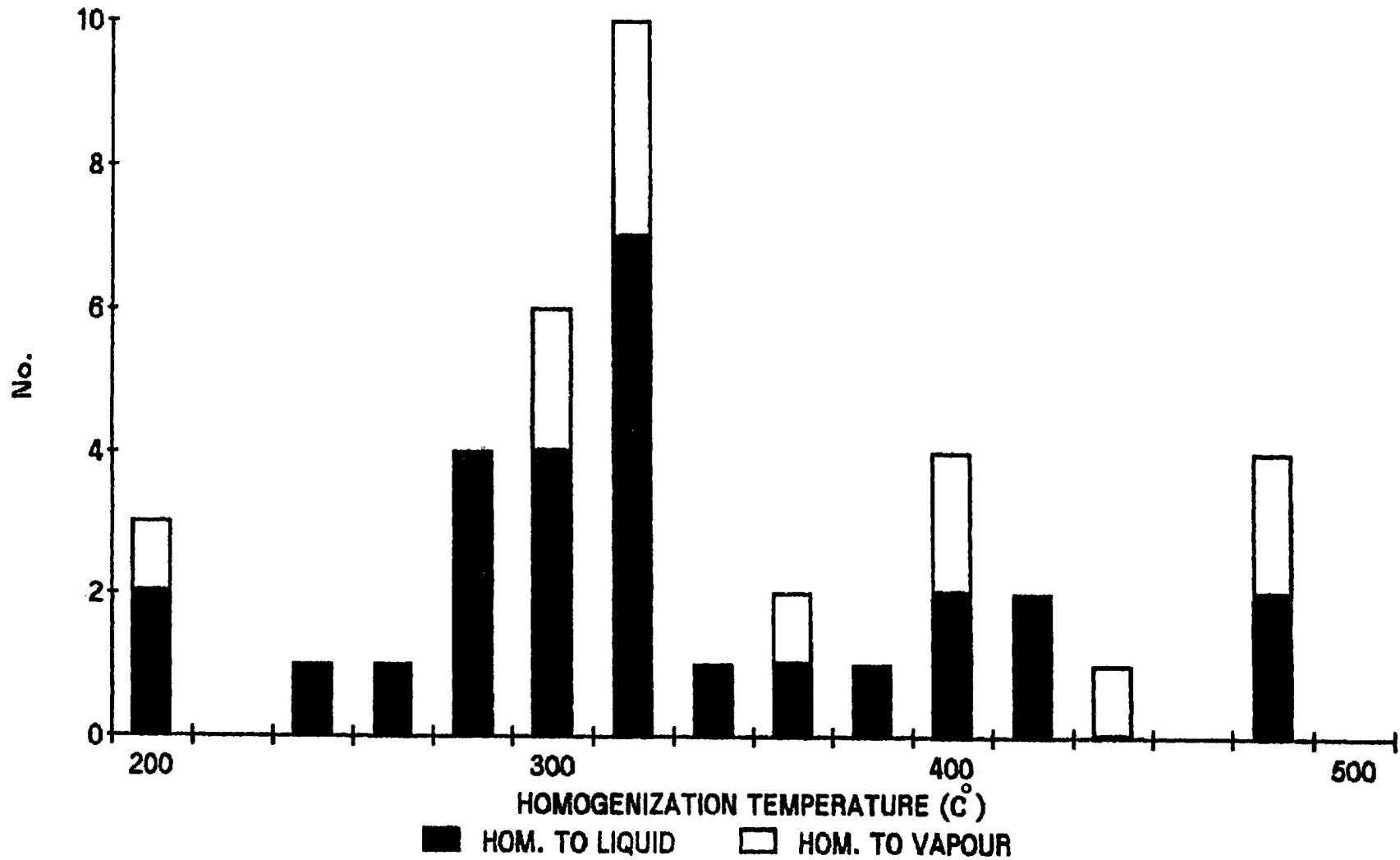


Figure 4-14. Histogram of forty homogenization temperatures from fluid inclusions hosted in quartz. Data are from the Keystone number six vein.

Homogenization Temperature

Homogenization temperatures were obtained from forty inclusions hosted in quartz. The results are graphed in fig. 4-14 and indicate that the fluid was boiling at 475, 410, 360, 300 and 200°C. These boiling temperatures are the result of discrete pulses of fluid injected into the vein system. Each pulse of fluid may or may not have an associated fracturing event.

The homogenization temperature was obtained for eight inclusions hosted in calcite. The results are graphed (fig. 4-15) as a function of depth. As with the Porcupine and the Shuniah Mines, there is a strong increase in temperature with depth.

Paragenesis

The paragenetic diagram for the Keystone Mine (fig. 4-16) is based on sixty fluid inclusion homogenization temperatures and examination of the vein cross section. The initial mineral to form was quartz, then fluorite from a boiling fluid at 300°C. The solution cooled, and quartz again precipitated at 160°C. When the solution reached a temperature of 80°C, calcite and the bulk of the sulfides precipitated. There was a fracturing episode and renewed injection of boiling fluid from which quartz precipitated at 475°C, 410°C and 360°C. When the solution cooled to about 100°C, calcite and the bulk of the sulphides precipitated.

KEYSTONE MINE FLUID INCLUSION DATA CALCITE HOMOGENIZATION TEMPERATURES

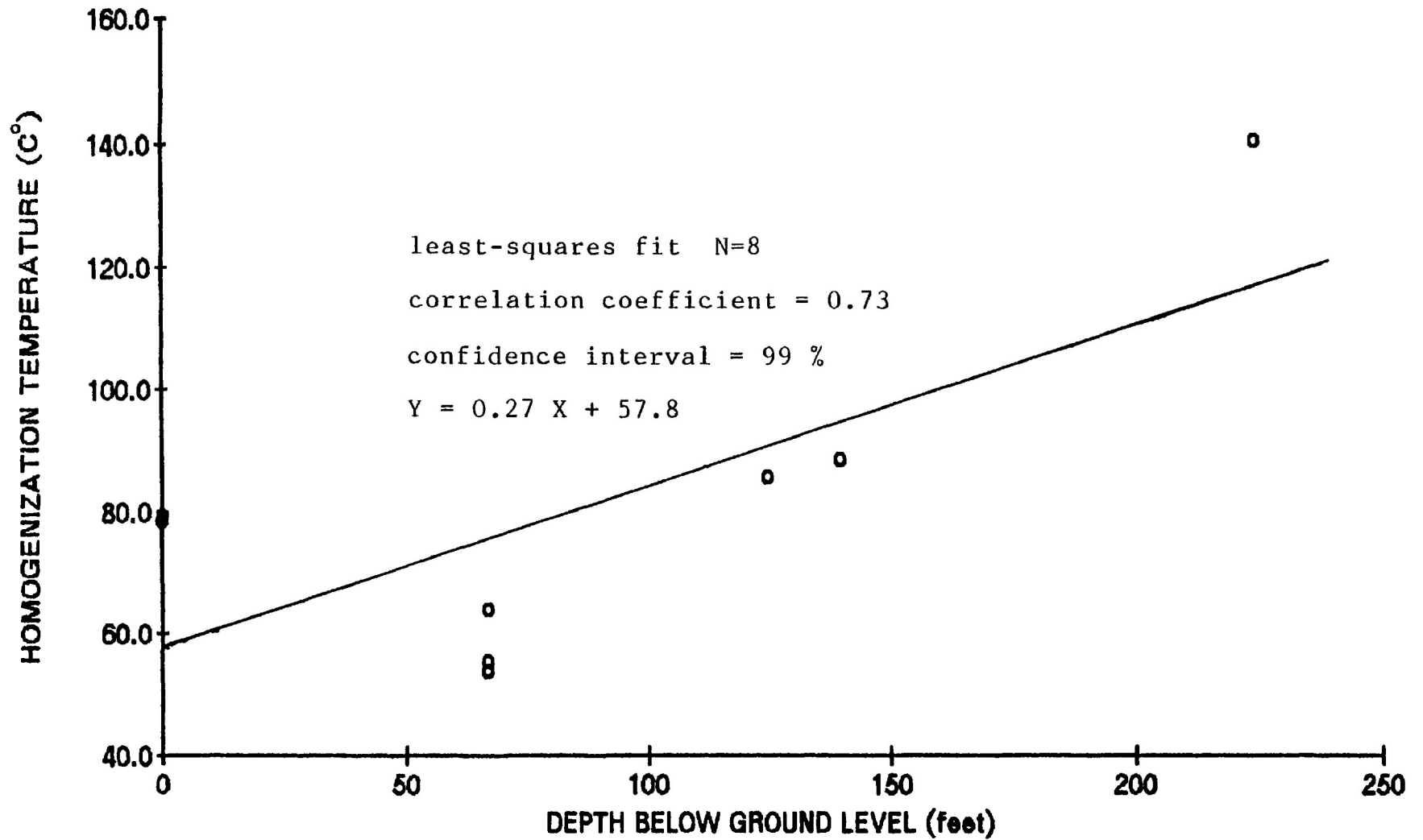


Figure 4-15. Graph of homogenization temperatures from fluid inclusions hosted in calcite as a function of depth. Data is from the Keystone number six vein.

Keystone vein no. 6

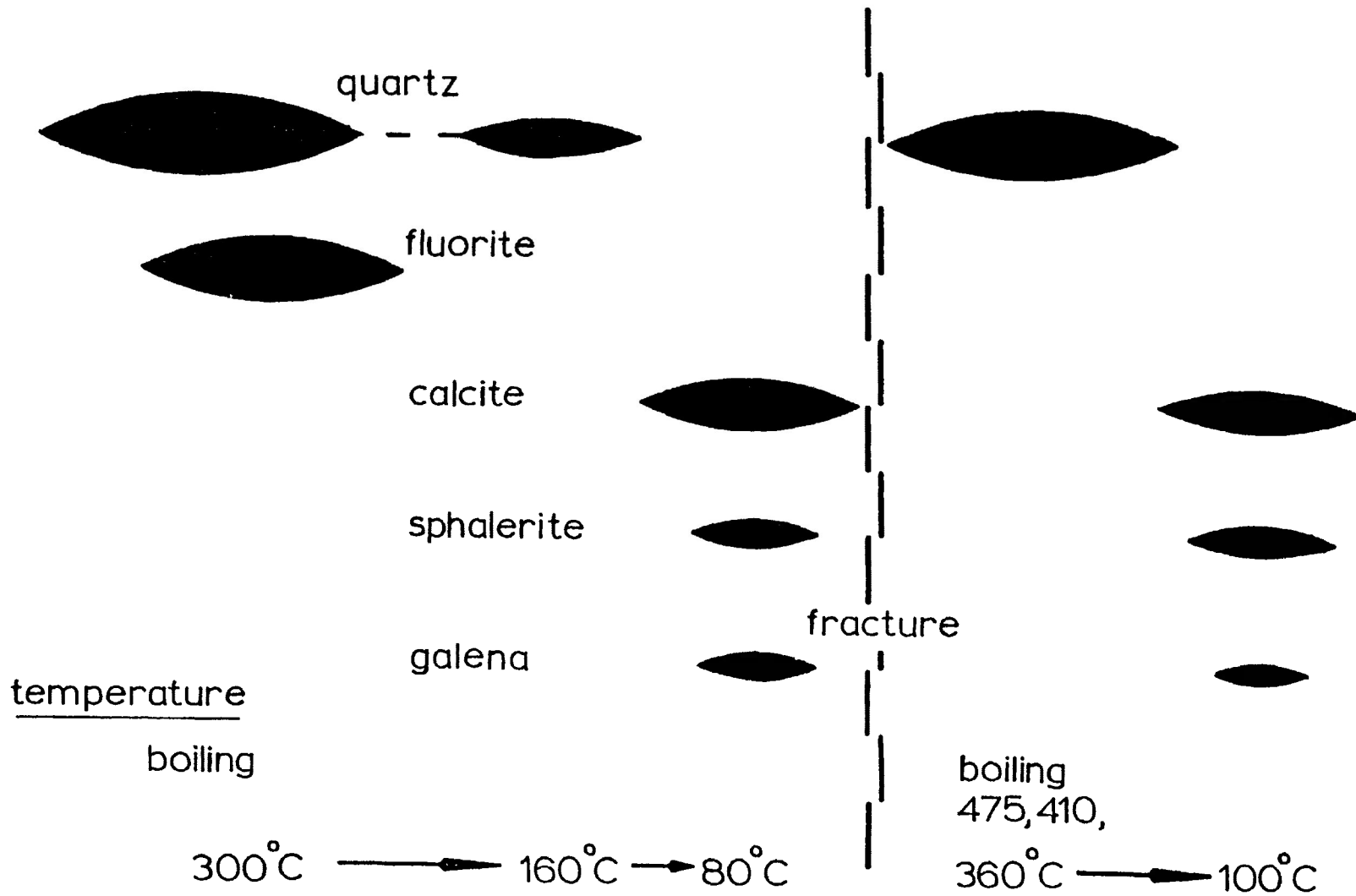


Figure 4-16. Paragenetic diagram for the Keystone number six vein.

Stable Isotope Data

Five samples of calcite from the Porcupine vein and three samples from the Keystone vein were analyzed for carbon and oxygen isotope ratios from both core and surface samples. The samples were selected to give an indication of how the isotopic ratios vary with depth. The maximum depth from which samples were available is four hundred forty feet. Each sample had a fluid inclusion homogenization temperature, so a fractionation factor for calcite-H₂O and calcite-HCO₃⁻ was calculated (table 4-1).

The plot of $\delta^{18}\text{O}$ as a function of depth (fig. 4-17) shows a trend for increasingly positive ratios with depth. This indicates that the water's oxygen ratio tended to become progressively lighter as the fluid migrated upwards. This could be the result of mixing of an originally isotopically heavy fluid with a isotopically lighter fluid. It could also be the result of fluid boiling. In either case the isotopic signature of the most pristine fluid is indicated by the isotopic values for the deepest sample. This sample would form from a fluid that had undergone the least amount of contamination and had also undergone the least amount of boiling. The initial fluid composition probably had an oxygen isotope ratio of around 2 to 6‰.

TABLE 4-1

CRESWEL STABLE ISOTOPE DATA

PORCUPINE MINE
CARBONATE OXYGEN AND CARBON ISOTOPE RATIOS

<u>SAMPLE No.</u>	<u>DEPTH (feet)</u>	<u>TEMP. (C°)</u>	<u>δ ¹⁸O_{cc}</u>	<u>δ ¹⁸O_{WATER}</u>
PO4	0	92.4	10.8	-7.1
68-13-42	42	80.0	15.2	-4.2
68-13-54	54	94.0	12.6	-5.1
68-13-56	56	84.9	10.4	-8.4
68-03-440	440	194.5	12.0	2.1

<u>SAMPLE No.</u>	<u>DEPTH (feet)</u>	<u>TEMP. (C°)</u>	<u>δ ¹³C_{cc}</u>	<u>δ ¹³C_{CHCO3}</u>
PO4	0	92.4	-8.4	-8.2
68-13-42	42	80.0	-8.1	-7.9
68-13-54	54	94.0	-8.1	-7.9
68-13-56	56	84.9	-8.1	-7.9
68-03-440	440	194.5	-7.4	-7.0

KEYSTONE MINE
CARBONATE OXYGEN AND CARBON ISOTOPE RATIOS

<u>SAMPLE No.</u>	<u>DEPTH (feet)</u>	<u>TEMP. (C°)</u>	<u>δ ¹⁸O_{cc}</u>	<u>δ ¹⁸O_{WATER}</u>
5-125	125	85.8	11.3	-7.4
5-140	140	88.6	11.0	-7.4
6-225	225	140.6	20.0	6.6

<u>SAMPLE No.</u>	<u>DEPTH (feet)</u>	<u>TEMP. (C°)</u>	<u>δ ¹³C_{cc}</u>	<u>δ ¹³C_{CHCO3}</u>
5-125	125	85.8	-7.1	-6.9
5-140	140	88.6	-7.1	-6.9
6-225	225	140.6	-7.8	-7.5

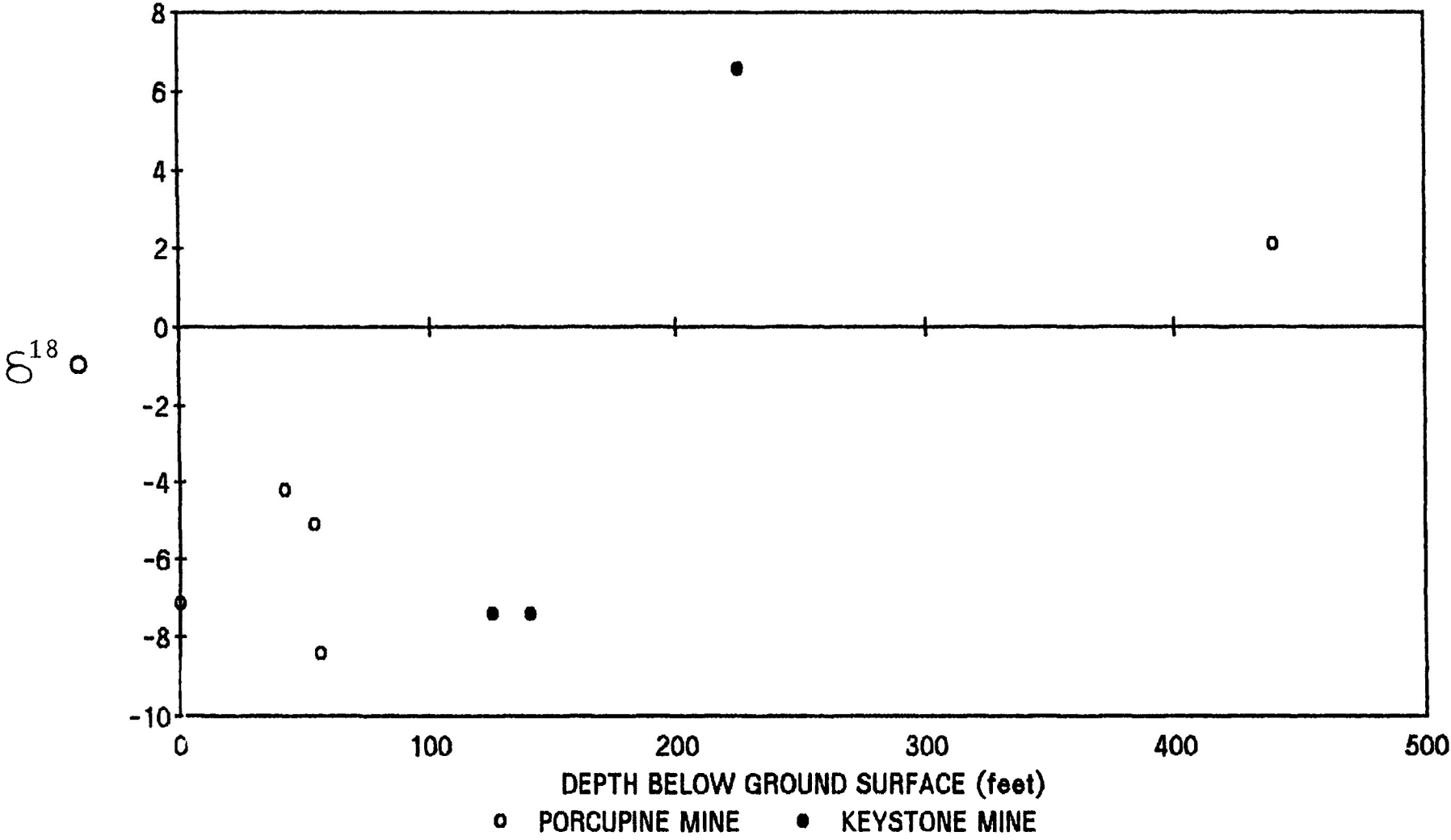
OXYGEN AND DEUTERIUM ISOTOPE RATIOS

<u>SAMPLE No.</u>	<u>DEPTH (feet)</u>	<u>TEMP. (C°)</u>	<u>δ ¹⁸O_{ILLITE}</u>	<u>δ ¹⁸O_{WATER}</u>
SM	0	129.6	12.1	1.9
EA53	0	102.4	12.4	1.4

<u>SAMPLE No.</u>	<u>DEPTH (feet)</u>	<u>TEMP. (C°)</u>	<u>δ D_{ILLITE}</u>	<u>δ D_{WATER}</u>
SM	0	129.6	-66	-42.3
EA53	0	102.4	-68	-40.8

OXYGEN ISOTOPE VARIATION WITH DEPTH

DATA FROM CRESWEL GROUP



Page 4-34

Figure 4-17. Graph of oxygen isotope variations as a function of depth. Data is from the Porcupine (n=5) and the Keystone (n=3) Mines.

The carbon isotope ratios are very consistent. They average -7.5‰ with a standard deviation of 0.5‰ . This indicates that the carbon source for the hydrothermal fluids was homogeneous and constant with time.

Two samples of illite, one from the Keystone vein (EA53) and one from Silver Mountain (SM), were analyzed for both oxygen and deuterium isotope ratios. These samples were intergrown with quartz that contained fluid inclusions, which allowed a fluid inclusion homogenization temperature to be calculated. This temperature allowed the fractionation between the illite and the fluid to be calculated. The results indicate $\delta^{18}\text{O}$ of 1.9 and 1.4 and δD of -42.3 and -40.8 for SM and EA53 respectively (table 4-1).

Comparison of Porcupine and Keystone Mines

For both the Keystone and the Porcupine Mines the vein forming fluid was of the same composition, dominated by a NaCl-MgCl₂-CaCl₂ solution. In both vein systems the salinity was variable. This is probably attributable to mixing of the solution combined with boiling of the fluid.

The homogenization temperature data for the two mines are remarkably similar. Both mines show a similar paragenesis with the quartz phase precipitating from a boiling solution. The solution was injected as discrete pulses of boiling fluid at different temperatures. The solution then cooled, and calcite and the sulfides precipitated out of a non-boiling fluid around 100°C.

One of the main differences in the homogenization temperatures is that fluid inclusions hosted in Keystone Mine calcite homogenizes at about 33° lower than the Porcupine Mine's calcite. Since both mines indicate strong trends of increasing homogenization temperatures with depth, the lower homogenization temperature of the Keystone vein suggests that it was at a stratigraphically higher level than was the Porcupine Mine.

The oxygen isotope ratios exhibit the same trend for both the Porcupine and the Keystone Mines. Both vein

systems exhibit increasingly positive oxygen ratios with depth. A similar mechanism must have operated on both systems to increasingly fractionate the hydrothermal fluid to lighter oxygen isotopes. This can be attributed to either mixing or boiling as will be discussed latter.

The carbon isotope ratios are very similar. The value of $\delta^{13}\text{C} = -7.5 \text{ ‰}$ is not diagnostic of any particular environment. However, the similarity of the carbon ratios indicates that the source of the carbon was constant and similar for both vein systems.

There are some differences in the mineralogy of the two vein systems. The main difference is in the abundance and the composition of sphalerite. In the Keystone vein sphalerite is a very common vein component, easily the most abundant metallic mineral. In the Porcupine vein sphalerite is present, but it is not as common as in the Keystone vein. The composition of the sphalerite is also distinctly different. Sphalerite at the Keystone vein has anomalous concentrations of cadmium (Jennings, 1987), with concentrations ranging from 0.34 to 1.50 weight percent cadmium. Jennings (1987) found no evidence of cadmium in sphalerite from the Porcupine vein.

Cadmium is a fairly common component of sphalerite in the Thunder Bay silver district, occurring in

the Keystone, Silver Mountain, West Beaver, Rabbit Mountain, Big Harry and Edward Island veins (Jennings, 1987). The presence of cadmium in the Keystone sphalerite and not in the Porcupine sphalerite is not readily explained. The two veins are only about one kilometer apart, and the fluid inclusion and stable isotope data indicate that they shared a common or similar fluid source. There do not appear to be significant differences in the chemistry or concentrations of the two vein fluids, so salinity is not a likely cause. The Keystone vein has high fluid inclusion homogenization temperatures in excess of 475°C, which are significantly higher than the Porcupine vein fluid inclusion homogenization temperatures that never exceed 400°C. These higher fluid temperatures in the Keystone vein may be necessary for the transport of cadmium. The lower fluid temperatures in the Porcupine vein would not enhance cadmium transport, explaining its absence from the sphalerite.

Implications of the Fluid Inclusion Study

Homogenization Temperatures

The fluid inclusion homogenization temperatures present perhaps the most significant aspects of this study. For any phase of quartz or calcite identified the homogenization temperature invariably increases with depth. This trend suggests that the heat source for the fluid may not have been the hypabyssal intrusions as proposed by previous authors (Franklin, 1970, Franklin et al., 1986). If the diabase sills acted as a heat source, then the fluid inclusion homogenization temperature would be a maximum at the diabase margins and decrease with distance away from the sill. Instead the homogenization temperature increases with depth, which implies that a deep seated source must have supplied heat to the vein system.

Evidence for boiling is seen in fluid inclusions within this study. Ramboz et al. (1982) have outlined two criteria that must be observed within fluid inclusions as evidence of boiling. Adjacent primary inclusions must homogenize to a liquid and to a vapor or decrepitate at approximately the same temperature. The inclusions must be of the same generation, which gives them approximately the same time of formation. These criteria are met in the growth

zones of quartz (photo 3-2, 3-3) that are hosted in shale immediately underlying the shale-diabase contact.

The fluid inclusion homogenization temperatures indicate that the hydrothermal fluids were injected as a series of discrete pulses. Each pulse migrated upwards and entered a zone of dilation and expanded causing sporadic boiling (photo 3-3). This zone of dilation was caused by the extensional faulting associated with the Keweenawan rift system (Franklin *et al.*, 1986) and hydrofracturing of the shale. Boiling is very evident in the areas where the vein is hosted in shale. Where the vein is hosted in diabase, chert or the lithologies forming the Archean terrane there is little evidence for boiling. This is due to their greater competencies, which have a tendency to throttle the vein system and restricts boiling to zones that are easily hydrofractured.

The boiling temperatures obtained from homogenizing the fluid inclusions indicate the trapping pressure of the fluid inclusions. If boiling of the fluid has occurred, then the fluid must occupy the two-phase curve on a temperature, pressure, and composition phase diagram (Bischoff and Pitzer, 1985; Sourirajan and Kennedy, 1962; Henley, 1984 a). For the veins examined the initial quartz phase shows a boiling temperature between approximately 375°C and 400°C. These boiling temperatures indicate a

trapping pressure of between 225 and 250 bars (Bischoff and Pitzer, 1985). There are some indications of higher boiling temperatures that exceed 450°C at the Thunder Bay Mine and the latter stages of the Keystone Mine. These temperatures indicate higher trapping pressures, up to 350 to 400 bars (Sourirajan and Kennedy, 1962). There is also evidence for lower boiling temperatures, found in fluorite and in some quartz phases. These boiling temperatures range from 300°C to around 250°C. The lower boiling temperatures indicate a lower trapping pressure of approximately 50 to 100 bars (Henley, 1984 a).

It is not possible to determine an exact trapping pressure, since the fluid inclusions formed from a boiling solution. The effect of boiling concentrates the solution and varies the salinity, so the composition axis on the phase diagram (Bischoff and Pitzer, 1985; Sourirjan and Kennedy, 1962) is not known exactly. However, the salinity values obtained in this study were found to range between one and twenty four equivalent weight percent NaCl. The trapping pressure is therefore given as a range to account for the variations in salinity.

The fluctuation between high and low pressure environments probably indicates an alternation between hydrostatic and lithostatic loads. The trapping pressure of 225 to 250 bars indicates a lithostatic load of

approximately one kilometer. The lower trapping pressure of 50 to 100 bars indicate a hydrostatic load of one half to one kilometer. These pressures indicate that the depth of formation of these deposits was approximately one kilometer. The alternation between hydrostatic and lithostatic loads is the result of the vein system alternating between being open and closed to the surface. If the veins were initially open to the surface, it would have a hydrostatic load. As the fluid then precipitated minerals it would choke the system, closing it and resulting in a lithostatic load. Renewed movement along the fault would fracture the vein, opening it to the surface and producing a hydrostatic load.

Trapping pressures that exceeded the lithostatic load are seen in trapping pressures that approach 400 bars. These overpressures were capable of hydrofracturing the wall rock, resulting in the brecciated nature of the veins. The hydrofracturing was probably associated with renewed movement along the fault. The pressure would increase from hydrostatic to lithostatic to overpressures, then fracturing of the vein system would open the system decreasing the pressure resulting in hydrostatic loads. In all the veins examined hydrofracturing is commonly observed, accounting for the high trapping pressures.

Knowledge of the trapping pressure allows for the determination of the temperature correction due to the

effect of pressure. Since in any one vein system studied there is a range in salinity as well as a range of pressures involved, the temperature correction cannot be determined exactly. However, for all the pressures and salinities involved, the temperature correction is between 25 and 50°C (Potter, 1977). Since the maximum temperature correction is less than 50°C, and the pressure was not constant, the temperature correction was not applied to the homogenization temperatures.

Jennings (1986) calculated the trapping pressure for inclusions, based on the thickness of the Animikie sediments. The maximum depth of burial for these veins was estimated to be nine hundred and sixty meters. This results in a lithostatic load of 250 bars, and is consistent with the results of this study.

The trapping pressure as determined from fluid inclusions also concurs with the regional geology. The presence of greenalite and minnesotaite (Moorehouse, 1960) in the Gunflint Formation indicates that the Animikie Group has not been buried more than one kilometer (James, 1954)

Freezing Data

The eutectic temperatures determined from fluid inclusions are variable and indicate locally heterogeneous

fluid compositions. The fluids are seen to be NaCl-H₂O, NaCl-MgCl₂-H₂O, NaCl-CaCl₂-H₂O, and NaCl-MgCl₂-CaCl₂-H₂O. This variation in the fluid composition can only be attributed to mixing of two or more distinct fluids. Further evidence of mixing will be presented in the stable isotope data. However, the bulk composition of the fluid is dominated by NaCl, MgCl₂ and, to a lesser extent, CaCl₂.

There is some evidence for a CO₂-H₂O fluid as indicated by inclusions with a eutectic temperature less than -70°C. These inclusions are almost exclusively hosted in calcite and are restricted to late in the paragenesis. These CO₂-rich fluids could be attributed to the fluid becoming richer in CO₂ with time by the condensation of volatiles that entered the gas phase upon boiling. No trends in variation of fluid composition with host mineralogy or with depth could be distinguished.

The salinity of the fluid inclusions is variable. The salinity ranges from one to twenty-four equivalent weight percent NaCl. As with the eutectic composition, no trend in the salinity with host mineralogy or with depth was seen. The variations in salinity are interpreted to be the result of boiling. Shelton (1983) has interpreted similar variations in salinity to be the results of changes in ambient pressure. If the pressure regime switched from hydrostatic to lithostatic, the fluid may have intersected

the two-phase field, resulting in the separation of a high- and a low-salinity phase. These variable salinity fluids may then have been trapped as fluid inclusions. The salinity variations could also be partially attributed to dilution of saline connate waters with meteoric waters.

Although the salinity is variable, it is still quite low. There is no evidence of halite daughter crystals in any of the fluid inclusions examined. This indicates that the fluid was unsaturated with respect to alkali halides. This is unusual in five element ore suites. Changkakoti et al. (1986 a), reported salinities of fifteen to thirty-five equivalent weight percent NaCl from fluid inclusion in the Great Bear Lake District, and Kerrich et al. (1986) reported salinities from the Cobalt Gowganda District of up to fifty-four equivalent weight percent NaCl.

Implications of the Mineralogy

Paragenesis

The paragenetic sequence in all the veins examined is similar, which implies that similar fluid compositions and similar controls on deposition of vein material acted throughout the district. The suggestion of a region-wide mechanism for the formation of the veins is also consistent with fluid inclusion data and geological field relationships.

All the veins initially precipitated quartz from a high-temperature fluid, generally around 375°C. The fluid cooled until around 300°C at which time green or purple fluorite precipitated. The fluid cooled further to about 100°C, when the bulk of the vein material precipitated as calcite. It is at this late stage that sulfates precipitated. No homogenization temperatures were determined on sulfates, but barite at Silver Mountain was found to be precipitated at a late stage (Jennings, 1987).

The sulfide mineralogy also has a characteristic paragenesis. Pyrite and silver, as native silver and argentite, precipitated at fairly high temperatures, generally after the onset of fluorite precipitation. Argentite is also found in the cleavage planes of calcite,

which implies that it also formed at a latter stage. The bulk of the sulfides formed coevaly with the late calcite at temperatures around 100°C.

The veins examined are almost all composite veins composed of several generations of fracturing and renewed deposition of vein material. Each episode of vein deposition shows the same paragenesis as outlined above. The larger veins, such as the Shuniah, show evidence for at least three fracturing events. It has been suggested (Chambers, 1986) that the secondary fracturing is necessary for silver deposition. However, several veins were seen to be the result of only one fracturing event. For example, the Thunder Bay vein is the result of only one episode of fracturing, and it was a past silver producer. Another example is found in reports of the miners from the Shuniah Mine. Curtis (1887) reported that the Main or Champion vein, which is the result of several fracturing events, is barren and is dominantly calcite with large pods of sulphides. The smaller, anastomosing veinlets, which are the result of only one fracturing event and are composed of dominantly high-temperature quartz, carried the bulk of the ore. The Champion Vein hosted silver only when these veinlets cut it.

Controls on Mineral Deposition

In the Thunder Bay silver district the silver mineralization is restricted to areas immediately underlying the diabase-shale contact. It is in these areas where strong evidence of boiling is seen. This suggests that boiling is one control on ore mineralization. The result of boiling a fluid is three fold. Initially, there is a significant loss of H^+ due to the partitioning of volatiles (CO_2 , H_2S , CH_4 and H_2) into a vapor phase. This has the result of increasing pH. Secondly, there is a net cooling of the fluid as a result of boiling. Thirdly, there is also the effect of concentrating the fluid phase and supersaturating it with respect to dissolved species. Any combination of these effects is an effective mechanism for causing precipitation from the fluids.

When boiling is initiated at high pressures, the density difference between the exsolved vapor phase and the liquid phase is small. This reduces the tendency for physical separation of the two phases, increasing the interaction between the phases and decreasing the effect of boiling. Bischoff and Pitzer (1985) have suggested that a boiling system, under the pressures associated with oceanic vents (200-250 bars), is much closer to a closed system than an open system as defined by Drummond and Ohmoto (1985). In closed systems, no mass escapes the system and all vapor

produced is in equilibrium with the fluid. This drastically reduces the changes that can occur as a result of boiling. However, Drummond and Ohmoto (1985) have demonstrated that a boiling solution in a closed system at 300°C prior to boiling would experience a pH increase of 0.5 units in the first 10% of boiling and a pH increase of 1.5 units after 25% boiling. Drummond and Ohmoto (1985) have also demonstrated that at temperatures greater than 300°C the tendency for the volatiles to partition into a vapor phase decreases with temperature. This will decrease the effect that boiling has on fluid chemistry.

Boiling episodes tend to be isoenthalpic rather than isothermal (Drummond and Ohmoto, 1985). This means that the enthalpy of a liquid and vapor after boiling will be equal to the enthalpy of the fluid before boiling. As a fluid boils the solution will lose heat to the vapor phase and cool as boiling proceeds. Drummond and Ohmoto (1985) have demonstrated that an open system at 300°C undergoing isoenthalpic boiling will cool by 110°C in the first 25% of boiling. The cooling of the fluid would have the effect of reducing the solubility of species in solution. The solution would become supersaturated with the species causing precipitation. The concentration of the fluid as a result of boiling has the same effect as cooling. The solutions become supersaturated with the species causing precipitation.

The cooling of the fluid is further enhanced by mixing of the fluid with cooler meteoric waters. This mixing is suggested in the salinity data as well as in the stable isotope data.

Different mineral stabilities are affected differently in boiling solutions. Quartz is generally present in hydrothermal fluids as silicic acid, and boiling will have little effect on it. Deposition of quartz is effected only by the concentration of silicic acid within the solution. When the solution becomes supersaturated with silicic acid, either as a result of cooling or concentrating the liquid phases, quartz will precipitate (Henley, 1984 b).

Calcite is unlike quartz in that calcite tends to precipitate rapidly at the onset of boiling. Drummond and Ohmoto (1985) have shown that it is possible to remove several hundred ppm Ca as calcite from solution with a few percent boiling. Sulfides, oxides and native metals are very similar to calcite and will precipitate from solution at the onset of boiling. The actual paragenetic sequence will depend upon the initial fluid chemistry, but generally calcite will form contemporaneously with the bulk of the sulfide, oxides and native metals (Drummond and Ohmoto, 1985). This paragenetic sequence is recognized in all the veins examined during the course of this study.

Sulfate minerals are not commonly associated with precipitation from a boiling fluid. Most hydrothermal fluids have a composition lying in the field dominated by SO_4^{2-} . In this field boiling will have little effect on the sulfate concentrations. If the solution were dilute and acidic, HSO_4^- would be the dominant sulfate species. In this case a pH increase could generate SO_4^{2-} and cause sulfate minerals to form (Drummond and Ohmoto, 1985).

Mineralogy

It has long been noted by miners of the Thunder Bay silver veins that rich ore zones are invariably adjacent to exceptionally carbon-rich areas of country rock. During this study, this feature was observed at the Thunder Bay Mine, where the wall-rock is composed mainly of silicified shale with pods of graphite. Polished thin section examination of the graphitic areas showed that native silver and pyrite were absorbed onto the graphite. This suggests that graphite served as absorption sites for the ore species, which nucleated the ore minerals, facilitating their precipitation. It is also likely that the carbon served as a site for local reduction of the fluid resulting in the precipitation of silver.

A sample of wavellite was collected from the Shuniah Mine and identified, using pinhole and Gandolfi

camera techniques. This is the first time this mineral has been identified in the Thunder Bay silver district. It is interesting to note that the only vein system found hosting wavellite is the only vein system that is dominantly hosted in the Gunflint Formation. To form wavellite a source of phosphate is necessary. Fralick (personal communication, 1989) has identified concentrations of phosphate in the Gunflint Formation. It is likely that these anomalous concentration of phosphate served as the source for the wavellite.

Implications of the Stable Isotope Data

Oxygen Isotope Data

The most striking trend seen in the stable isotope data is the variation of the oxygen ratio as a function of depth (fig. 5-1). It is apparent that the fluid's oxygen composition became progressively lighter as it rose vertically towards the surface. This variation in oxygen isotope ratio can be viewed as a result of mixing two distinct fluids. The initial fluid's composition can be approximated by the composition of the deepest samples and the early, high temperature quartz. These samples precipitated from the most pristine or undiluted fluid. This indicates that the initial fluid composition would have an oxygen isotope ratio of +10‰ (Table 3-1, 4-1). As the fluid rose vertically, it became increasingly diluted with a meteoric fluid. This enriches the fluid in ^{16}O and shifts the $\delta^{18}\text{O}$ to progressively negative values.

The oxygen isotopic ratio of +10‰ is consistent with a connate water source. Figure 5-2 shows the trend of the oxygen data with respect to reference waters. This suggests that the water initially was a deep, basinal brine, derived from dewatering of the Rove and Gunflint Formations. As the fluid migrated vertically, the hydrothermal fluid became progressively enriched in ^{16}O .

OXYGEN ISOTOPE VARIATION WITH DEPTH

Page 5-16

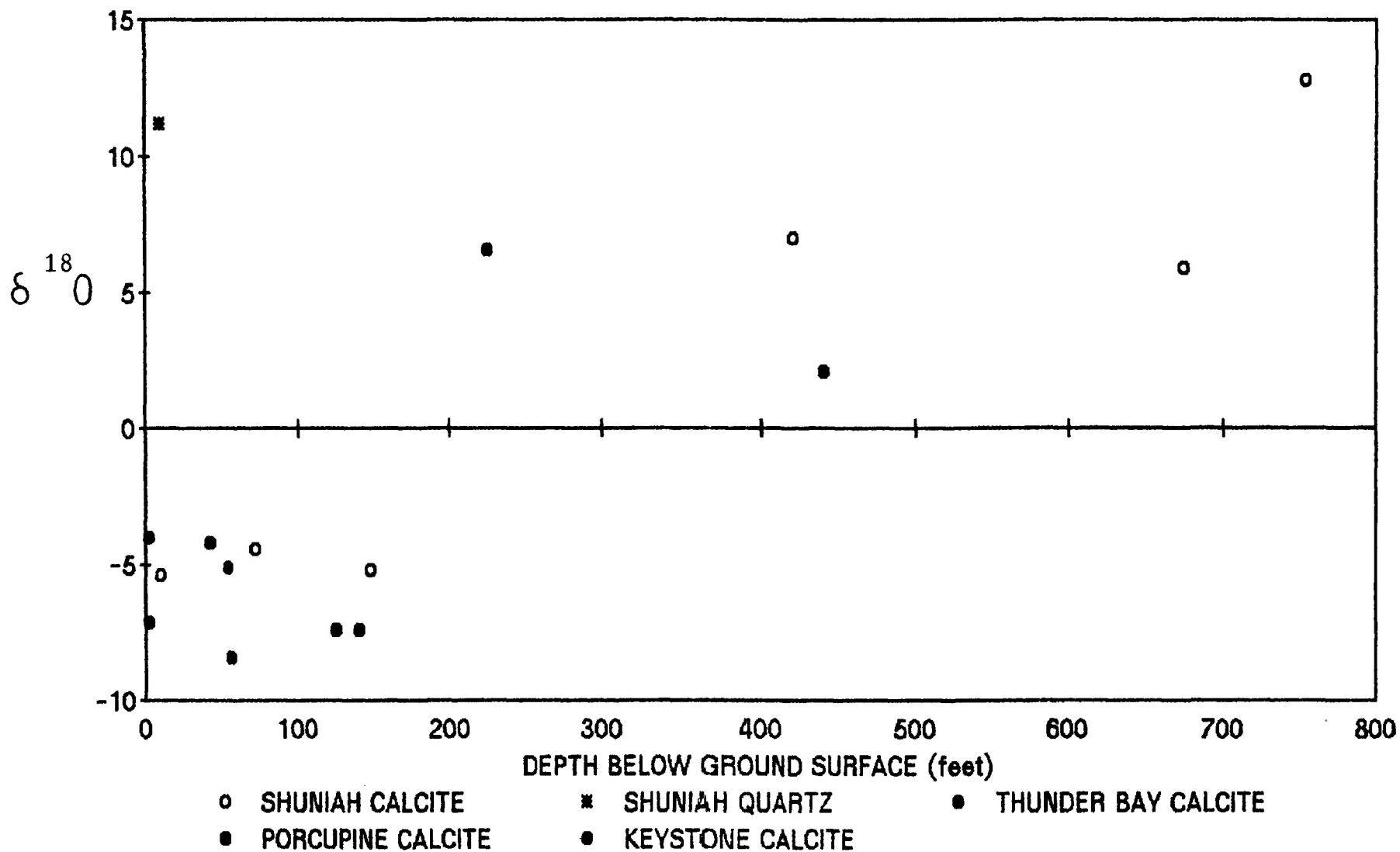


Figure 5-1. Variation in oxygen isotope ratios as a function of depth. Data are combined from the Port Arthur and Creswel Groups.

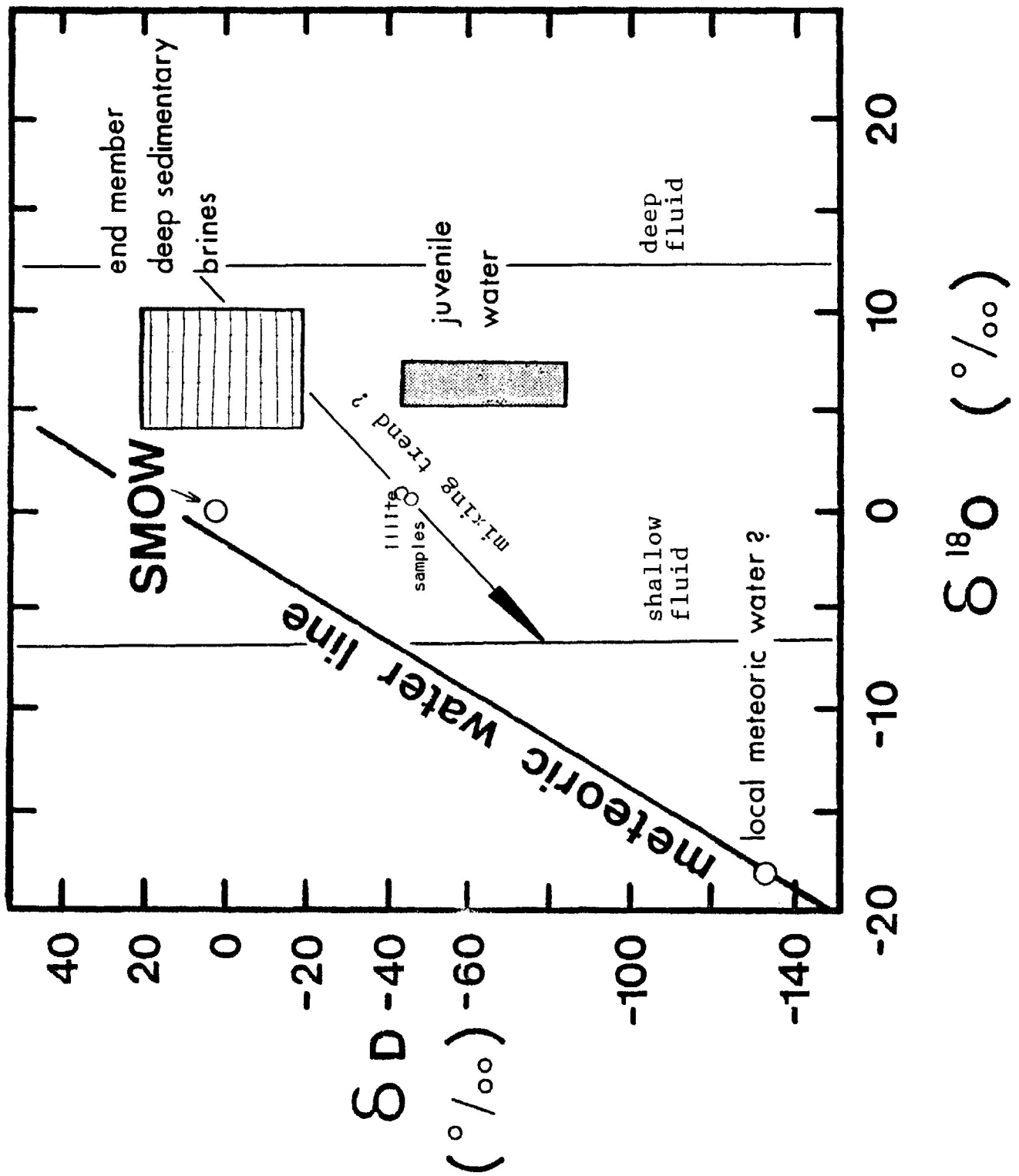


Figure 5-2. Graph of deuterium vs oxygen isotopic ratios showing reference waters and proposed mixing trend.

The two samples of illite that were analyzed for both deuterium and oxygen isotope ratios (table 4-1) constrain the mixing line. These values plot at an intermediate position on the mixing trend between the connate and the meteoric fluids.

Figure 5-2 does indicate that strictly on the basis of oxygen isotope data, there is a possibility that the pristine water could have originated from other sources such as an igneous intrusion or due to metamorphic dewatering. However, there is neither evidence for a deep seated pluton nor a metamorphic event coeval with vein formation. There is also no evidence for any internal differentiation nor hydrothermal alteration within the hypabyssal intrusions, which indicates that they were not likely hydrothermal fluid sources. The data strongly indicate that the fluid was a connate brine originating from the dewatering of the Animikie sediments. The fluid was diluted with a meteoric component as it migrated vertically resulting in the mixing trend shown in figure 5-2.

The depletion in ^{18}O as the fluid migrated vertically is likely the result of dilution from a meteoric water. However, increasingly negative $\delta^{18}\text{O}$ values could also be due to the fluid boiling. Higgins and Kerrich (1982) have shown that a boiling fluid in the temperature range 300-400°C will show a 7‰ depletion in ^{18}O as a result of 40

mol% CO₂ loss. However, in the trend seen in this study there is 10 to 15‰ depletion of ¹⁸O in the fluid. This would necessitate a large loss in CO₂ from the system. As indicated earlier, at the pressures where boiling took place the density difference between vapor and liquid is small, and the fluid would approximate a closed system (Bischoff and Pitzer, 1985). This would decrease the amount of vapor lost to the fluid, reducing the fluid's depletion in ¹⁸O. Therefore, it is unlikely that the trend in δ¹⁸O values is due solely to boiling.

It is not likely that the trend observed is the result of the hydrothermal fluids equilibrating with wall rocks of different oxygen ratios. There is no evidence for any significant hydrothermal alteration of the wall rock. If the fluids were to equilibrate with the wall rock, then the rocks would show extensive hydrothermal alteration and this is not observed. Also the trend is independent of the wall-rock lithology. The same trend is observed when the vein is hosted within the Rove Formation, Gunflint Formation or within the Archean rocks. For these reasons it is likely that vein emplacement was very rapid. The vein fluids would migrate up the fault system and rapidly precipitate the vein material without equilibrating with the wall-rock.

It is probable that the ^{18}O depletion as seen in this study is not the result of any single process, but the result of both processes. Dilution of a connate brine with a lighter meteoric water combined with fluid boiling both serve to form the trend seen in the oxygen isotope ratios (fig. 5-1).

Carbon Isotope Data

The carbon isotope ratios in carbonates are very constant in the samples analyzed (fig. 5-3). The average value is -6.6‰ with a standard deviation of 3.1‰ . The data are variable, when the vein is hosted outside of the Rove Formation. The deeper samples from the Shuniah Mine (SH-29, SH-48, SH-190) are hosted in the Gunflint Formation, and the carbon isotope ratios show a wide range in values. If these values are excluded, then the average $\delta^{13}\text{C}$ value is 7.0‰ with a standard deviation of 0.9‰ .

As discussed in chapter three this variation in carbon isotope ratios is probably due to the Gunflint Formation being a poor and non-uniform carbon source. The consistency of the carbon isotope ratios in vein hosted in the Rove Formation is due to the abundance and uniform composition of the carbon in the Rove shale.

CARBON ISOTOPE VARIATION WITH HOST LITHOLOGY

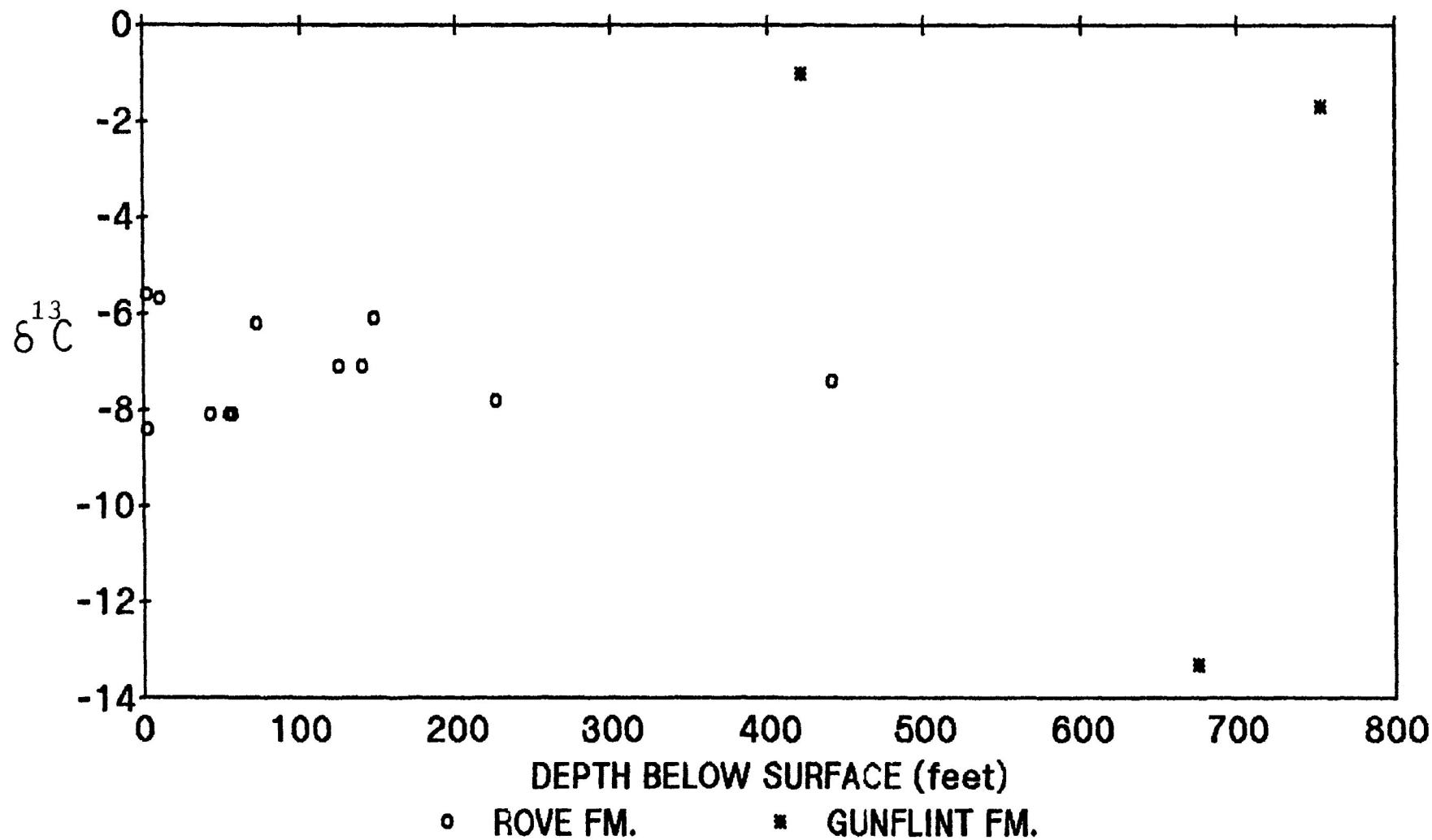


Figure 5-3. Graph demonstrating the variation in carbon isotope ratios for the different wall-rock lithologies.

Elemental Carbon Isotope Data

Four samples of graphite were analyzed for elemental carbon ratios. Two samples were from the Thunder Bay Mine area, and two samples were from Silver Islet grab samples. One of the two samples from the Thunder Bay Mine was collected from the vein wall-rock. This sample was intergrown with carbonate vein material. The sample was crushed and the calcite and graphite were separated, the calcite fraction was analyzed for oxygen and carbon isotopic ratios and the graphite fraction was analyzed for elemental carbon isotopic ratios. The observed carbon fractionation between the graphite and the calcite is 26.3‰ at 95.0°C. The second graphite sample from the Thunder Bay Mine area was collected from the shale-d diabase contact in a diabase quarry approximately 1 km southeast of the mine site. This sample was removed from any known hydrothermal activity and is believed to be primary carbon recrystallized by contact metamorphism from the intrusion of the diabase sill. The carbon ratios for both the vein wall rock and the primary graphite are equivalent at approximately -31.5‰. These values are consistent with the ratios expected for recrystallized organic carbon (Schoell, 1984; summarized by Ohmoto, 1986).

Two samples from Silver Islet were analyzed for carbon isotope ratios. One sample which had graphite and

dolomite intergrown was crushed and separated. The graphite fraction was analyzed for its carbon isotopic ratio, and the dolomite fraction was analyzed for carbon and oxygen isotopic ratios. The observed fractionation between the dolomite and the graphite was 22.2‰ at 177.5°C. The second sample from Silver Islet was only graphite and was analyzed for carbon isotope ratios. The two elemental carbon ratios from Silver Islet graphite are consistent at approximately -34‰. These values are consistent with the elemental carbon values obtained from the Thunder Bay Mine and indicate a recrystallized organic carbon source (Schoell, 1984; summarized by Ohmoto, 1986).

The two pairs of graphite/carbonate analysis indicate consistent results. The pair from the Thunder Bay Mine shows a fractionation of 26.3‰ at 95.0°C. The pair from the Silver Islet grab sample shows a fractionation 22.2‰ at 177.5 °C. The object of these analysis was to determine if the graphitic wall-rock could act as a carbon source for the vein carbonate. Eichman and Schidlowski (1975) found unmetamorphosed co-existing organic carbon/carbonate pairs in Precambrian sediments, with a $\Delta_{\text{calcite-graphite}}$ = 20-30, with increasing fractionation with decreasing temperature. However, Friedman and O'Neil (1977; summarized by Field and Fifarek 1985), reported calcite-graphite fractionations of 18.0 and 13.9 for 95°C and 175°C respectively, considerably lower than the

fractionation reported by Eichman and Schidlowski (1975). Compilation of the fractionation factors between calcite and graphite (Valley, 1986) indicates a large range in $\delta^{13}C$ values particularly in the lower temperatures. Although the data are variable, they indicate that the fractionation between calcite and graphite is large, and that the fractionation observed in this study is within published limits. This suggests that the graphite from the Rove shale could act as a carbon source for the hydrothermal carbonate.

There are several lines of evidence that support the carbon source being the Rove shale. In the Shuniah Mine, where the vein system extends beyond the Rove Formation the presence of calcite as vein gangue is reduced. The vein gangue at depth is dominantly quartz with only minor calcite. This indicates that the hydrothermal fluids became saturated with calcite only in the upper portions of the vein system. This is not due to temperature differences, since the deep carbonates formed at fairly low temperatures. It is also not due to a lack of aqueous Ca, since the fluid inclusion eutectic temperatures indicate the presence of $CaCl_2$ in solution. It is proposed that the absence of calcite from the vein when it is not hosted in shale is due to a lack of carbon in the source rock.

Three samples of calcite from the Shuniah vein that were hosted in the Gunflint Formation were analyzed for

carbon isotope ratios. These samples yielded greatly variable results, which indicate a nonuniform carbon source. If the hydrothermal fluids were leaching carbon from the wall-rock as proposed, then the Gunflint Formation, which is dominantly chert, would be a poor and nonuniform carbon source and would result in a vein with only minor calcite with nonuniform isotope ratios.

The carbonate samples from the vein systems hosted in the Rove shale yielded very consistent carbon isotope ratios. This indicates that the carbon source was uniform throughout this area of the veins. The four samples of elemental carbon from the Rove shale that was analyzed for carbon ratios showed consistent carbon isotope ratios. The Rove shale has high carbon content, averaging around 2 weight percent carbon (Harvey, 1985), indicating that the Rove shale could act as a suitable carbon source.

There is some evidence that refutes the possibility that the Rove shale served as a carbon source for the vein carbonate. In the Shuniah vein there are large volumes of calcite. The vein cross section contains approximately 100 m² of calcite (appendix 5). From calculations shown in appendix 5 the hydrothermal fluids would have to completely leach all the carbon for 12.1 meters on either side of the vein to form the required vein carbonate. This is not seen; hydrothermal alteration of the

country rock is limited to approximately one half of the veins width into the wall rock (Franklin, 1970). Also, in many of the veins there is graphite in contact with the vein material indicating that the hydrothermal fluids did not leach all of the carbon from the country rock. In order for the Rove shale to act as a carbon source for the Shuniah vein, there must have been thicker sequences of shale than what is seen now to account for the carbon or the shale must have higher concentrations of carbon than what is seen in other areas. The other veins examined are much smaller, with much less calcite than the Shuniah vein. For the smaller veins it is much easier to propose that the Rove shale acted as a carbon source.

In summary the isotopic data indicate that the presence of the Animikie sediments is essential for the formation of the veins studied. The oxygen isotopic ratios indicate that the hydrothermal fluid originated from the dewatering of the sediments and was later diluted with local meteoric water. The fluid scavenged carbon, and by analogy metals, from the Animikie sediments, and deposited them at the contact with the diabase. The graphitic wall-rock that is prevalent in the veins is recrystallized organic carbon. The contact metamorphism due to the hypabyssal intrusives mobilized and recrystallized primary organic carbon present in the shale.

Summary

The purpose of this study was to examine the variations in the hydrothermal fluid with depth in past-producing silver veins in the Thunder Bay area. The methodology used in this study included fluid inclusions and stable isotope analysis from drill core samples. The fluid inclusion analysis consisted of three hundred forty-four fluid inclusion homogenization temperatures, one hundred twenty-five fluid inclusion eutectic temperatures and one hundred twenty-four fluid inclusion salinity determinations. The results of the fluid inclusion segment of the study, combined with examination of vein cross-section and polished thin sections, has indicated the following:

1. The heat source for the fluid was deep-seated.
2. Vein emplacement was synkinematic with fault movement. The vein formation was episodic; fracturing and renewed movement along the fault punctuated vein mineralization.
3. The vein systems were emplaced at about 1 km depth. The pressure regime alternated between hydrostatic and lithostatic loads.

4. Ore mineralization was at least partially controlled by boiling.

5. Boiling was localized at the diabase-shale contact due to the throttling caused by a highly competent lithology overlying a fissile lithology. Boiling could also have been the result of alternating pressure regimes as seen from the boiling temperatures. If the pressure regime switched from lithostatic to hydrostatic, as a result of fracturing the vein system, then the decreased pressure could result in sporadic boiling.

6. Ore fluids boiled initially at temperatures approaching 400°C, at which time quartz and minor sulfides with native silver precipitated. The fluid then cooled to approximately 100°C as a result of boiling and dilution of meteoric waters. At this point the bulk of the vein precipitated as calcite and sulfides with native silver.

7. The hydrothermal fluids were intruded as a series of pulses that may or may not have had an associated fracturing event.

8. The graphitic wall-rock acted as nucleation sites or as areas of local reduction, initiating the precipitation of ore minerals.
9. The hydrothermal fluids were dominantly NaCl, MgCl₂ and CaCl₂ brines. The fluid was always undersaturated with respect to these salts.

The fluid inclusion analysis has indicated the nature and composition of the hydrothermal fluids. To determine the origin of the fluid and its constituents, stable isotope analysis of the vein material was conducted. The stable isotope segment of this study consisted of fifteen samples of calcite, which were analyzed for oxygen and carbon isotopic ratios, four samples of elemental carbon, which were analyzed for carbon isotopic ratios, and one sample of dolomite, which was analyzed for carbon and oxygen isotopic ratios. The stable isotope analysis has indicated the following:

1. The Rove shale is a probable carbon source, as well as being a likely metal source.
2. The original fluid was a connate brine, which became diluted with a meteoric component, as it migrated vertically.

Conditions of the Ore-Forming Vein Systems

A number of factors must be considered when proposing a model for the formation of the Thunder Bay silver district:

1. Origin of the hydrothermal fluid.
2. Heat source of the fluids.
3. Driving force for the fluids.
4. Chemistry of the fluid.
5. Transport of metal ligands.
6. Metal source.
7. Factors that localize the silver ore.
8. The range in vein types, from barren to base metal-silver, to five element assemblages.

Each of these factors will be addressed, with specific reference to the findings of this study, in order to form a genetic model for the formation of the veins.

1. The oxygen isotopic ratios of the most pristine hydrothermal fluids are consistent with a connate fluid. As the fluid migrated vertically up the fracture system, it became increasingly diluted with a meteoric component. The connate fluids were probably derived from dewatering of the Rove and Gunflint Formations.

2. The heat source of the fluids is deep seated. Kissin (1988 a) has shown that there is a strong association between five-element ore types and a rifting environment. The thermal anomaly associated with rifting can produce temperatures up to 400°C at shallow depths. It is proposed that the formation of the Keweenawan rift system acted as the heat source for the fluids.

3. The mobilization of the fluids is attributed to the formation of extensional faults associated with the Keweenawan rifting. The faults are open structures and therefore areas of low pressure. Fluids heated by high thermal gradients would be mobilized and migrate towards the areas of low pressure. In the fault system the fluids would rise vertically due to thermal gradients.

4. One of the main problems in outlining the fluid chemistry of five-element ore suites is the transport of nickel and cobalt. Crerar et al. (1985) have shown that higher temperatures and higher salinities favor the

stability of tetrahedral over octahedral nickel and cobalt complexes, which enhances solubility. Examination of Eh-pH diagrams generated at 100, 250 and 400°C (Sherlock, unpublished data) has shown that the solubility of nickel and cobalt is enhanced at high temperatures and high salinities. If the solution is relatively oxidizing the transport of iron is greatly reduced, which accounts for the low iron content characteristic of these vein systems (Kissin, 1988 b). Jennings (1987), using the Fe content of sphalerite, calculated the activity of sulphur, to be 10^{-18} to 10^{-28} . In summary, the fluids are likely to be high temperature, moderately saline, of low sulphur content, and are relatively oxidizing lying on the magnetite-hematite buffer (Kissin, 1988 b).

5. Little is actually known about the hydrothermal transport of Ni, and Co. All that can be suggested from this study is indirect evidence. Previous fluid inclusion studies of other five-element assemblages has demonstrated that the fluids are supersaturated brines (Kerrick et al., 1986; Changkakoti et al., 1986 a). The fluid inclusions from this study indicate that the fluids were invariably undersaturated brines. The veins from this study were not of the five-element assemblage, in that they lack the characteristic mineralization. However, they are genetically related to the five-element ore suite by their spatial and temporal association to Silver Islet and their similar

geological relationships. The reason for the variation in ore types may be due to the salinity of the hydrothermal fluids. It is proposed that the fluids must be very saline brines to mobilize As, Ni, Co and Bi and transport them as chloride complexes. An undersaturated fluid will not mobilize those elements and will form base metal-silver veins such as were examined in this study.

6. Franklin (1970) proposed that the Rove shale was a suitable metal source and lateral secretion was the mechanism that mobilized the metal into solution. A test of this hypothesis was made by Harvey (1985) who compared the concentration of elements with distance away from the vein system. No strong trends in depletion of the shale proximal to the vein system were seen. It is likely that the Rove shale did act as a metal source, with fluids scavenging metals occurring over large areas but from narrow alteration zones (Kissin, 1988 b). Indirect evidence derived from this study supports the Rove shale acting as a metal source. The stable isotope data has indicated that the Rove shale is a possible source for hydrothermal carbon. If the fluids scavenged carbon from the shale then they may also have derived metals from it as well. However, mechanism rather than source rock is the important idea. The metals may have been remobilized from anywhere; it is the high-temperature, high salinity fluid that is needed to mobilize the elements of the five-element suite.

7. Silver ore is invariably localized at the zone of shale that is in contact with the diabase. Fluid inclusion evidence from these zones indicate that sporadic boiling occurred here. The boiling was due to the greater competency of the diabase than of the shale. The vein system was throttled by the diabase. The fluid would then expand below the diabase causing local hydrofracturing of the shale and expansion of the fluid. The expansion of the fluid would allow boiling. The boiling resulted in partitioning of volatiles from the fluid, causing cooling and an increase in pH. This supersaturated the solution resulting in precipitation of vein material.

Silver ore is often found in contact with graphitic wall rock. Native silver has been observed to be absorbed onto the graphite. It is probable that the graphite acted as a local reduction site, initiating mineralization. This resulted in the ore being localized in pods in areas where the country rock is carbon-rich. The carbon-rich areas appear to be concentrated at the diabase shale contact. This is likely the result of the carbon being recrystallized as graphite by contact metamorphism during the intrusion of the diabase sills.

8. There is a large range of vein types in the Thunder Bay silver district. The veins range from five-

element assemblages to base metal-silver types to barren veins. The veins are all related, showing common textures, fluid temperatures and fluid chemistry. One possible difference is that the five element vein type needs a highly saline fluid to mobilized the ore suite. However, much more detailed studies of the different vein types are needed before any conclusion can be made.

Model for the Formation of the Thunder Bay Silver Veins

Kissin (1988 b) proposed the following model for the formation of the Thunder Bay silver vein systems; this model is presented diagrammatically in fig. 6-1. The Keweenaw rift system produced the necessary thermal anomaly needed to generate the high fluid temperatures seen. Connate waters, mobilized by the high temperature gradient, scavenged metals from the Rove shale in a narrow alteration zone, but over large areas. The fluids were saline and relatively oxidizing, which allowed them to transport the ore suite associated with the five-element veins. This also suppressed the transportation of iron, resulting in the characteristic low iron content of the system. The fluid migrated to zones of dilation, which were normal extensional faults associated with the rifting. The hydrothermal fluids then rose due to adiabatic expansion. The fluids rose to about one kilometer below the paleosurface, where they precipitated vein material as a result of boiling and cooling due to dilution from a meteoric water component. The pressure regime on the fluid fluctuated from hydrostatic to lithostatic to overpressures. This fluctuation was due to the opening and closing of the vein system to the surface. The vein was open to the surface, as a result of movement along the fault. The hydrothermal fluid precipitated vein material, which choked the system and applied a lithostatic load. The pressure continued to build resulting in

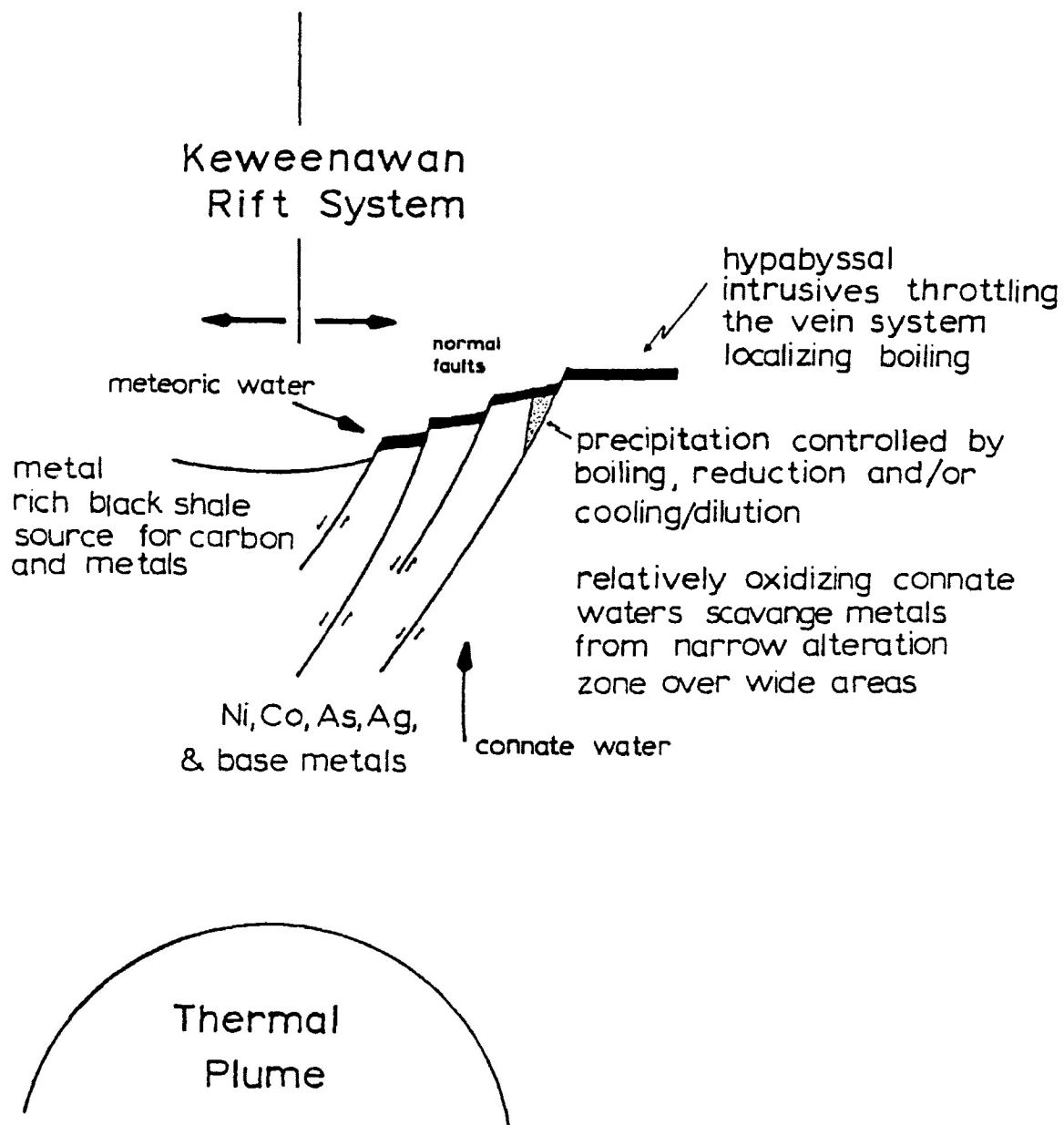


Figure 6-1. Model for the formation of Mainland Belt silver veins after Kissin (1988b).

overpressures, which hydrofractured the host rock. This renewed movement along the fault opened the vein system to the surface resulting in a hydrostatic load. The fluctuation in ambient pressure produced the sporadic boiling, as well as the hydrofracturing that was prevalent throughout the vein systems. The boiling was localized by throttling due to competency of the diabase sills. Local reduction by carbonaceous materials also aided in deposition.

Recommendations for Future Research

One of the most promising directions that future research should take is to further investigate the variations in oxygen isotope ratios with depth. A possible method would be to extract fluid from fluid inclusions directly and analyze it for deuterium and oxygen isotopic ratios. The carbonate is often very rich in primary fluid inclusions and would be suitable for this technique.

Also an experimental geochemical investigation should be undertaken to determine the hydrothermal conditions of transport needed for mobilization and precipitation of the five element suite.

References

- Bischoff, J.L. and Pitzer, K.S.
1985: Phase relations and adiabats in boiling seafloor geothermal systems. Earth and Planetary Science Letters, vol. 75, pp. 327-338.
- Blackadar, R.G.
1956: Differentiation and assimilation in the Logan Sills, Lake Superior District, Ontario. American Journal of Science, vol. 254, pp. 623-655.
- Bowen, N.L.
1911: Silver in the Thunder Bay District. Annual Report, Ontario Bureau of Mines, vol. 20, pt. 2, pp. 119-132.
- Chambers, B.
1986: Geology and mineralogy of the Creswel silver deposits, Mainland Belt silver region. Honors B.Sc. thesis, Lakehead University, Thunder Bay, Ontario. 68 p.
- Changkakoti, A., Morton, R.D., and Gray, J.
1986 a: Hydrothermal environments during the genesis of silver deposits in the Northwest Territories of Canada: Evidence from fluid inclusions. Mineralium Deposita, vol. 21, pp. 63-69.
- Changkakoti, A., Morton, R.D., Gray, J., and Young, C.J.
1986 b: Oxygen, hydrogen, and carbon isotopic studies of the Great Bear Lake silver deposits, Northwest Territories. Canadian Journal of Earth Science, vol. 23, pp. 1463-1469.
- Clayton, R.N., O'Neil, J.R., and Mayeda, T.K.
1972: Oxygen isotope exchange between quartz and water. Journal Geophysical Research, vol. 77, pp. 3057-3067.
- Cole, B.L.
1978: Geology and mineralogy of the Beaver Junior Mine, Mainland Belt silver region, Thunder Bay District. Honors B.Sc. thesis, Lakehead University, Thunder Bay, Ontario. 54 p.
- Courtis, W.M.
1887: The Animikie rocks and their vein phenomena as shown at the Duncan mine, Lake Superior. American Institute of Mining and Metallurgical and Petroleum Engineers, Transactions, vol. 15, pp. 671-677.

- Crawford, M.L.
1981: Phase equilibria in aqueous fluid inclusions. in Fluid Inclusions: Application to Petrology, MAC Short Course vol. 6. Edited by L.S. Hollister and M.L. Crawford. pp. 75-100.
- Crerar, David, Wood, Scott, Brantley, Susan, Bocarsly, Andrew,
1985: Chemical controls on solubility of ore-forming minerals in hydrothermal solutions. Canadian Mineralogist, vol. 23, pp. 333-352.
- Davis, D.W. and Sutcliffe, R.H.
1984: U-Pb ages from the Nipigon Plate (abst.) in GAC-MAC 1984 Program with Abstracts. Joint Annual Meeting, vol. 9, pp. 57.
- Davis, D.W., Lowenstein, T.K., and Spencer, R.J.
1988: Melting behavior of fluid inclusions in laboratory grown halite crystals in the systems NaCl-H₂O, NaCl-KCl-H₂O, and NaCl-MgCl₂-H₂O (abst # 5353) in GSA Program with Abstracts 1988. pp. A152.
- Deines, P., Langmuir, D., and Harmon, R.S.
1974: Stable isotope ratios and the existence of a gas phase in the evolution of carbonate ground waters. Geochimica et Cosmochimica Acta, vol. 38, pp. 1147-1164.
- Drummond, S.E., and Ohmoto, H.
1985: Chemical evolution and mineral deposition in boiling hydrothermal systems. Economic Geology, vol. 80, pp. 26-147.
- DuBois, P.M.
1962: Paleomagnetism and correlation of Keweenawan rocks. Geological Survey of Canada Bulletin 71. 75 p.
- Eichmann, R., and Schidolwski, M.
1975: Isotopic fractionation between co-existing organic carbon-carbonate pairs in Precambrian sediments. Geochimica et Cosmochimica Acta, vol. 39, pp. 585-595.
- Eslinger, E.V., and Savin, S.M.
1973: Mineralogy and oxygen isotope geochemistry of the hydrothermally altered rocks of the Ohaki-Broadlands, New Zealand geothermal area. American Journal of Science, vol. 273. pp. 240-270.
- Field, C.W., and Fifarek, R.H.
1985: Light stable-isotope systematics in the epithermal environments. in Geology and geochemistry of epithermal systems, Reviews in Economic Geology vol. 2. Edited by B.R. Berger and P.M. Bethke. pp. 73-98.

Franklin, J.M.

1970: Metallogeny of the Proterozoic rocks of the Thunder Bay District, Ontario. Ph.D. thesis, the University of Western Ontario, London, Ontario, 317p.

Franklin, J.M.

1978: Rubidium-strontium age determinations of the Rove Formation shale. in Rubidium-strontium isochron age studies, report 2. Edited by R.K. Wanless and W.D. Loveridge, Geological Survey of Canada Paper 77-14. pp. 35-39.

Franklin, J.M.

1982: Introduction to Proterozoic Geology of the Northern Lake Superior in Proterozoic geology of the northern Lake Superior area. Edited by J.M. Franklin. Geological Association of Canada, Winnipeg Manitoba Guidebook, Field Trip 4, pp. 1-13.

Franklin, J.M., Kissin, S.A., Smyk, M.C., Scott, S.D.

1986: Silver deposits associated with the Proterozoic rocks of the Thunder Bay District, Ontario. Canadian Journal of Earth Sciences, vol. 23, pp. 1576-1591.

Franklin, J.M., McIlwaine, W.H., Poulsen, K.H., and Wanless, R.K.

1980: Stratigraphy and depositional setting of the Sibley Group, Thunder Bay District, Ontario. Canadian Journal of Earth Sciences, vol. 17, pp. 633-651.

Friedman, I., and O'Neil, J.R.

1977: Compilation of stable isotope fractionation factors of geochemical interest. in Data of Geochemistry, Sixth Edition. Edited by M. Fleischer. United States Geological Survey, Professional Paper 440-KK. pp. KK1-KK12.

Goodwin, A.M.

1960: Gunflint Iron Formation in the Whitefish Lake area. Ontario Department of Mines, Annual Report, Vol. 69, Part 7, pp. 41-63.

Harvey, P.L.

1985: A test of the lateral secretion hypothesis at the Rabbit Mountain Mine, Mainland Belt silver region, Thunder Bay District, Ontario. Honors B.Sc. thesis, Lakehead University, Thunder Bay, Ontario. 75 p.

Henley, R.W.

1984 a: Chemical structure of geothermal systems. in Fluid-Mineral Equilibria in Hydrothermal Systems, Reviews in Economic Geology Vol. 1. Society of Economic Geologists. Edited by R.W. Henley, A.H. Truesdell and P.E. Barton, Jr. pp. 9-30.

Henley, R.W.

1984 b: High temperature calculations in geothermal development. in Fluid-Mineral Equilibria in Hydrothermal Systems, Reviews in Economic Geology Vol. 1. Society of Economic Geologists. Edited by R.W. Henley, A.H. Truesdell and P.B. Barton, Jr. pp. 177-190.

Higgins, N.C., and Kerrich, R.

1982: Progressive ¹⁸O depletion during CO₂ separation from a carbon dioxide-rich hydrothermal fluid: evidence from the Grey River tungsten deposit, Newfoundland. Canadian Journal of Earth Science, vol. 19, pp. 2247-2257.

Hurley, P.M., Fairbairn, H.W., Pinson, Jr., W.H., and Hower, J.

1962: Unmetamorphosed minerals in the Gunflint Formation used to test the age of the Animikie. Journal of Geology, vol. 70, pp. 489-492.

Ingall, E.D.

1888: Report on mines and mining on Lake Superior. Geological and Natural History Survey of Canada, Annual Report for 1887-8, new series, No. 3, Part H, pp. 1-131.

James, H.L.

1954: Sedimentary facies of iron formation. Economic Geology, vol. 49. pp. 235-293.

Jennings, E.A.

1987: A survey of the Mainland and Island Belts, Thunder Bay silver district, Ontario: Fluid inclusions, mineralogy, and stable isotopes. M.Sc. thesis, Lakehead University, Thunder Bay, Ontario. 159 p.

Kerrich, R., Strong, D.F., Andrews, A.J., and Owsiacski, L.

1986: The silver deposits at Cobalt and Gowganda, Ontario. III Hydrothermal regimes and source reservoirs-evidence from H, O, C and Sr isotopes and fluid inclusions. Canadian Journal of Earth Science, vol. 23, pp. 1519-1550.

Kissin, S.A.

1988 a: Nickel-cobalt-native silver (five element) veins: A rift related ore type. in Proceedings Volume, North American Conference on Tectonic Control of Ore Deposits and the Vertical and Horizontal Extent of Ore Systems. University of Missouri-Rolla. Edited by Geza Kisvarsanyi and S.K. Grant. pp. 268-279.

- Kissin, S.A.
1988 b: The five-element suite: An indication of non-magmatic ore types related to rifting and basin development. *Explore*, no. 64, pp. 5-7.
- Kissin, S.A. and McCuaig, T.C.
1988: The genesis of silver vein deposits in the Thunder Bay area, Northwestern Ontario; Grant 300, pp. 146-156 in *Geoscience Research Grant Program, Summary of Research, 1987-1988*, Edited by V.G. Milne, Ontario Geological Survey, Miscellaneous Paper 140. 251p.
- Kovach, J. and Faure, G.
1969: The age of the Gunflint Iron Formation of the Animikie series in Ontario, Canada. *Geological Society of America Bulletin*, vol. 80, pp. 1725-1736
- Kustra, C.A., McIlwaine, W.H., Fenwick, K.G., Scott, J.
1977: Proterozoic Rocks of the Thunder Bay Area Northwestern Ontario. *Field Excursion Guide*. Institute on Lake Superior Geology, Twenty Third Annual Meeting, Proterozoic Field Trip 47 p.
- Kyser, T.K.
1987: Equilibrium fractionation factors for stable isotopes. in *Stable isotope geochemistry of low temperature fluids*. Mineralogical Association of Canada Short Course vol. 13. Edited by T.K. Kyser. pp. 1-84
- Maunula, T.L.
1979: Geology and mineralogy of the Little Pig vein, Mainland Belt silver region, Thunder Bay District, Ontario. Honors B.Sc. thesis, Lakehead University, Thunder Bay, Ontario. 48 p.
- Matthews, A., and Katz, A.
1977: Oxygen isotope fractionation during dolomitization of calcium carbonate. *Geochimica et Cosmochimica Acta*, vol. 41, pp. 1431-1438.
- McGlynn, J.C.
1970: Geology of the Canadian Shield-Superior Province. in *Geology and Economic Minerals of Canada*. Geological Survey of Canada, Economic Geology Report No. 1 pp. 66.
- Miles, H.C.
1933: Report on the Animikie Mines Gillies and O'Connor Township, Thunder Bay District, Ontario. Animikie Mines Limited.
- Moorehouse, W.W.
1960: Gunflint Iron Range in the vicinity of Port Arthur. Ontario Department of Mines Annual Report, vol. 69, part 7. pp. 1-40.

- Morey, E.B.
1969: The geology of the Middle Precambrian Rove Formation in northeastern Minnesota. Minnesota Geological Survey, Special Publication Series, SP7, 62 p.
- Morey, E.B.
1972: The Gunflint Range. *in* Geology of Minnesota, a Centennial Volume, Edited by P.K.Sims and G.B. Morey, Minnesota Geological Survey. pp. 218-225.
- Mosley, E.B.
1977: Geology and mineralogy of the Rabbit Mountain Mine, Mainland Belt silver region, Thunder Bay District, Ontario. Honors B.Sc. thesis, Lakehead University, Thunder Bay, Ontario. 94 p.
- Ohmoto, H.
1986: Stable isotope geochemistry of ore deposits. *in* Stable Isotopes in High Temperature Geological Processes, Reviews in Mineralogy, vol. 16. Edited by. J.W. Valley, H.P. Taylor, Jr., J.R. O'Neil, pp. 491-560.
- Oja, R.V.
1967: Geochemical investigations of the Thunder Bay silver area. *in* Proceedings, Symposium on Geochemical Prospecting, Geological Survey of Canada Paper 66-54, Edited by E.M. Cameron. pp. 211-221.
- O'Neil, J.R., Clayton, R.N. and Mayeda, T.K.
1969: Oxygen isotope fractionation in divalent metal carbonates. Journal Chemical Physics, vol. 51, pp. 5547-5558.
- Peterman, Z.E.
1966: Rb-Sr dating of middle Precambrian metasedimentary rocks of Minnesota. Geological Society of America Bulletin, vol. 77, pp. 1031-1044.
- Potter, R.W., II.
1977: Pressure corrections for fluid-inclusion homogenization temperatures based on the volumetric properties of the system NaCl-H₂O. United States Geological Survey Journal of Research, vol. 5, pp. 603-607.
- Potter, R.W., II., Clyne, M.A., and Brown, D.L.
1978: Freezing point depression of aqueous sodium chloride solutions. Economic Geology, vol. 73, pp. 284-285.
- Roedder, E.
1984: Fluid Inclusions. Reviews in Mineralogy vol. 12. Mineralogical Society of America. 644 p.

Schoell, M.

1984: Stable isotopes in petroleum research. in Advances in Petroleum Geochemistry, vol. 1. Edited by J.D. Brooks and D. Welte. Academic Press, London. pp. 215-243.

Shegelski, R.J.

1982: The Gunflint Formation. in Proterozoic geology of the northern Lake Superior area. Edited by J.M. Franklin. Geological Association of Canada, Winnipeg Manitoba Guidebook, Field Trip 4, pp. 15-41.

Shelton, K.L.

1983: Composition and origin of ore-forming fluids in a carbonate-hosted porphyry copper and skarn deposit: a fluid inclusion and stable isotope study of Mines Gaspe Quebec. Economic Geology, vol. 78, pp. 387-421.

Smyk, M.C.

1984: A comparative study of silver occurrences, Island Belt silver region, Thunder Bay District, Ontario, Honors B.Sc. thesis, Lakehead University, Thunder Bay, Ontario. 132 p.

Sourirajan, S. and Kennedy, G.C.

1962: The system H₂O-NaCl at elevated temperatures and pressures. American Journal of Science, vol. 260, pp. 115-141.

Stille, P. and Clauer, N.

1986: Sm-Nd isochron-age and provenance of the argillites of the Gunflint Iron Formation in Ontario Canada. Geochimica et Cosmochimica Acta, vol. 50, pp. 1141-1146.

Tanton, T.L.

1931: Fort William and Port Arthur and Thunder Cap map areas, Thunder Bay District, Ontario. Geological Survey of Canada, Memoir 167, 222p.

Taylor, H.P. Jr.

1967: Oxygen isotope studies of hydrothermal mineral deposits in Geochemistry of hydrothermal ore deposits. Edited by H.L. Barnes. Holt, Rinehart and Winston New York. pp. 109-142.

Truesdell, A.H.

1974: Oxygen isotope activities and concentrations in aqueous salt solutions at elevated temperature: consequences for isotope geochemistry. Earth and Planetary Science Letters, vol. 23, pp. 387-396.

Valley, J.W.

1986: Stable isotope geochemistry of metamorphic rocks in
Stable Isotopes in High Temperature Geological
Processes, Reviews in Mineralogy, vol. 16. Edited by.
J.W. Valley, H.P. Taylor, Jr., J.R. O'Neil,
pp. 445-490.

Wallace, H.

1981: Keweenawan geology of the Lake Superior Basin. in
Proterozoic Basins of Canada. Edited by F.H.A.
Campbell. Geological Survey of Canada paper 81-10,
pp. 399-417.

Yeh, H.

1980: D/H ratios and late-stage dehydration of shales during
burial. Geochimica et Cosmochimica Acta, vol. 44,
pp. 341-352.

SHUNIAH MINE FLUID INCLUSION DATA
HOMOGENIZATION TEMPERATURE OF QUARTZ I

SAMPLE No.	DEPTH (feet)	HOST	T HOM. (C°)	HOM. PHASE
SHA-10-1	10	QTZ I	375.0	V
SHA-10-1	10	QTZ I	375.4	V
SHA-10-1	10	QTZ I	376.4	L
SH-79	21	QTZ I	359.8	V
SH-79	21	QTZ I	362.8	L
SH-112	385	QTZ I	423.0	V
SH-112	385	QTZ I	436.1	V
SH-112	385	QTZ I	450.1	V
SH-127	389	QTZ I	390.6	L
SH-128	395	QTZ I	359.8	L
SH-130	398	QTZ I	419.6	V
SH-130	398	QTZ I	420.3	V
SH-133	405	QTZ I	442.6	V
SH-133	405	QTZ I	389.8	L
SH-52	411	QTZ I	374.2	L
SH-52	411	QTZ I	380.3	L
SH-150	489	QTZ I	448.8	L
SH-150	489	QTZ I	440.3	V
SH-177	572	QTZ I	445.6	L
SH-177	572	QTZ I	433.2	V

SHUNIAH MINE FLUID INCLUSION DATA
HOMOGENIZATION TEMPERATURE OF QUARTZ II

SAMPLE No.	DEPTH (feet)	HOST	T HOM. (C°)	HOM. PHASE
SHA-2	10	QTZ II	349.4	L
SHA-6	10	QTZ II	385.4	V
SHA-6	10	QTZ II	390.0	L
SHA-6	10	QTZ II	402.3	L
SHA-6	10	QTZ II	378.9	V
SHA-6	10	QTZ II	375.6	V
SH-76	16	QTZ II	400.0	V
SH-76	16	QTZ II	402.9	L
SH-76	16	QTZ II	420.0	L
SH-76	16	QTZ II	400.7	V
SH-78	20	QTZ II	360.0	L
SH-78	20	QTZ II	365.4	L
SH-78	20	QTZ II	418.9	V
SH-78	20	QTZ II	424.5	V
SH-2	384	QTZ II	444.5	V
SH-2	384	QTZ II	449.5	V

SHUNIAH MINE FLUID INCLUSION DATA
HOMOGENIZATION TEMPERATURE OF QUARTZ II

SAMPLE No.	DEPTH (feet)	HOST	T HOM. (C°)	HOM. PHASE
SH-2	384	QTZ II	471.8	V
SH-2	384	QTZ II	430.9	L
SH-112	385	QTZ II	381.3	L
SH-112	385	QTZ II	441.2	V
SH-112	385	QTZ II	442.8	L
SH-112	385	QTZ II	457.5	V
SH-127	389	QTZ II	410.6	V
SH-82	394	QTZ II	429.4	L
SH-82	394	QTZ II	439.3	V
SH-128	395	QTZ II	456.7	L
SH-128	395	QTZ II	482.0	L
SH-128	395	QTZ II	482.2	V
SH-130	398	QTZ II	462.3	L
SH-130	398	QTZ II	511.2	V
SH-130	398	QTZ II	524.5	V
SH-131	399	QTZ II	402.8	L
SH-131	399	QTZ II	414.4	L
SH-131	399	QTZ II	420.6	V
SH-133	405	QTZ II	444.9	L
SH-133	405	QTZ II	357.4	V
SH-52	411	QTZ II	389.3	L
SH-52	411	QTZ II	407.6	L
SH-53	411	QTZ II	410.9	L
SH-52	411	QTZ II	424.4	L
SH-52	411	QTZ II	435.1	L
SH-52	411	QTZ II	444.4	V
SH-52	411	QTZ II	450.0	L
SH-147	419	QTZ II	455.6	V
SH-109	451	QTZ II	402.4	L
SH-109	451	QTZ II	451.1	L
SH-110	455	QTZ II	371.8	L
SH-123	465	QTZ II	385.6	L
SH-123	465	QTZ II	398.8	L
SH-123	465	QTZ II	439.8	L
SH-123	465	QTZ II	380.0	L
SH-124	468	QTZ II	374.1	V
SH-150	489	QTZ II	433.2	V
SH-175	528	QTZ II	355.4	L
SH-177	572	QTZ II	368.4	L
SH-177	572	QTZ II	391.7	L
SH-177	572	QTZ II	401.2	L
SH-177	572	QTZ II	415.0	L
SH-177	572	QTZ II	423.4	L
SH-177	572	QTZ II	428.8	L
SH-177	572	QTZ II	430.5	V
SH-177	572	QTZ II	400.2	L
SH-177	572	QTZ II	357.4	L

SHUNIAH MINE FLUID INCLUSION DATA
HOMOGENIZATION TEMPERATURE OF QUARTZ III

SAMPLE No.	DEPTH (feet)	HOST	T HOM. (C°)	HOM. PHASE
SHA-10-3	10	QTZ III	491.6	L
SHA-10-3	10	QTZ III	504.2	L
SHA-10-3	10	QTZ III	510.0	L
SHA-6	10	QTZ III	552.6	L
SHA-8	10	QTZ III	192.4	L
SHA-2	10	QTZ III	297.8	L
SH-77	19	QTZ III	196.1	V
SH-77	19	QTZ III	199.0	V
SH-77	19	QTZ III	247.0	L
SH-77	19	QTZ III	267.3	L
SH-71	57	QTZ III	203.0	L
SH-71	57	QTZ III	258.2	L
SH-3	384	QTZ III	285.7	L
SH-3	384	QTZ III	296.6	L
SH-3	384	QTZ III	303.5	L
SH-3	384	QTZ III	310.0	L
SH-3	384	QTZ III	312.8	L
SH-3	384	QTZ III	333.4	L
SH-127	389	QTZ III	172.4	L
SH-127	389	QTZ III	242.4	L
SH-51	395	QTZ III	223.2	L
SH-51	395	QTZ III	255.3	L
SH-51	395	QTZ III	264.8	L
SH-129	397	QTZ III	262.3	V
SH-129	397	QTZ III	277.8	V
SH-133	405	QTZ III	85.6	L
SH-133	405	QTZ III	251.7	L
SH-133	405	QTZ III	264.7	L
SH-133	405	QTZ III	338.1	L
SH-133	405	QTZ III	340.4	V
SH-133	405	QTZ III	386.4	L
SH-83	414	QTZ III	270.0	L
SH-83	414	QTZ III	285.1	L
SH-83	414	QTZ III	322.2	L
SH-83	414	QTZ III	327.8	L
SH-30	424	QTZ III	248.8	L
SH-30	424	QTZ III	276.6	L
SH-30	424	QTZ III	308.7	L
SH-30	424	QTZ III	312.0	L
SH-30	424	QTZ III	317.7	L
SH-150	489	QTZ III	303.0	L
SH-48	674	QTZ III	458.0	D
SH-190	754	QTZ III	337.8	L

**SHUNIAH MINE FLUID INCLUSION DATA
HOMOGENIZATION TEMPERATURE OF CALCITE**

SAMPLE No.	DEPTH (feet)	HOST	T HOM. (C°)	HOM. PHASE
SHA-10-3	10	CC	189.5	L
SHA-10-2	10	CC	193.0	L
SHA-8	10	CC	252.7	L
SHA-8	10	CC	272.4	L
SHA-8	10	CC	300.9	L
SH-70	54	CC	222.2	L
SH-70	54	CC	227.8	L
SH-70	54	CC	236.4	V
SH-190	754	CC	295.7	L
SH-190	754	CC	343.0	V
SHA-3	10	CC I	87.0	L
SHA-3	10	CC I	87.8	V
SHA-6	10	CC I	97.6	L
SHA-4	10	CC I	97.6	L
SHA-3	10	CC I	98.1	L
SHA-3	10	CC I	98.8	L
SHA-6	10	CC I	106.0	L
SHA-4	10	CC I	117.5	L
SHA-10-4	10	CC I	118.2	L
SHA-4	10	CC I	132.5	L
SH-154	72	CC I	89.7	L
SH-154	72	CC I	107.0	L
SH-154	72	CC I	108.0	L
SH-154	72	CC I	108.0	L
SH-154	72	CC I	119.4	L
SH-156	148	CC I	103.0	L
SH-156	148	CC I	106.0	L
SH-50	392	CC I	118.2	L
SH-50	392	CC I	125.4	L
SH-50	392	CC I	152.5	L
SH-130	398	CC I	115.7	L
SH-130	398	CC I	121.2	L
SH-130	398	CC I	135.8	L
SH-133	405	CC I	107.8	L
SH-133	405	CC I	164.7	L
SH-133	405	CC I	166.6	L
SH-133	405	CC I	167.6	L
SH-133	405	CC I	169.7	L
SH-133	405	CC I	170.7	L
SH-133	405	CC I	182.6	L
SH-83	414	CC I	150.5	L
SH-29	421	CC I	160.4	L
SH-18	491	CC I	142.2	L

**SHUNIAH MINE FLUID INCLUSION DATA
HOMOGENIZATION TEMPERATURE**

SAMPLE No.	DEPTH (feet)	HOST	T HOM. (C°)	HOM. PHASE
SH-177	572	CC I	210.6	L
SH-43	590	CC I	150.1	L
SH-48	674	CC I	157.8	L
SH-48	674	CC I	158.0	L
SH-48	674	CC I	180.0	L
SHA-7	10	CC II	55.8	L
SH-130	398	CC II	99.1	L
SH-133	405	CC II	66.6	L
SH-133	405	CC II	68.9	L
SH-106	408	CC II	62.7	L
SH-106	408	CC II	65.6	L
SH-83	414	CC II	87.6	L
SH-83	414	CC II	91.2	L
SH-18	491	CC II	87.1	L
SH-18	491	CC II	87.4	L
SH-43	590	CC II	113.9	L
SH-43	590	CC II	127.7	L
SH-44	611	CC II	104.3	V
SH-147	419	AMY	56.8	L
SH-133	405	GF	227.8	L
SH-133	405	GF	237.0	L
SH-133	405	GF	276.3	V
SH-133	405	GF	278.2	L
SH-133	405	GF	281.7	V
SH-29	421	GF	258.6	L
SH-29	421	GF	262.2	L
SH-29	421	GF	263.6	L
SH-29	421	GF	285.7	L
SH-29	421	GF	292.2	V
SH-29	421	GF	294.7	V
SH-29	421	GF	297.2	L
SH-30	424	GF	267.3	L
SH-30	424	GF	308.7	L
SH-130	398	SPH	110.0	L
SH-130	398	SPH	112.1	L
SH-130	398	SPH	113.6	L
SH-130	398	SPH	114.0	L
SH-130	398	SPH	124.6	L
SH-130	398	SPH	124.8	L

SHUNIAH MINE FLUID INCLUSION DATA
QUARTZ FREEZING DATA

SAMPLE No.	DEPTH (feet)	HOST	T EUT. (C°)	T FIN. (C°)	SALINITY WT % NaCl
SH-52	411	QTZ I	-62.2	-16.5	20.0
SH-53	411	QTZ I	-59.0	-16.1	19.7
SHA-10-3	10	QTZ I	-57.8	-18.0	21.2
SH-52	411	QTZ I	-57.6	-22.1	24.1
SHA-10-1	10	QTZ I	-56.6	-11.4	15.4
SHA-10-3	10	QTZ I	-54.3	-17.6	20.9
SH-79	21	QTZ I	-53.6	-9.1	13.0
SH-127	389	QTZ I	-48.2	-12.2	16.2
SH-109	451	QTZ I	-47.2	-15.0	18.8
SH-109	451	QTZ I	-45.6	-14.4	18.3
SH-110	455	QTZ I	-44.4	-11.2	15.2
SH-112	385	QTZ I	-41.9	-4.6	7.3
SH-123	465	QTZ I	-40.4	-10.1	14.1
SH-130	398	QTZ I	-39.8	-18.9	21.9
SH-76	16	QTZ II	-79.2	-8.5	12.3
SH-128	395	QTZ II	-44.8	-4.0	6.4
SH-78	20	QTZ II	-44.0	-10.6	14.6
SHA-2	10	QTZ II	-42.7	-2.8	4.6
SH-2	384	QTZ II	-41.8	-8.5	12.3
SH-2	384	QTZ II	-38.2	-7.2	10.7
SH-77	19	QTZ III	-71.5	-34.2	32.1
SHA-8	10	QTZ III	-63.2	-23.0	24.7
SH-133	405	QTZ III	-55.5	-18.6	21.6
SHA-6	10	QTZ III	-53.3	-6.8	10.2
SH-133	405	QTZ III	-52.2	-21.7	23.8
SH-51	395	QTZ III	-47.0	-4.9	7.7
SH-124	468	QTZ III	-43.8	-7.9	11.6
SH-150	489	QTZ III	-26.0	-5.4	8.4
SH-176	539	QTZ III	-32.6	-1.0	1.7
SH-150	489	QTZ III	-29.7	-11.2	15.2
SH-48	674	QTZ III	-22.0	-2.4	4.0

**SHUNIAH MINE FLUID INCLUSION DATA
CALCITE FREEZING DATA**

SAMPLE No.	DEPTH (feet)	HOST	T EUT. (C°)	T FIN. (C°)	SALINITY WT. % NaCl
SHA-10-3	10	CC	-51.9	-3.5	5.7
SHA-8	10	CC	-42.8	-6.6	10.0
SHA-8	10	CC	-57.9	-24.6	25.7
SHA-4	10	CC	-48.1	-9.4	13.3
SHA-10-2	10	CC	-48.4	-12.8	16.8
SHA-7	10	CC	-48.0	-6.9	10.4
SHA-7	10	CC	-47.5	-9.8	13.8
SHA-6	10	CC	-43.8	-6.8	10.2
SH-70	54	CC	-37.6	-2.8	4.6
SH-156	148	CC	-34.0	-1.0	1.7
SH-156	148	CC	-34.0	-0.5	0.9
SH-133	405	CC	-86.2	-36.0	33.4
SH-18	491	CC	-47.6	-1.0	1.7
SH-175	528	CC	-51.9	-6.9	10.4
SH-44	611	CC	-45.6	-4.6	7.3
SH-190	754	CC	-44.6	-13.3	17.3
SHA-3	10	CC I	-51.6	-14.3	18.2
SHA-3	10	CC I	-48.8	-15.0	18.8
SHA-6	10	CC I	-44.8	-3.2	5.2
SHA-4	10	CC I	-43.3	-10.6	14.6
SHA-3	10	CC I	-46.2	-20.7	23.2
SHA-3	10	CC I	-46.1	-12.8	16.8
SHA-10-4	10	CC I	-43.7	-5.7	8.8
SHA-4	10	CC I	-38.6	-7.3	10.9
SH-154	72	CC I	-43.2	-13.3	17.3
SH-154	72	CC I	-44.5	-3.0	4.9
SH-154	72	CC I	-35.5	-2.2	3.7
SH-154	72	CC I	-34.6	-2.0	3.4
SH-154	72	CC I	-38.6	-3.8	6.1
SH-156	148	CC I	-32.0	-0.2	0.4
SH-156	148	CC I	-32.0	-0.5	0.9
SH-50	392	CC I	-60.4	-10.9	14.9
SH-133	405	CC I	-74.8	-37.4	34.5
SH-133	405	CC I	-77.9	-47.8	45.4
SH-18	491	CC I	-48.4	-4.7	7.4

**SHUNIAH MINE FLUID INCLUSION DATA
CALCITE FREEZING DATA**

SAMPLE No.	DEPTH (feet)	HOST	T EUT. (C°)	T FIN. (C°)	SALINITY WT. % NaCl
SH-177	572	CC I	-50.2	-4.3	6.9
SH-48	674	CC I	-47.0	-15.8	19.5
SH-130	398	CC II	-43.1	-7.0	10.5
SH-133	405	CC II	-60.0	-45.1	42.0
SH-133	405	CC II	-62.4	-44.3	41.1
SH-106	408	CC II	-51.3	-19.2	22.1
SH-106	408	CC II	-51.3	-18.7	21.7
SH-83	414	CC II	-45.5	-15.5	19.2
SH-18	491	CC II	-47.0	-18.8	21.8
SH-43	590	CC II	-48.6	-5.0	7.9
SH-44	611	CC II	-45.2	-7.0	10.5
SH-147	419	AMY	-38.8	-16.6	20.1
SH-29	421	GF	-44.9	-11.9	15.9
SH-130	398	SPH	-38.5	-7.8	11.5
SH-130	398	SPH	-37.8	-7.5	11.1

THUNDER BAY MINE FLUID INCLUSION DATA

SAMPLE No.	HOST	T HOM. (C°)	HOM PHASE
TB-5	CC	81.3	L
TB-5	CC	91.1	L
TB-5	CC	92.5	L
TB-5	CC	95.9	L
TB-5	CC	97.0	L
TB-5	CC	109.2	L
TB2-2	QTZ	390.6	L
TB2-1	QTZ	401.0	L
TB2-1	QTZ	404.4	L
TB2-1	QTZ	416.3	L
TB2-2	QTZ	425.7	L
TB2-1	QTZ	438.5	V
TB2-1	QTZ	457.7	V
TB2-1	QTZ	461.0	V

SAMPLE No.	HOST	T EUT. (C°)	T FIN. (C°)	SALINITY
TB-5	CC	-48.3	-7.5	11.1
TB-5	CC	-47.2	-7.5	11.1
TB-5	CC	-47.0	-6.7	10.1
TB2-2	QTZ	-47.5	-15.2	19.0
TB2-2	QTZ	-47.5	-14.6	18.4
TB2-1	QTZ	-46.8	-16.6	20.1

KEYSTONE MINE FLUID INCLUSION DATA

SAMPLE No.	DEPTH (feet)	HOST	T HOM. (C°)	HOM. PHASE	
KS-6-3	0	QTZ	275.8	L	
KS-6-3	0	QTZ	282.2	L	
KS-6	0	QTZ	301.4	V	
KS-6-3	0	QTZ	312.0	V	
KS-6	0	QTZ	316.4	L	
KS-6	0	QTZ	324.8	V	
5-120	120	QTZ	275.4	L	
5-120	120	QTZ	316.3	V	
5-120	120	QTZ	317.4	L	
6-219.5	219.5	QTZ	410.3	L	
6-219.5	219.5	QTZ	421.3	L	
6-219.5	219.5	QTZ	423.2	L	
6-219.5	219.5	QTZ	430.6	V	
6-220	220	QTZ	358.8	L	
6-220	220	QTZ	362.2	V	
6-220	220	QTZ	479.0	V	
6-220	220	QTZ	479.4	V	
6-221-2	221	QTZ	246.7	L	
6-221-2	221	QTZ	255.1	L	
6-221-1	221	QTZ	299.8	L	
6-221-2	221	QTZ	373.8	L	
6-221-2	221	QTZ	396.2	L	
6-221-2	221	QTZ	409.1	V	
6-221-2	221	QTZ	410.0	V	
6-221-1	221	QTZ	488.8	L	
6-223	223	QTZ	285.4	L	
6-223	223	QTZ	315.6	L	
6-223	223	QTZ	323.3	L	
6-223	223	QTZ	325.9	L	
6-223	223	QTZ	336.4	L	
6-224	224	QTZ	190.3	L	
06-224	224	QTZ	192.4	V	
6-224	224	QTZ	204.3	L	
6-225	225	QTZ	293.1	L	
6-225	225	QTZ	298.1	L	
6-225	225	QTZ	307.1	L	
6-225	225	QTZ	321.7	L	
6-225	225	QTZ	473.0	L	
6-220.75	225.75	QTZ	294.7	V	
6-280	280	QTZ	323.5	L	

SAMPLE No.	DEPTH (feet)	HOST	T EUT (C°)	T FIN. (C°)	SALINITY
KS-6-3	0	QTZ	-42.8	-7.8	11.6
5-120	120	QTZ	-36.6	-15.7	19.6
6-219.5	219.5	QTZ	-41.9	-13.1	17.3
6-221-2	221	QTZ	-47.7	-16.1	20.0
6-223	223	QTZ	-36.7	-18.4	21.8
06-224	224	QTZ	-35.0	-1.0	1.7

KEYSTONE MINE FLUID INCLUSION DATA

SAMPLE No.	DEPTH (feet)	HOST	T HOM. (C°)	HOM. PHASE
06-67	67	CC	54.0	L
06-67	67	CC	55.4	L
06-67	67	CC	64.1	L
KS2-4	0	CC	78.5	L
KS2-4	0	CC	79.4	L
5-125	125	CC	85.8	L
5-140	140	CC	88.6	L
6-225-1	225	CC	140.6	L
KS-6	0	GF	278.0	L
KS-6	0	GF	308.0	L
KS-6	0	GF	317.8	L
6-225-2	225	PF	266.6	L
6-225-2	225	PF	268.4	L
6-225-2	225	PF	287.5	L
6-225-2	225	PF	290.1	V
6-225-1	225	PF	310.7	L
6-225-1	225	PF	327.4	V
KS2-4	0	SPH	92.9	L
K6	0	SPH	93.6	L
KS2-4	0	SPH	103.8	L

SAMPLE No.	DEPTH (feet)	HOST	T EUT (C°)	T FIN. (C°)	SALINITY
06-67	67	CC	-58.6	-13.6	17.8
KS2-4	0	CC	-32.8	-5.6	8.8
KS2-4	0	CC	-33.4	-5.1	8.1
5-125	125	CC	-40.2	-6.9	10.5
5-140	140	CC	-40.1	-11.9	16.2
6-225-1	225	CC	-66.2	-44.2	41.7
KS-6	0	GF	-39.4	-7.3	11.0
6-225-2	225	PF	-47.0	-11.6	15.8
6-225-2	225	PF	-48.2	-8.8	12.8
KS2-4	0	SPH	-23.4	-3.5	5.8
KS2-4	0	SPH	-24.0	-3.0	5.0

PORCUPINE MINE FLUID INCLUSION DATA

SAMPLE No.	DEPTH (feet)	HOST	T HOM. (C°)	HOM. PHASE
13-56	56	QTZ	163.9	L
13-56	56	QTZ	170.4	L
13-42	42	QTZ	180.5	L
13-42	42	QTZ	192.5	L
13-42	42	QTZ	259.5	L
13-42	42	QTZ	266.6	V
13-30	30	QTZ	267.4	L
13-48	48	QTZ	272.5	L
13-48	48	QTZ	277.3	V
13-48	48	QTZ	278.0	V
13-42	42	QTZ	286.2	L
13-48	48	QTZ	286.4	L
13-42	42	QTZ	288.2	L
13-42	42	QTZ	294.6	L
PO-1	0	QTZ	295.7	L
13-48	48	QTZ	299.6	L
PO-1	0	QTZ	300.0	V
13-48	48	QTZ	301.3	L
13-42	42	QTZ	302.6	L
13-30	30	QTZ	308.8	L
13-68	68	QTZ	322.8	L
13-30	30	QTZ	338.2	V
13-42	42	QTZ	363.6	L
13-36	36	QTZ	365.0	L
13-42	42	QTZ	370.8	V
PO-5	0	QTZ	386.0	L
PO-5	0	QTZ	389.6	L
13-36	36	QTZ	393.4	L
13-68	68	QTZ	444.4	V

SAMPLE No.	DEPTH (feet)	HOST	T EUT (C°)	T FIN (C°)	SALINITY
13-56	56	QTZ	-25.4	-4.6	7.3
13-42	42	QTZ	-45.6	-6.3	9.6
13-42	42	QTZ	-36.7	-2.0	3.4
13-42	42	QTZ	-39.5	-3.5	5.7
13-48	48	QTZ	-37.0	-2.3	3.9
13-68	68	QTZ	-42.1	-1.0	1.7
PO-10	0	QTZ	-31.0	-3.1	5.1

PORCUPINE MINE FLUID INCLUSION DATA

SAMPLE No.	DEPTH (feet)	HOST	T HOM. (C°)	HOM PHASE
PO-3	0	CC	84.8	L
PO-4	0	CC	87.7	L
PO-4	0	CC	92.4	L
13-51	51	CC	104.6	L
13-51	51	CC	114.7	L
13-51	51	CC	353.1	V
13-51	51	CC	357.1	V
13-56	56	CC	84.8	L
13-68	68	CC	108.9	L
13-68	68	CC	343.5	L
13-80	80	CC	73.1	L
13-80	80	CC	83.3	L
03-358.6	358.6	CC	163.0	L
03-358.6	358.6	CC	170.6	V
03-360	360	CC	116.8	L
03-410	410	CC	287.7	L
03-410	410	CC	306.2	V
03-440	440	CC	168.9	L
03-440	440	CC	196.2	L
03-440	440	CC	218.3	L
PO-1	0	GF	158.0	L
PO-1	0	GF	220.0	L
PO-1	0	GF	238.6	L
PO-1	0	GF	253.7	L
PO-1	0	GF	256.4	L
PO-1	0	GF	258.0	V
PO-1	0	GF	275.6	V
PG-4	0	PF	260.6	V
PG-4	0	PF	262.4	V
PG-4	0	PF	268.2	L
PG-4	0	PF	270.5	L
PO-5	0	SPH	72.4	L
PO-5	0	SPH	92.5	L

SAMPLE No.	DEPTH (feet)	HOST	T EUT (C°)	T FIN (C°)	SALINITY
PO-3	0	CC	-35.0	-5.6	8.7
PO-4	0	CC	-35.8	-5.7	8.8
PO-4	0	CC	-35.0		
13-51	51	CC	-38.0	-0.3	0.5
13-51	51	CC	-38.2	-6.0	9.2
13-56	56	CC	-35.6	-10.5	14.5
13-68	68	CC	-51.5	-13.4	17.4
13-80	80	CC	-44.2	-5.8	8.9
03-358.6	358.6	CC	-40.5	-5.6	8.7
03-360	360	CC	-38.8	-4.1	6.6
03-410	410	CC	-69.5	-5.0	7.9
PO-1	0	GF	-43.0	-8.4	12.2
PG-4	0	PF	-44.0	-8.7	12.5
PO-5	0	SPH	-33.0	-8.0	11.7

STABLE ISOTOPE SAMPLES FLUID INCLUSION DATA

SAMPLE No.	DEPTH (feet)	HOST	T HOM (C°)	HOM. PHASE
SI	GRAB	DOLOMITE	183.0	L
SI	GRAB	DOLOMITE	172.1	L
SM	0	QUARTZ	129.6	L
EA53	0	QUARTZ	102.4	L

Appendix 1
explanation of headings

Depth	depth below ground surface in feet
Host	mineral that hosted the fluid inclusion
T HOM	homogenization temperature for the fluid inclusion in degrees Celsius
HOM PHASE	phase that the fluid inclusion homogenized to, either liquid (L) or vapor (V)
T EUT	eutectic temperature for the fluid inclusion in degrees Celsius
T Fin	final melting temperature for the fluid inclusion in degrees Celsius
Salinity	salinity of the fluid inclusion as calculated from the final melting temperature using the equations of Potter <u>et al.</u> (1978)

Appendix 2

Preparation of double polished thin sections without heating (modified from Jennings, 1987).

1. Trim the samples to fit a 1" diameter bakelite mounting ring. Grind the sample on 400 grit to remove saw marks. Clean the sample and leave it to dry overnight. Allow to air dry do not heat the sample.
2. Mount the sample in the bakelite mounting ring in a conventional manner using a cold setting epoxy such as Araldite. Care must be taken when preparing the epoxy, not to add too much hardener to the mixture. Too much hardener will cause the epoxy to heat up upon setting and possibly damaging the fluid inclusions.
3. After the epoxy has set grind the sample to a 600 grit. Then polish the sample to 1 micron with a lead lap. Clean and allow the sample to air dry overnight.
4. Mount the sample on a glass plate that has been lightly ground to roughen its surface. The epoxy used to mount the sample is Clearcast epoxy which is a polyester casting resin produced by MIA Chemicals. Allow the sample to air dry overnight.
5. Cut the sample, using the thin-sectioning saw, in the same manner used to make thin sections. Using the thin-section grinding wheel, grind the sample until it is translucent. Then grind the sample on 600 grit. Clean and allow the sample to air dry overnight.
6. Polish the sample, on a lead lap down to 1 micron.
7. Soak the sample in acetone for 24 hours to remove it from the glass plate.

Sample preparation in this manner will produce double polished section that have not been heated above 30°C.

Shuniah Sample

Pinhole	d spacings measured ¹ Gandolfi	standard ²	Intensity
8.799 VS		8.39	100
		5.64	60
		4.82	50
4.079 W	4.27 VW	4.30	20
		4.03	40
		3.79	40
3.454 VS	3.37 S	3.44	80
3.239 S		3.20	80
	3.04 M	3.05	40
		2.95	60
2.7206 M	2.83 M	2.78	60
	2.52 S	2.56	80
2.398 W	2.44 M	2.37	40
	2.27 W	2.25	20
2.1142 W	2.12 M	2.09	60
		2.03	20
	1.98 S	1.95	60
		1.88	40
	1.81 M	1.82	40
		1.75	50
		1.70	40
	1.66 W	1.66	20
		1.60	50
	1.54 W	1.56	40
		1.52	40
	1.49 M	1.48	20
		1.45	50
		1.40	40
	1.37 W	1.37	20
		1.34	60
	present but VW not measured	1.30	40
		1.26	40
		1.23	20
		1.20	20
	1.18 M	1.18	40

Shuniah Sample Cont.

d spacings measured ¹ Pinhole	standard ² Gandolfi	Intensity
	1.16	40
	1.14	20
	1.11	40
	1.09	20
	1.08	20
	1.06	20
	1.05	40
	1.03	20
	1.00	20

Identified as wavellite $\text{Al}_3(\text{OH})_3(\text{PO}_4)_5 \cdot 5\text{H}_2\text{O}$

1 Relative intensities expressed as S = strong,
M = moderate, W = weak and V = very

2 Standard from Selected Powder Diffraction Data for
Minerals Search Manual, Joint Committee on Powder
Diffraction Standards, 1974. File number 2-0075

Silver Mountain Sample

Pinhole Camera

d spacings measured

4.458	strong
2.776	
1.781	
3.327	
7.305	
12.70	
4.46	
3.36	
2.57	weak

sample identified as 2 M illite $K-Na-Mg-Fe-Al-Si-O-H_2O$

Appendix 4

Explanation of sample labels

All the samples of core from the Shuniah Mine are from a collection at the Geological Survey of Canada. This collection is comprised of a series of samples taken from the core by Curtis and then donated to the Geological Survey of Canada. The samples are catalogued in "Catalogue of Specimens of Rock, Gangue, and Ores Passed through by the Diamond Drill at the Duncan Silver Mine Thunder Bay, Lake Superior W.M. Curtis M.E. 1877-1878"

All samples that were used from this collection during this study are identified as SH-###., where the number refers to the catalogued number.

Other samples that are identified as SHA-## were collected from a vein cross section that was exposed in an old adit that was opened during the course of this study.

Samples from the Thunder Bay vein are identified as TB#-#, these were collected during the course of this study.

Samples of core from the Creswel Group are from the collection J.M. Franklin. This samples are labeled 68-#-###. The first number refers to the diamond drill core number. The second set of numbers refers to the vertical depth of the sample. These were calculated using the depth along the core and the angle of the drill hole.

Samples of the Porcupine vein were collected from a surface exposure during this study and are labeled PO-# and PG-#.

Samples of the Keystone vein were collected from a surface exposure during this study and are labeled KS-#-#.

One sample of illite from the Keystone mine was collected and identified by Jennings (1987), labeled EA53.

One sample of illite was collected from Silver Mountain during the course of this study and identified, and is labeled SM.

Sample descriptions

Shuniah vein

Sample	DDH	Wall Rock	Vein Material
SH-2	01	shale	quartz, calcite
SH-3	01	shale	quartz
SH-18	03	shale	calcite, chlorite?
SH-29	04	shale	quartz, calcite, sphalerite, pyrite, marcasite, galena, argentite
SH-30	04	chert	quartz, green fluorite, pyrite
SH-43	04	syenite	quartz, calcite
SH-44	04	syenite	quartz, calcite
SH-48	04	syenite	quartz, calcite veinlets
SH-50	05	shale	quartz, calcite, pyrite and sphalerite
SH-51	05	foliated granitoid	quartz
SH-52	05	none seen	quartz
SH-70	06	shale	calcite
SH-71	07	shale	quartz vein
SH-76	08	shale	quartz
SH-77	08	shale	quartz
SH-78	08	shale	quartz
SH-79	08	green shale	quartz
SH-82	09	shale	quartz
SH-83	09	shale	quartz, calcite
SH-106	10	shale	quartz, calcite
SH-109	10	chlorite?	quartz
SH-110	10	chlorite?	quartz
SH-199	10	none seen	quartz, calcite, green fluorite, pyrite
SH-112	11	shale	quartz
SH-123	13	green shale	quartz
SH-124	13	green shale + pyrite	quartz

Shuniah vein cont.

Sample	DDH	Wall Rock	Vein Material
SH-127	14	shale	quartz
SH-128	14	black shale	quartz vein
SH-129	14	brecciated shale	quartz veinlets
SH-130	14	shale	quartz, calcite, sphalerite
SH-131	14	black shale	quartz veinlets
SH-133	14	shale	quartz, marcasite, pyrite, sphalerite, green fluorite, calcite
SH-147	16	shale	quartz, amethyst
SH-150	16	shale	quartz
SH-154	17	shale	calcite
SH-156	18	shale	calcite
SH-175	18	granite	quartz, calcite
SH-176	18	chert	quartz
SH-177	18	shale	quartz, calcite
SH-190	18	syenite	quartz, calcite, pyrite, marcasite, galena, sphalerite, green fluorite
SHA 1-8	surface	silicified shale	calcite, quartz, pyrite, sphalerite, galena, argentite, native silver, wavellite

Thunder Bay vein

Sample #	Wall Rock	Vein Material
TB-2	silicified shale, graphite	quartz, calcite, pyrite, sphalerite, galena, native silver
TB-2-1	silicified shale	quartz
TB-2-2	silicified shale	quartz
TB-5	silicified shale	calcite

Keystone vein

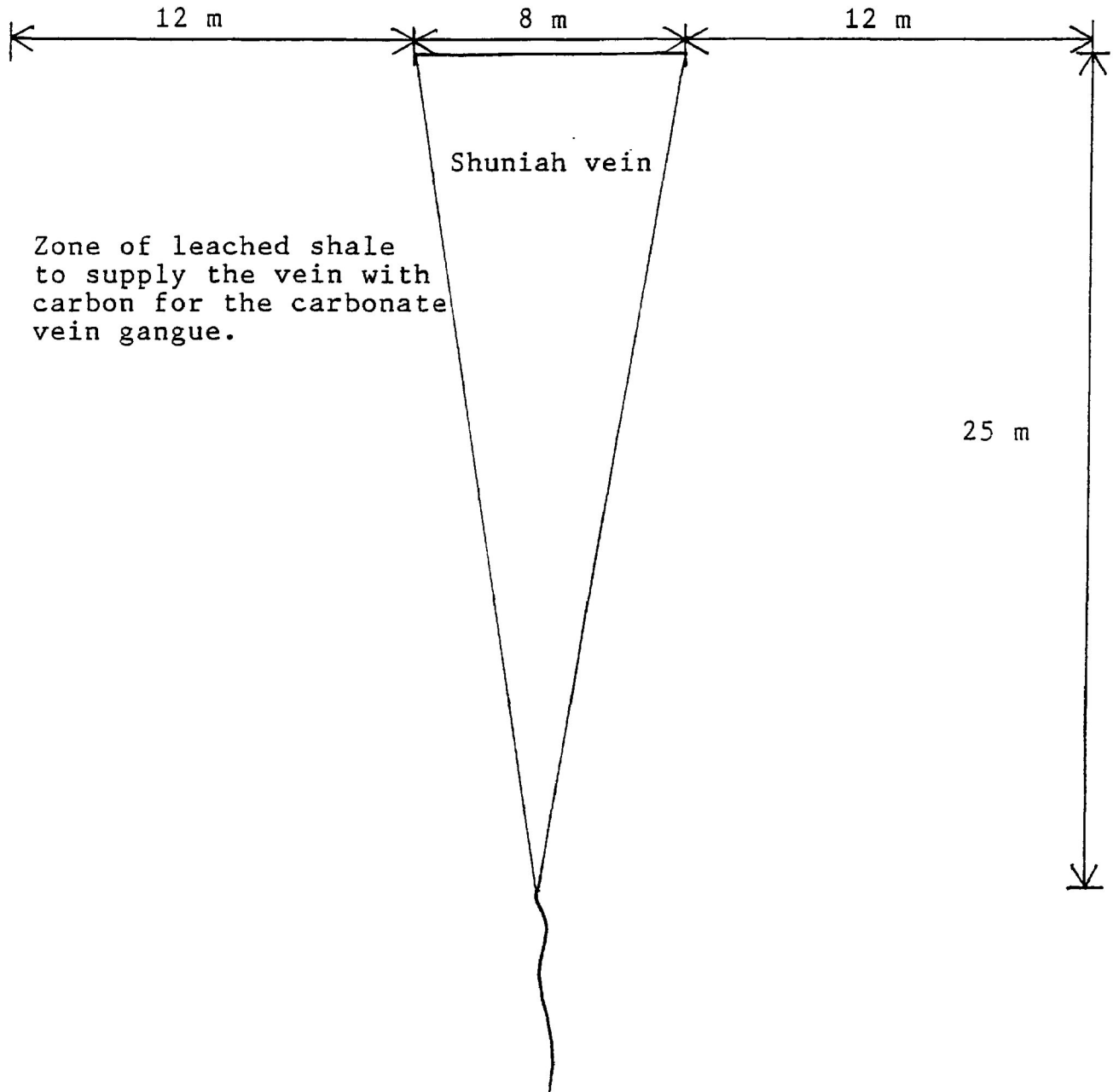
Sample #	Wall Rock	Vein Material
6-67	shale	calcite
6-219.5	shale	quartz
6-220	shale	quartz
6-220.75	shale	quartz
6-221-1	shale	quartz, calcite
6-221-2	shale	quartz
6-223	shale	quartz
6-223-5	shale, graphite	quartz, sphalerite, pyrite
6-224	shale	quartz
6-225	shale	quartz, calcite purple
6-225-1	shale	purple fluorite, calcite
6-225-2	shale	purple fluorite
6-280	shale	quartz, galena
6-280	shale	quartz, galena fluorite, native silver
5-120	shale	quartz
5-125	shale	calcite, quartz
5-140	shale	calcite
K6	shale	sphalerite
KS6-2	shale	quartz
KS2-4	shale	sphalerite, calcite
KS-6	shale	green fluorite
KS6-3	shale	quartz

Porcupine vein

Sample #	Wall Rock	Vein Material
13-30	shale	quartz
13-36	shale	quartz
13-42	shale	quartz
13-48	shale	quartz, pyrite
13-51	shale	quartz, calcite
13-56	shale	quartz, calcite
13-68	shale	quartz, calcite
13-80	shale	quartz, calcite
3-358.6	chert	calcite
3-360	shale	calcite
3-410	chert	calcite
3-440	shale	calcite
PG-4	shale	purple fluorite, calcite, quartz
PO-1	shale	quartz, green fluorite
PO-3	shale	calcite
PO-4	shale	calcite
PO-5	shale	sphalerite, quartz, calcite
PO-10	shale	quartz

Appendix 5

Generalized Cross Section Through The Shuniah Vein System



Generalized diagram illustrating the volume of shale that must be completely leached of all carbon to act as a source for the vein carbonate. The actual limit of hydrothermal alteration is only 4m on either side of the vein. Calculations are given on the following page.

Appendix 5

Calculation for the limit of hydrothermal leaching of carbon from the wall-rock shale.

A cross section of the Shuniah vein can be approximated as a triangle 8 m across and 25 m deep. For each one meter along strike there is 100 cubic meters of vein material. In this zone the vein is composed exclusively of calcite, so for each meter along strike there is $2.7E5$ kg of calcite, or $3.2E4$ kg of carbon.

If we assume that the carbon source was graphite, then 14.0 cubic meters of graphite are needed to account for the calcite. The Rove shale averages 2 wt. % carbon; then in one cubic meter of shale there is 53.4 kg of graphite.

Therefore, a hydrothermal fluid would have to leach 607 cubic meters of shale to supply the carbon for the carbonate. If the vein is completely enclosed in shale then the shale must be completely leached of carbon for 12.1 meters on either side of the vein.

constants used.

density of calcite = 2.7 g/cc
density of graphite = 2.32 g/cc
density of shale = 2.67 g/cc
carbon makes up 12.00 weight % of calcite.